Electronic Supplementary Information (ESI)

Annulated oxazolium anion–π^+ AIEgens

Samim Sohel Rana,[a] Surajit Manna[b] and Joyanta Choudhury*[a]

[a]Organometallics & Smart Materials Laboratory, Department of Chemistry
Indian Institute of Science Education and Research Bhopal
Bhopal 462 066, India
[b]Indian Institute of Science Education and Research (IISER) Berhampur, Berhampur, Odisha, India
*E-mail: joyanta@iiserb.ac.in

Table of Content

1. General methods and materials

Bruker AVANCE III 400, 500MHz, and 700 MHz NMR spectrometers were used to record ^{1}H, ^{13}C, and ^{31}P spectra at room temperature unless otherwise indicated. Chemical shifts are represented in parts ppm using the solvents residual proton resonance as an internal reference ($CHCl_3$: = 7.26 ppm for ^{1}H spectra, 77.2 ppm for ^{13}C spectra; CH_3CN: = 1.94 ppm for ^{1}H spectra, 1.3 ppm for ^{13}C spectra; DMSO: 2.5 ppm for ^{1}H spectra). Unless otherwise specified, all coupling constants (*J*) are reported in hertz (Hz) and are exclusively given for ^{1}H-^{1}H couplings. To signify multiplicity, the following acronyms were used: s (singlet), d (doublet), t (triplet), q (quartet), dd (doublet of doublet), dt (triplet of triplets), m (multiplet), br (broad). A Bruker microTOF QII instrument was used for ESI mass spectrometry. The products were purified chromatographically using column chromatography on silica gel (230-400 mesh). For each crystal, single-crystal X-ray diffraction data were acquired using a Bruker SMART APEX II CCD diffractometer with graphite monochromated MoKα (= 0.71073) and CuKα (λ = 1.54178) radiation at various low temperatures. The UV-visible absorption spectra were obtained using a Cary 100 UV-Vis spectrophotometer at room temperature. Fluorescence emission experiments were carried out with a Jobin Yvon Horiba Model Fluorolog-3-21. EPR spectra were recorded using Bruker EMX micro-X CW-EPR spectrometer in dry CH_2Cl_2 at 100 K (microwave frequency = 9.389156 GHz). Cyclic voltammetry (CV) experiments were performed using a CHI 620E electrochemical workstation. Dry solvents and reagents were purchased from commercial suppliers and used without further purification. Deuterated solvents and $RhCl_3.xH_2O$ were purchased from Aldrich. $[RhCp^*Cl_2]_2$ was synthesized according to the reported procedure.[S1]

2. General procedure for the synthesis of oxazolium salts

The oxazolium salts were synthesized using the following reported procedure. The synthesized compounds (**1a**-**1f**) were already reported in that literature.[S2] The following three steps as given below:

Step 1. In an oven-dried round-bottomed flask aryl aniline (32.9 mmol) and acetoin (65.8 mmol) were dissolved in toluene (110 mL). Then 0.1 mL of concentrated HCl (catalytic amount) was added to the reaction mixture and stirred for 18 h at 140 ^{o}C. The formed water from the reaction was removed by using the Dean-Stark apparatus. After that, the reaction mixture was concentrated and purified by silica gel column chromatography to obtain the desired product (65-80%). R_f = 0.4 (5% EtOAc in hexane)

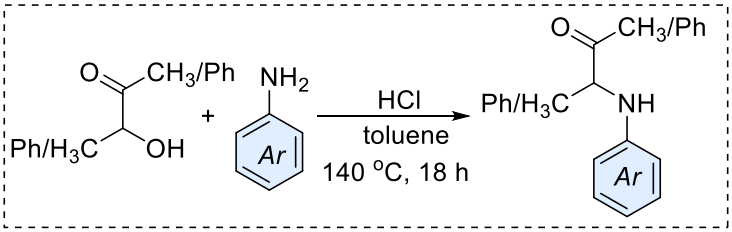

Scheme S1: Synthetic procedure for aryl amino ketone

Step 2. Formic acid (1.16 mL, 30.4 mmol) was added to acetic anhydride (2.17 mL, 23 mmol) in 10 mL round-bottomed flask, then stirred at 60 ^{o} C for 2 h. The resulting mixed anhydride was added slowly to a stirred solution of aryl amino ketone (15.3 mmol) in THF (50 mL) and stirred at room temperature for 16 h. The reaction mixture was concentrated, followed by co-concentration with toluene (3x50 mL). The crude compound was purified by silica gel column chromatography to obtain (75-85%) of the product.

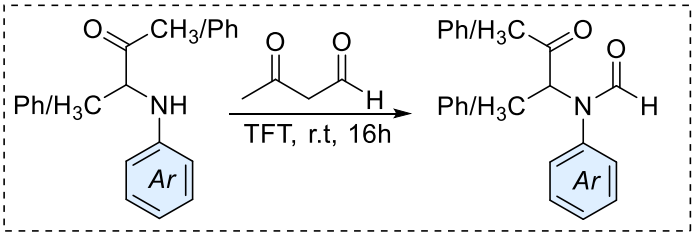

Scheme S2: Synthetic procedure for N-aryl formamide

Step 3. 6.28 mmol of the above compound dissolved in polyphosphoric acid (PPA) 6.0 mL in a 10 mL R.B. and heated at 80 ^{o} C for 18 h. Then cool the mixture to room temperature and added KPF_6 solution to the reaction mixture. Extract the mixture with DCM (4x30 mL) and dry it over

anhydrous Na_2SO_4. After that the mixture is concentrated and recrystallized in dry diethyl ether to obtain various oxazolium salts.

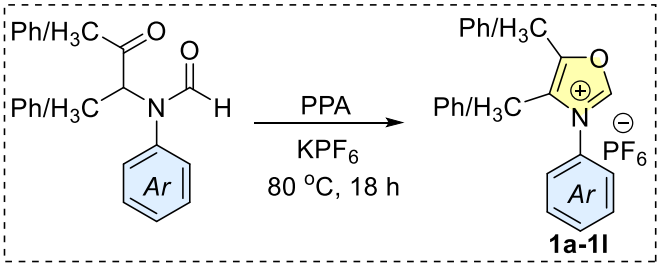

Scheme S3: Synthetic procedure for oxazolium salts

3. Experimental characteristic data for 1a-1l salts

4,5-dimethyl-3-phenyloxazol-3-ium hexafluorophosphate (1a): Yield = 60%. **^{1}H NMR** (400 MHz, $CDCl_3$) δ 9.23 (s, 1H), 7.64 (dt, *J* = 21.1, 7.3 Hz, 3H), 7.53 (d, *J* = 7.7 Hz, 2H), 2.50 (s, 3H), 2.13 (s, 3H).

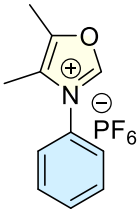

4,5-dimethyl-3-(p-tolyl)oxazol-3-ium hexafluorophosphate (1b): Yield = 50%. **^{1}H NMR** (400 MHz, $CDCl_3$) δ 9.20 (s, 1H), 7.42 (s, 4H), 2.54 (s, 3H), 2.47 (s, 3H), 2.15 (s, 3H).

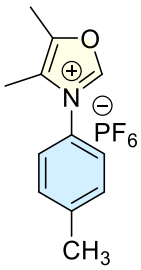

3-(4-methoxyphenyl)-4,5-dimethyloxazol-3-ium hexafluorophosphate (1c): Yield = 70%. **^{1}H NMR** (400 MHz, $CDCl_3$) δ 9.18 (s, 1H), 7.45 (d, *J* = 8.5 Hz, 2H), 7.08 (d, *J* = 8.4 Hz, 2H), 3.88 (s, 3H), 2.51 (s, 3H), 2.13 (s, 3H).

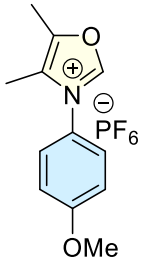

3-(4-bromophenyl)-4,5-dimethyloxazol-3-ium hexafluorophosphate (1d): Yield = 75%. **^{1}H NMR** (400 MHz, $CDCl_3$) δ 9.29 (s, 1H), 7.74 (d, *J* = 7.8 Hz, 2H), 7.41 (d, *J* = 7.7 Hz, 2H), 2.49 (s, 3H), 2.10 (s, 3H).

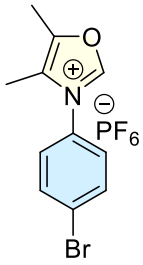

3-(4-fluorophenyl)-4,5-dimethyloxazol-3-ium hexafluorophosphate (1e): Yield = 65%. **^{1}H NMR** (400 MHz, $CDCl_3$) δ 9.49 (s, 1H), 7.61 (dd, *J* = 8.1, 4.3 Hz, 2H), 7.30 – 7.23 (m, 2H), 2.49 (s, 3H), 2.12 (s, 3H).

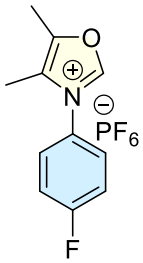

3-(4-isopropylphenyl)-4,5-dimethyloxazol-3-ium hexafluorophosphate (1f): Yield = 40%. **^{1}H NMR** (400 MHz, $CDCl_3$) δ 9.44 (s, 1H), 7.46 (dd, *J* = 21.9, 8.0 Hz, 4H), 3.06 – 2.92 (m, 1H), 2.50 (s, 3H), 2.16 (s, 3H), 1.28 (d, *J* = 6.8 Hz, 6H).

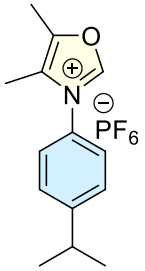

3,4,5-triphenyloxazol-3-ium hexafluorophosphate (1g): Yield = 70%. **^{1}H NMR** (400 MHz, CD_3CN) δ 9.74 (s, 1H), 7.63 – 7.44 (m, 13H), 7.40 (m, 2H). **^{13}C NMR** (126 MHz, CD_3CN) δ 153.0, 151.4, 132.9, 132.5, 132.5, 131.9, 131.1, 131.0, 130.5, 130.4, 129.9, 127.4, 127.2, 124.9, 122.9.

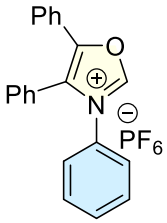

4,5-diphenyl-3-(p-tolyl)oxazol-3-ium hexafluorophosphate (1h): Yield = 75%. **^{1}H NMR** (400 MHz, CD_3CN) δ 9.70 (s, 1H), 7.56 (d, *J* = 7.8 Hz, 4H), 7.49 (t, *J* = 7.6 Hz, 4H), 7.40 (d, *J* = 7.5 Hz, 2H), 7.34 (br, 4H), 2.38 (s, 3H). **^{13}C NMR** (126 MHz, CD_3CN) δ 152.9, 151.3, 143.7, 132.5, 131.9, 131.4, 130.5, 130.4, 129.9, 128.6, 127.4, 126.9, 125.03, 123.0, 21.1.

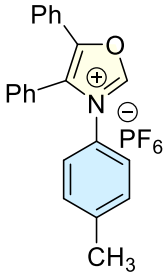

3-(4-methoxyphenyl)-4,5-diphenyloxazol-3-ium hexafluorophosphate (1i): Yield = 70%. **^{1}H NMR** (400 MHz, CD_3CN) δ 9.69 (s, 1H), 7.60 – 7.53 (m, 4H), 7.49 (t, *J* = 7.3 Hz, 4H), 7.37 (dd, *J* = 15.0, 8.0 Hz, 4H), 7.02 (d, *J* = 8.3 Hz, 2H), 3.81 (s, 3H). **^{13}C NMR** (176 MHz, CD_3CN) δ 162.8, 152.9, 151.2, 132.4, 131.9, 130.5, 130.4, 130.1, 128.6, 127.4, 125.1, 123.5, 123.1, 115.9, 56.5.

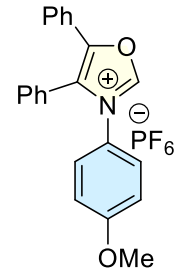

3-(4-fluorophenyl)-4,5-diphenyloxazol-3-ium hexafluorophosphate (1j): Yield = 65%. **^{1}H NMR** (400 MHz, CD_3CN) δ 9.73 (s, 1H), 7.56 (d, *J* = 6.5 Hz, 4H), 7.48 (d, *J* = 7.2 Hz, 6H), 7.39 (d, *J* = 7.5 Hz, 2H), 7.28 (t, *J* = 7.9 Hz, 2H). **^{13}C NMR** (126 MHz, CD_3CN) δ 165.9, 163.9, 153.2, 151.4, 132.6, 131.9, 130.6, 130.4, 130.0, 129.8, 129.7, 127.4, 127.2, 127.2, 124.9, 122.7.

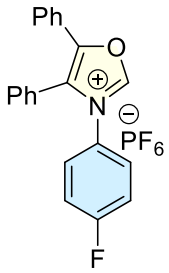

4,5-diphenyl-3-(4-(trifluoromethyl)phenyl)oxazol-3-ium hexafluorophosphate (1k): Yield = 60%. **^{1}H NMR** (400 MHz, CD_3CN) δ 9.81 (s, 1H), 7.86 (d, *J* = 8.5 Hz, 2H), 7.65 (d, *J* = 8.4 Hz, 2H), 7.60 – 7.55 (m, 4H), 7.52 – 7.46 (m, 4H), 7.42 – 7.38 (m, 2H). **^{13}C NMR** (126 MHz, CD_3CN) δ 153.4, 151.6, 134.3, 134.0, 133.8, 133.5, 132.7, 132.7, 131.9, 130.7, 130.4, 129.7, 128.4, 128.2, 128.2, 128.1, 128.1, 127.4, 125.34, 124.76, 123.1, 122.5.

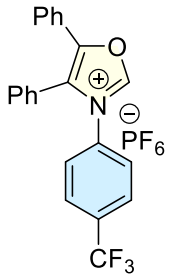

3-(4-fluorophenyl)-4,5-diphenyloxazol-3-ium hexafluorophosphate (1l): Yield = 65%. **^{1}H NMR** (700 MHz, CD_3CN) δ 9.79 (s, 1H), 7.71 (t, *J* = 8.5 Hz, 2H), 7.62 – 7.53 (m, 4H), 7.52 – 7.46 (m, 4H), 7.40 (m, 4H).**^{13}C NMR** (176 MHz, CD3CN) δ 153.1, 153.1, 151.4, 134.1, 132.6, 132.5, 131.9, 130.6, 130.3, 129.7, 129.0, 127.4, 126.7, 124.8, 122.6.

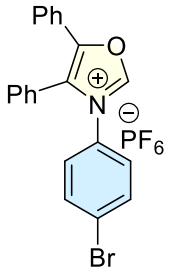

4. General procedure for the synthesis of N-aryl benzoxazole salts

The synthesis of N-aryl benzoxazole salts were performed using the following reported procedure [S3]. The following steps as given below:

Step 1. Copper iodide (CuI) (10 mol%), aryl iodide (1 mmol), 2-aminophenol (1.2 mmol), and K_3PO_4 (1.5 eq) were added to 100 ml two neck RB with a magnetic bead. Then RB was evacuated for 5 minutes and filled back with nitrogen. After that 1,4-dioxane (40 mL) was added by syringe and the reaction mixture was stirred vigorously for 24 h at 110 ^{o}C. After 24 h the reaction mixture

was cooled to room temperature and the reaction mixture was extracted by adding ethyl acetate (50 mL) and water (30 mL). The extracted organic layer is then dried over anhydrous Na_2SO_4. The filtrate is concentrated and purified by silica gel column chromatography to obtain (80-85%) of the product.

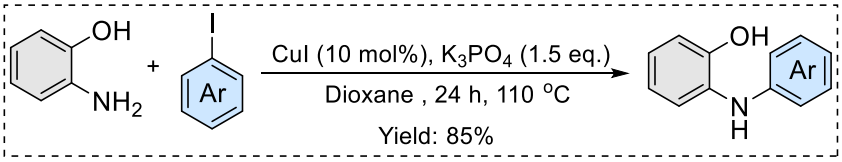

Scheme S4: Synthetic procedure for 2-(arylamino)phenol

Step 2. A solution of $HBF_4.OEt_2$ (1 mmol) was added to a solution of the above synthesized starting material (1 mmol) in 10 mL of MeOH. The mixture was stirred for 1 h at room temperature and then the solvent was removed by vacuum. After that triethyl orthoformate (15 mL) was added to the reaction mixture. The resulting mixture was stirred for 24 h at ambient temperature and then the volatiles was removed by vacuum. After that 30 mL of diethyl ether was added to the crude product to give a white precipitate, yielding benzfused oxazolium salts.

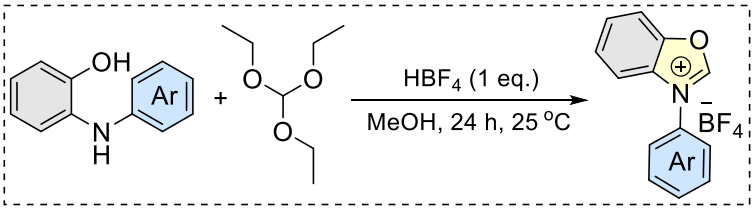

Scheme S5: Synthetic procedure for Benzoxazolium salts

5. Experimental character data for 1m and 1n salts

3-phenylbenzo[d]oxazol-3-ium hexafluorophosphate (1m): Yield = 65%. **^{1}H NMR** (400 MHz, CD_3CN) δ 9.96 (s, 1H), 8.15 (d, *J* = 8.5 Hz, 1H), 7.94 (d, *J* = 3.7 Hz, 1H), 7.83 (m, 7H)

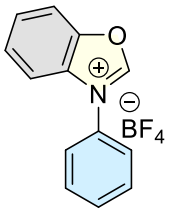

3-(4-methoxyphenyl)benzo[d]oxazol-3-ium tetrafluoroborate (1n): Yield = 62%. **^{1}H NMR** (400 MHz, CD_3CN) δ 9.90 (s, 1H), 8.13 (d, *J* = 8.4 Hz, 1H), 7.93 (t, J = 7.6 Hz, 1H), 7.84 (q, *J* = 8.2 Hz, 2H), 7.71 (d, *J* = 8.5 Hz, 2H), 7.29 (d, *J* = 8.5 Hz, 2H), 3.94 (s, 3H).

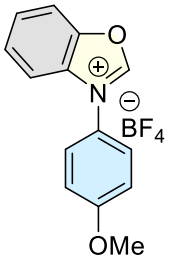

6. Optimization of the reaction conditions

To an oven-dried Schlenk tube, **1a** (0.1 mmol), base (0.42 mmol), catalyst (0.003 mmol), oxidant (0.25 mmol), and **2a** (0.1 mmol) were loaded and then the tube was kept under vacuum for 5 minutes. After that, the tube was filled with N_2 gas. To this mixture, dry and degassed solvent (2.0 mL) was added under the Schlenk technique and the reaction mixture was left with stirring at 110 °C in the dark. After a certain time, the whole reaction mixture was passed through a short *C*elite pad which was thereafter washed with dichloromethane (30 mL). The combined filtrate was concentrated under reduced pressure. The final product was separated by silica gel column chromatography and eluted with a $CHCl_3$/MeOH solvent mixture as an eluent. For optimization studies, The yields were calculated as isolated yields. Conditions were varied as shown in Table S1 to optimize the catalytic protocol.

Table S1: Optimization of the catalytic reaction conditions

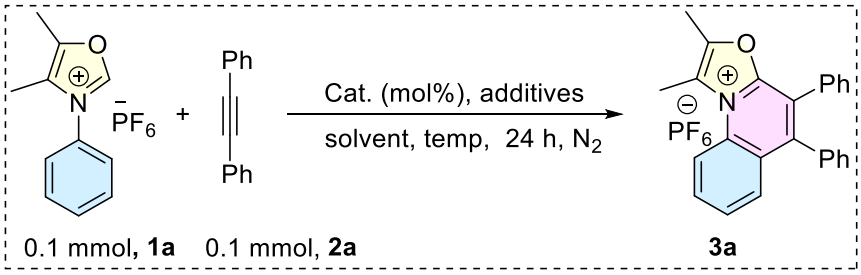

Scheme S6: Synthetic procedure for optimization reaction

Entry	Catalyst	Additives (Equiv.)	Solvent &Temp.°C	Yield[a]
1.	**$[RhCp^*Cl_2]_2$**	**NaOAc (4.2) + AgOTf (2.5)**	**DCE, 110 °C**	**85 (isolated yield)**
2.	$[RhCp^*Cl_2]_2$	NaOAc (4.2) + AgOTf (2.5)	DCE, r.t	45%
3.	$[RhCp^*Cl_2]_2$	Cu $(OAc)_2.H_2O$ (4.2)	MeOH	ND
4.	$[RhCp^*Cl_2]_2$	AgOTf (2.5)	DCM, 110 °C	50%
5.	$[RhCp^*Cl_2]_2$	Cs_2CO_3 (1.5) + AgOTf (2.5)	DCE	35%
6.	$[IrCp^*Cl_2]_2$	NaOAc (4.2) + AgOTf (2.5)	DCE	ND
7.	$CoCp^*COI_2$	NaOAc (4.2) + AgOTf (2.5)	DCE	ND
8.	---	NaOAc (4.2) + AgOTf (2.5)	DCE, 110 °C	ND

Note: Maximum yield was observed after 24 hours of reaction time. [a]isolated yield

7. General procedure for the catalytic annulation reactions

In a Schlenk tube, oxazolium salt (0.1 mmol), NaOAc (4.2 equiv.), $[RhCp^*Cl_2]_2$ (1.8 mg, 3 mol%), AgOTf (64.3 mg, 0.25 mmol), and alkyne (0.12 mmol) were loaded. Then the system was evacuated for 5 minutes to remove any residual air or moisture and filled with N_2 gas. Subsequently, dry and degassed dichloroethane (DCE, 2.0 mL) was added to the mixture and the reaction was carried out at 110 °C for 24 hours in the dark. The reaction mixture was subsequently passed through a short column of Celite and washed with dichloromethane (DCM, 30 mL). The combined filtrate was concentrated under reduced pressure and the final product was isolated using column chromatography eluting with a mixture of dichloromethane and methanol (2% DCM/MeOH).

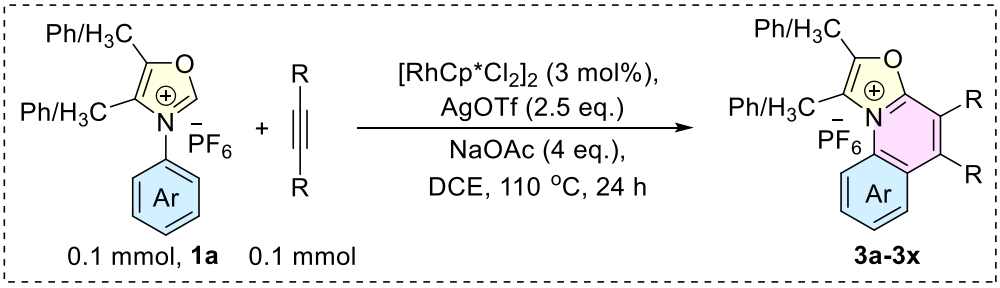

Scheme S7: Synthesis of cationic N,O doped molecules

8. Experimental characterization data for the annulated products 3a–3x

1,2-dimethyl-4,5-diphenyloxazolo[3,2-a]quinolin-10-ium trifluoromethanesulfonate (3a):

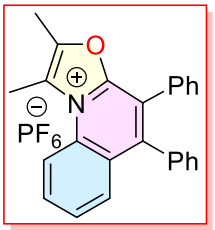

Yield = 85%, 42 mg, **^{1}H NMR** (400 MHz, CD_3CN) δ 8.84 (d, *J* = 8.7 Hz, 1H), 8.16 – 8.07 (m, 1H), 7.85 (m, 2H), 7.47 – 7.26 (m, 10H), 3.03 (s, 3H), 2.56 (s, 3H). **^{13}C NMR** (126 MHz, CD_3CN) δ 153.4, 152.4, 150.2, 134.7, 133.9, 133.3, 131.4, 131.2, 130.9, 130.6, 130.19, 130.0, 129.9, 129.4, 129.4, 127.4, 124.9, 122.9, 12.7, 10.7. **^{31}P NMR** (162 MHz, CD_3CN, 300K): δ -144.66 (hept, *J* = 706.5 Hz). **HRMS** (ESI, positive ion): M^+ = 350.1510 (calculated 350.1540 for $[C_{25}H_{20}NO]^+$)

4,5-bis(4-(tert-butyl)phenyl)-1,2-dimethyloxazolo[3,2-a]quinolin-10-ium

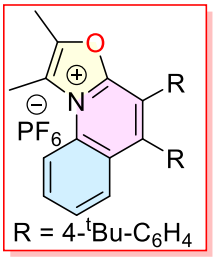

trifluoromethanesulfonate (3b): Yield = 91%, 55 mg, **^{1}H NMR** (500 MHz, CD_3CN) δ 8.83 (d, *J* = 8.9 Hz, 1H), 8.11 (m, 1H), 7.89 – 7.81 (m, 2H), 7.47 (d, *J* = 8.3 Hz, 2H), 7.41 (d, *J* = 8.4 Hz, 2H), 7.24 (d, *J* = 8.4 Hz, 2H), 7.19 (d, *J* = 8.3 Hz, 2H), 3.03 (s, 3H), 2.57 (s, 3H), 1.32 (s, 9H), 1.29 (s, 9H). **^{13}C NMR** (126 MHz, CD_3CN) δ 153.6, 153.4, 150.5, 136.4, 132.5, 131.3, 131.1, 130.7, 129.2, 128.0, 126.4, 126.3, 124.9, 124.2, 123.2, 120.6, 31.3, 31.3, 12.6, 10.7. **HRMS** (ESI, positive ion): M^+ = 462.3112 (calculated 462.2792 for $[C_{33}H_{36}NO]^+$)

1,2-dimethyl-4,5,7-triphenyloxazolo[3,2-a]quinolin-10-iumtrifluoromethanesulfonate (3c):

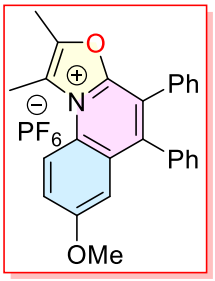

Yield = 86%, 45 mg, **^{1}H NMR** (400 MHz, CD_3CN) δ 8.75 (d, *J* = 9.5 Hz, 1H), 7.70 (d, *J* = 9.5 Hz, 1H), 7.47 – 7.27 (m, 10H), 7.14 (s, 1H), 3.77 (s, 3H), 2.99 (s, 3H), 2.54 (s, 3H). **^{13}C NMR** (126 MHz, CD_3CN) δ 159.9, 151.2, 150.1, 134.8, 131.4, 131.3, 130.8, 130.1, 130.0, 129.5, 129.4, 129.3, 128.0, 124.6, 123.5, 123.1, 120.2, 110.7, 56.4, 12.6, 10.7. **HRMS** (ESI, positive ion): M^+ = 380.1656 (calculated 380.1646 for $[C_{26}H_{22}NO_2]^+$)

4,5-bis(4-(tert-butyl)phenyl)-7-methoxy-1,2-dimethyloxazolo[3,2-a]quinolin-10-ium trifluoromethanesulfonate (3d):

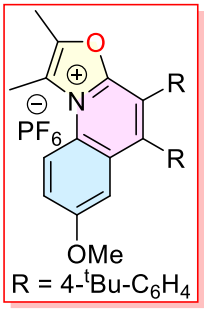

Yield = 90%, 58 mg, **^{1}H NMR** (400 MHz, CD_3CN) δ 8.74 (d, *J* = 9.5 Hz, 1H), 7.70 (d, *J* = 9.5 Hz, 1H), 7.47 (d, *J* = 7.5 Hz, 2H), 7.40 (d, *J* = 7.7 Hz, 2H), 7.21 (m, 4H), 7.15 (s, 1H), 3.78 (s, 3H), 2.99 (s, 3H), 2.55 (s, 3H), 1.32 (s, 9H), 1.29 (s, 9H). **^{13}C NMR** (176 MHz, $CDCl_3$) δ 159.18, 152.74, 152.46, 151.34, 149.50, 131.11, 130.50, 130.12, 128.78, 127.56, 127.21, 125.68, 125.61, 122.65, 122.49, 119.08, 111.13, 56.13, 35.07, 34.99, 31.44, 30.02, 12.88, 11.03. **HRMS** (ESI, positive ion): M^+ = 492.2889 (calculated 492.2898 for $[C_{34}H_{38}NO_2]^+$)

1,2,7-trimethyl-4,5-diphenyloxazolo[3,2-a]quinolin-10-iumtrifluoromethanesulfonate (3e):

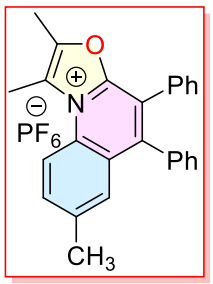

Yield = 85%, 44 mg, **^{1}H NMR** (500 MHz, CD_3CN) δ 8.72 (d, *J* = 9.0 Hz, 1H), 7.95 (dd, *J* = 9.0, 1.7 Hz, 1H), 7.61 (s, 1H), 7.46 – 7.41 (m, 3H), 7.36 (m, 3H), 7.33 – 7.28 (m, 2H), 7.26 (m, 2H), 3.01 (s, 3H), 2.54 (s, 3H), 2.48 (s, 3H). **^{13}C NMR** (126 MHz, CD_3CN) δ 153.0, 151.9, 150.0, 140.6, 135.4, 134.8, 131.5, 131.4, 131.3, 130.9, 130.1, 129.9, 129.7, 129.4, 127.5, 124.7, 122.8, 21.3, 12.6, 10.6. **HRMS** (ESI, positive ion): M^+ = 364.1682 (calculated 364.1696 for $[C_{26}H_{22}NO]^+$)

7-isopropyl-1,2-dimethyl-4,5-diphenyloxazolo[3,2-a]quinolin-10-ium trifluoromethanesulfonate (3f):

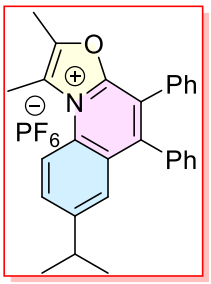

Yield = 85%, 46 mg, **^{1}H NMR** (400 MHz, CD_3CN) δ 8.77 (d, *J* = 8.9 Hz, 1H), 8.04 (d, *J* = 9.0 Hz, 1H), 7.65 (s, 1H), 7.47 – 7.25 (m, 10H), 3.09 (dt, *J* = 13.7, 6.8 Hz, 1H), 3.02 (s, 3H), 2.55 (s, 3H), 1.24 (s, 3H), 1.22 (s, 3H). **^{13}C NMR** (126 MHz, CD_3CN) δ 153.1, 152.1, 150.8, 150.0, 134.8, 133.0, 131.8, 131.4, 131.3, 130.9, 130.1, 130.0, 129.4, 129.4, 127.5, 127.3, 124.7, 122.8, 34.6, 23.7, 12.6, 10.7. **HRMS** (ESI, positive ion): M^+ = 392.2008 (calculated 392.2009 for $[C_{28}H_{26}NO]^+$)

7-bromo-1,2-dimethyl-4,5-diphenyloxazolo[3,2-a]quinolin-10-ium

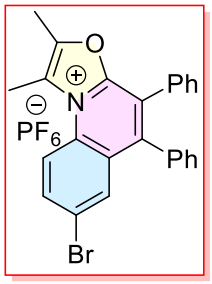

trifluoromethanesulfonate (3g): Yield = 92%, 53 mg, **^{1}H NMR** (400 MHz, CD_3CN) δ 8.73 (d, *J* = 9.3 Hz, 1H), 8.21 (d, *J* = 9.3 Hz, 1H), 7.92 (s, 1H), 7.36 (m, 10H), 3.00 (s, 3H), 2.56 (s, 3H). **^{13}C NMR** (126 MHz, CD_3CN) δ 153.3, 151.1, 150.6, 136.5, 134.1, 132.5, 132.1, 131.3, 130.8, 130.8, 130.4, 130.3, 129.5, 129.4, 129.0, 124.9, 124.1, 123.3, 120.6, 12.5, 10.6. **HRMS** (ESI, positive ion): M^+ = 428.0606 (calculated 428.0645 for $[C_{26}H_{22}NO_2]^+$)

7-bromo-4,5-bis(4-(tert-butyl)phenyl)-1,2-dimethyloxazolo[3,2-a]quinolin-10-ium

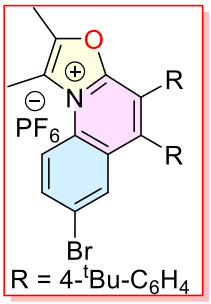

trifluoromethanesulfonate (3h): Yield = 95%, 65 mg, **^{1}H NMR** (400 MHz, CD_3CN) δ 8.72 (d, *J* = 9.2 Hz, 1H), 8.20 (d, *J* = 9.3 Hz,1H), 7.96 (s, 1H), 7.48 (d, *J* = 7.5 Hz, 2H), 7.40 (d, *J* = 7.5 Hz, 2H), 7.20 (m, 4H), 3.00 (s, 3H), 2.57 (s, 3H), 1.32 (s, 9H), 1.29 (s, 9H). **^{13}C NMR** (126 MHz, CD_3CN) δ 153.6, 153.4, 150.5, 136.4, 132.5, 131.3, 131.1, 130.7, 129.2, 128.0, 126.4, 126.3, 124.9, 124.2, 123.2, 120.6, 31.3, 31.3, 12.6, 10.7. **HRMS** (ESI, positive ion): M^+ = 540.1874 (calculated 540.1897 for $[C_{33}H_{35}BrNO]^+$)

7-bromo-1,2-dimethyl-4,5-dipropyloxazolo[3,2-a]quinolin-10-ium

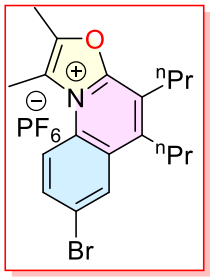

trifluoromethanesulfonate (3i): Yield = 82%, 41 mg, **^{1}H NMR** (400 MHz, CD_3CN) δ 8.59 (s, 1H), 8.57 (br, 1H), 8.12 (d, *J* = 9.3 Hz, 1H), 3.30 – 3.20 (m, 2H), 3.11 – 3.03 (m, 2H), 2.89 (s, 3H), 2.61 (s, 3H), 1.72 (td, *J* = 15.6, 7.7 Hz, 4H), 1.13 (t, *J* = 7.3 Hz, 3H), 1.07 (t, *J* = 7.3 Hz, 3H). **^{13}C NMR** (126 MHz, CD_3CN) δ 153.8, 152.2, 149.5, 135.6, 131.7, 130.2, 128.1, 124.4, 123.5, 123.1, 120.7, 31.1, 28.9, 24.7, 23.1, 14.3, 14.1, 12.5, 10.6. **HRMS** (ESI, positive ion): M^+ = 360.0931 (calculated 360.0958 for $[C_{19}H_{23}BrNO]^+$)

7-fluoro-1,2-dimethyl-4,5-diphenyloxazolo[3,2-a]quinolin-10-ium

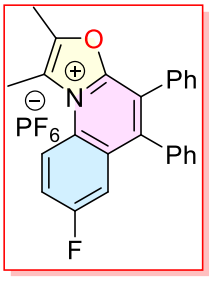

trifluoromethanesulfonate (3j): Yield = 75 %, 39 mg, **^{1}H NMR** (400 MHz, CD_3CN) δ 8.89 (m, 1H), 7.97 – 7.88 (m, 1H), 7.50 (s, 1H), 7.35 (m, 10H), 3.02 (s, 3H), 2.56 (s, 3H). **^{13}C NMR** (126 MHz, CD_3CN) δ 162.9, 160.9, 151.3, 151.3, 150.4, 134.3, 131.3, 131.0, 130.8, 130.2, 130.2, 129.5, 129.4, 125.0, 123.9, 122.6, 122.4, 121.7, 121.6, 115.2, 115.0, 12.6, 10.7. **HRMS** (ESI, positive ion): M^+ = 368.1444 (calculated 368.1446 for $[C_{25}H_{19}FNO]^+$)

1,2,4,5-tetraphenyloxazolo[3,2-a]quinolin-10-ium trifluoromethanesulfonate (3k): Yield = 90%, 56 mg, **^{1}H NMR** (400 MHz, CD_3CN) δ 7.95 – 7.89 (m, 1H), 7.89 – 7.81 (m, 5H), 7.77 – 7.69 (m, 2H), 7.51 (m, 1H), 7.50 – 7.43 (m, 9H), 7.43 – 7.37 (m, 4H), 7.37 – 7.32 (m, 2H). **^{13}C NMR** (176 MHz, CD_3CN) δ 153.6, 153.1, 150.0, 134.6, 133.8, 133.5, 133.0, 132.5, 132.4, 131.9, 131.4, 131.2, 131.1, 131.0, 130.4, 130.3, 130.2, 130.0, 129.6, 129.5, 127.8, 127.7, 126.3, 125.9, 125.3, 123.0. **HRMS** (ESI, positive ion): M^+ = 474.1826 (calculated 474.1853 for $[C_{35}H_{24}NO]^+$). **UV-Vis** (CH_3CN, c = 5.0 × 10^{-5} M): λ_{max} (ε, M^{-1} cm^{-1}) = 343 nm (20856).

((trifluoromethyl)sulfonyl)-l1-oxidane,4,5-bis(4-(tert-butyl)phenyl)-1,2-diphenyloxazolo[3,2-a]quinolin-10-ium salt (3l): Yield = 92%, 62 mg, **^{1}H NMR** (400 MHz, CD_3CN) δ 7.92 (m, 1H), 7.86 (m, 5H), 7.78 – 7.69 (m, 2H), 7.49 (m, 6H), 7.40 (m, 6H), 7.25 (d, *J* = 7.7 Hz, 2H). **^{13}C NMR** (126 MHz, CD_3CN) δ 153.7, 153.5, 153.4, 153.2, 149.9, 133.6, 133.5, 132.8, 132.5, 132.4, 131.8, 131.8, 131.2, 130.9, 130.8, 130.3, 129.9, 128.2, 127.8, 126.5, 126.4, 126.3, 126.0, 125.3, 123.0, 35.4, 35.3, 31.4, 31.3. **HRMS** (ESI, positive ion): M^+ = 586.3112 (calculated 586.3105 for $[C_{43}H_{40}NO]^+$)

((trifluoromethyl)sulfonyl)-l1-oxidane, 4,5-dibutyl-1,2-diphenyloxazolo[3,2-a]quinolin-10-ium salt (3m): Yield = 75%, 44 mg, **^{1}H NMR** (400 MHz, DMSO-d_6) δ 7.99 (d, *J* = 8.3 Hz, 1H), 7.34 (br, 1H), 7.30 (br, 5H), 7.18 (t, *J* = 7.9 Hz, 1H), 6.97 (m, 5H), 6.74 (d, *J* = 8.7 Hz, 1H), 2.82 (t, *J* = 7.3 Hz, 2H), 2.71 (t, *J* = 7.3 Hz, 2H), 1.29 – 1.21 (m, 2H), 1.05 (m, 6H), 0.50 – 0.41 (m, 6H). **^{13}C NMR** (126 MHz, DMSO-d_6) δ 152.7, 152.3, 146.8, 132.4, 131.6, 131.3, 131.2, 130.8, 129.5, 128.6, 127.4, 126.2, 125.4, 125.2, 124.9, 124.6, 121.0, 116.8, 32.5, 30.9, 28.0, 25.5, 22.3, 22.0, 13.8, 13.7. **HRMS** (ESI, positive ion): M^+ = 434.2476 (calculated 434.2479 for $[C_{31}H_{32}NO]^+$)

((trifluoromethyl)sulfonyl)-l1-oxidane, 4,5-dipentyl-1,2-diphenyloxazolo[3,2-a]quinolin-10-ium salt (3n): Yield = 76%, 45 mg, **^{1}H NMR** (400 MHz, DMSO-d_6) δ 8.55 (d, *J* = 8.2 Hz, 1H), 7.90 (m, 1H), 7.86 (br, 5H), 7.74 (t, *J* = 7.8 Hz, 1H), 7.53 (br, 5H), 7.30 (d, *J* = 8.8 Hz, 1H), 3.38 (m, 2H), 3.26 (m, 2H), 1.82 (m, 2H), 1.68 (m, 2H), 1.55 (m, 4H), 1.43 (m, 4H), 0.97 – 0.88 (m, 6H). **^{13}C NMR** (126 MHz, DMSO-d_6) δ 152.2, 146.8, 132.4, 131.6, 131.3, 131.2, 130.8, 129.4, 128.6, 127.4, 126.2, 125.4, 125.2, 124.9,

124.6, 121.0, 116.8, 31.3, 31.0, 30.2, 28.4, 28.2, 25.8, 21.9, 21.8, 13.8, 13.8. **HRMS** (ESI, positive ion): M^+ = 462.2803 (calculated 462.2792 for $[C_{43}H_{39}FNO]^+$)

4,5-bis(4-(tert-butyl)phenyl)-7-bromo-1,2-diphenyloxazolo[3,2-a]quinolin-10-ium trifluoromethanesulfonate (3o): Yield = 78 %, 57 mg, **^{1}H NMR** (700 MHz, CD_3CN) δ 7.94 (s, 1H), 7.93 – 7.91 (br, 1H), 7.86 (d, *J* = 8.0 Hz, 1H), 7.85 – 7.81 (m, 4H), 7.53 – 7.48 (m, 4H), 7.48 – 7.46 (m, 5H), 7.43 – 7.38 (m, 5H), 7.34 (m, 2H). **^{13}C NMR** (176 MHz, CD_3CN) δ 153.1, 152.3, 150.4, 136.6, 133.7, 132.9, 132.6, 132.3, 132.0, 131.3, 131.0, 130.5, 130.5, 130.3, 129.7, 129.6, 127.8, 126.3, 125.5, 125.1, 124.2, 123.5, 119.9. **HRMS** (ESI, positive ion): M^+ = 552.0969 (calculated 552.0958 for $[C_{35}H_{23}BrNO]^+$). **UV-Vis** (CH_3CN, c = 5.0 × 10^{-5} M): λ_{max} (ε, M^{-1} cm^{-1}) = 341 nm (23891).

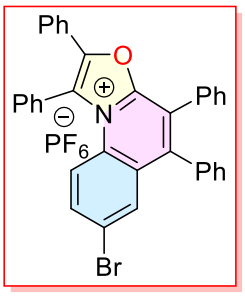

((trifluoromethyl)sulfonyl)-l1-oxidane, 7-fluoro-1,2,4,5-tetraphenyloxazolo[3,2-a]quinolin-10-ium salt (3p): Yield = 76%, 48 mg, **^{1}H NMR** (400 MHz, CD_3CN) δ 7.92 (m, 1H), 7.88 – 7.79 (m, 4H), 7.54 (s, 1H), 7.54 – 7.43 (m, 11H), 7.40 (br, 4H), 7.34 (d, *J* = 6.6 Hz, 2H).**^{13}C NMR** (126 MHz, CD_3CN) δ 162.9, 160.9, 152.9, 152.6, 150.3, 134.2, 133.6, 132.6, 132.3, 132.0, 131.4, 130.9, 130.8, 130.4, 130.3, 129.6, 127.8, 126.3, 125.6, 125.1, 124.0, 122.8, 122.6, 120.9, 120.8, 115.7, 115.5. **HRMS** (ESI, positive ion): M^+ = 492.1759 (calculated 492.1759 for $[C_{43}H_{39}FNO]^+$). **UV-Vis** (CH_3CN, c = 5.0 × 10^{-5} M): λ_{max} (ε, M^{-1} cm^{-1}) = 344 nm (17495).

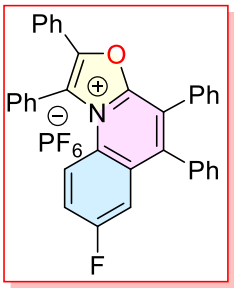

4,5-bis(4-(tert-butyl)phenyl)-7-fluoro-1,2-diphenyloxazolo[3,2-a]quinolin-10-ium trifluoromethanesulfonate (3q): Yield = 77 %, 53 mg, **^{1}H NMR** (400 MHz, CD_3CN) δ 7.92 (d, *J* = 6.4 Hz, 1H), 7.84 (m, 4H), 7.51 (m, 7H), 7.48 (s, 1H), 7.45 – 7.36 (m, 6H), 7.25 (d, *J* = 7.7 Hz, 2H), 1.33 (s, 9H), 1.32 (s, 9H). **^{13}C NMR** (126 MHz, CD_3CN) δ 162.4, 160.4, 153.4, 153.2, 152.4, 152.3, 149.7, 133.1, 132.1, 131.8, 131.5, 130.9, 130.6, 130.2, 129.8, 129.0, 127.4, 127.3, 126.0, 126.0, 125.8, 125.1, 124.7, 123.5, 122.1, 121.8, 120.4, 120.3, 115.1, 114.9, 35, 34.9, 30.9, 30.8. **HRMS** (ESI, positive ion): M^+ = 604.2986 (calculated 604.3011 for $[C_{43}H_{39}FNO]^+$)

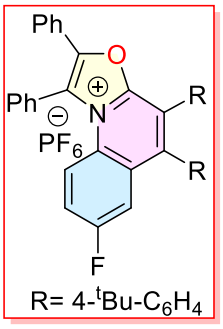

7-methyl-1,2,4,5-tetraphenyloxazolo[3,2-a]quinolin-10-ium trifluoromethanesulfonate (3r):

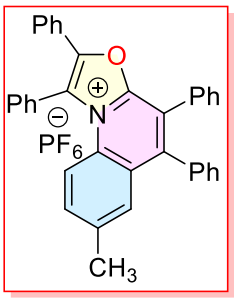

Yield = 91%, 58 mg, ^{1}H NMR (400 MHz, CD_3CN) δ 7.91 (m, 1H), 7.83 (m, 4H), 7.63 (s, 1H), 7.58 – 7.53 (m, 1H), 7.46 (m, 9H), 7.39 (m, 5H), 7.33 (d, *J* = 4.9 Hz, 2H), 2.39 (s, 3H). **^{13}C NMR** (126 MHz, CD_3CN) δ 152.2, 151.7, 149.0, 139.8, 134.4, 133.8, 132.5, 131.5, 131.4, 130.9, 130.5, 130.2, 130.0, 129.3, 129.3, 129.2, 129.1, 128.6, 128.5, 126.8, 126.8, 125.3, 125.0, 124.4, 122.0, 20.4. **HRMS** (ESI, positive ion): M^+ = 488.1991 (calculated 488.2009 for $[C_{36}H_{26}NO]^+$). **UV-Vis** (CH_3CN, c = 5.0 × 10^{-5} M): λ_{max} (ε, M^{-1} cm^{-1}) = 339 nm (27555).

4,5-bis(4-(tert-butyl)phenyl)-7-methyl-1,2-diphenyloxazolo[3,2-a]quinolin-10-ium trifluoromethanesulfonate (3s):

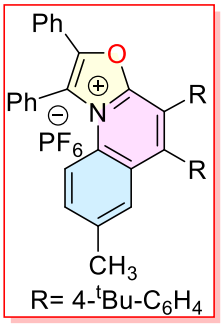

Yield = 85%, 63 mg, **^{1}H NMR** (400 MHz, CD_3CN) δ 7.91 (br, 1H), 7.84 (m, 4H), 7.67 (s, 1H), 7.58 – 7.44 (m, 7H), 7.42 (m, 4H), 7.37 (m, 3H), 7.24 (d, *J* = 7.6 Hz, 2H), 2.41 (s, 3H), 1.34 (s, 9H), 1.32 (s, 9H). **^{13}C NMR** (126 MHz, CD_3CN) δ 153.5, 153.3, 153.3, 152.7, 149.8, 140.6, 135.2, 133.4, 132.4, 132.4, 131.9, 131.8, 131.2, 131.0, 130.8, 130.3, 130.0, 128.3, 127.8, 127.7, 126.4, 126.2, 126.2, 126.0, 125.4, 122.9, 117.8, 116.7, 35.3, 31.3, 21.4. **HRMS** (ESI, positive ion): M^+ = 600.3244 (calculated 600.3261 for $[C_{44}H_{42}NO]^+$)

1,2,4,5-tetraphenyl-7-(trifluoromethyl)oxazolo[3,2-a]quinolin-10-ium trifluoromethanesulfonate (3t):

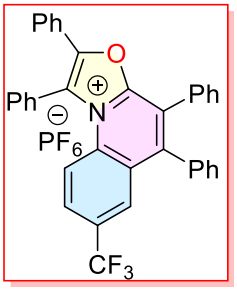

Yield = 70%, 49 mg, **^{1}H NMR** (400 MHz, CD_3CN) δ 8.12 (s, 1H), 8.00 – 7.91 (m, 2H), 7.90 – 7.84 (m, 4H), 7.70 (d, *J* = 9.2 Hz, 1H), 7.54 – 7.47 (m, 9H), 7.45 – 7.40 (m, 4H), 7.39 – 7.34 (m, 2H). **^{13}C NMR** (101 MHz, CD_3CN) δ 153.8, 153.5, 150.6, 134.6, 133.8, 133.7, 132.8, 132.3, 132.0, 131.3, 131.1, 130.7, 130.6, 130.5, 130.3, 129.7, 129.7, 129.6, 128.3, 128.2, 127.8, 127.6, 126.5, 125.4, 124.9, 124.6, 119.7. **HRMS** (ESI, positive ion): M^+ = 542.1700 (calculated 542.1727 for $[C_{36}H_{23}F_3NO]^+$). **UV-Vis** (CH_3CN, c = 5.0 × 10^{-5} M): λ_{max} (ε, M^{-1} cm^{-1}) = 345 nm (30937).

7-methoxy-1,2,4,5-tetraphenyloxazolo[3,2-a]quinolin-10-ium trifluoromethanesulfonate (3u):

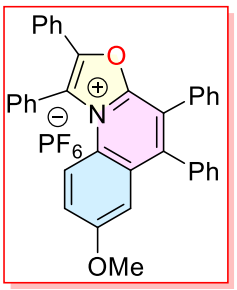

Yield = 82%, 53 mg, ^{1}H NMR (500 MHz, CD_3CN) δ 7.92 (m, 1H), 7.88 – 7.81 (m, 4H), 7.55 – 7.44 (m, 9H), 7.43 (s, 1H), 7.41 (m, 4H), 7.38 – 7.31 (m, 3H), 7.16 (s, 1H), 3.72 (s, 3H).**^{13}C NMR** (126 MHz, DMSO-d) δ 158.82, 151.55, 148.26, 133.9, 133.1, 131.9, 131.8, 131.5, 130.8, 130.5, 130.2, 130.0, 129.8, 129.2, 129.1, 128.3, 126.7, 125.5, 125.4, 124.8, 122.4, 118.8, 110.8, 56.2. **HRMS** (ESI, positive ion): M^+ = 504.1963 (calculated

504.1959 for $[C_{36}H_{26}NO_2]^+$). **UV-Vis** (CH_3CN, c = 5.0 × 10^{-5} M): λ_{max} (ε, M^{-1} cm^{-1}) = 338 nm (40216).

4,5-bis(4-(tert-butyl)phenyl)-7-methoxy-1,2-diphenyloxazolo[3,2-a]quinolin-10-ium

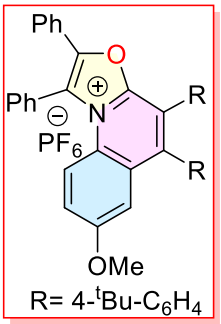

trifluoromethanesulfonate (3v) : Yield = 85%, 62 mg, **^{1}H NMR** (400 MHz, CD_3CN) δ 7.90 (m, 1H), 7.85 – 7.80 (m, 4H), 7.49 (m, 5H), 7.42 – 7.39 (m, 4H), 7.38 (br, 2H), 7.35 (s, 1H), 7.31 (m, 1H), 7.25 (m, 2H), 7.16 (d, *J* = 2.8 Hz, 1H), 3.71 (s, 3H). **^{13}C NMR** (126 MHz, CD_3CN) δ 159.8, 153.6, 153.4, 152.6, 152.1, 149.8, 133.5, 132.4, 132.4, 131.9, 131.9, 131.1, 130.7, 130.3, 129.7, 128.3, 127.7, 127.4, 126.4, 126.4, 126.1, 126.0, 125.4, 123.1, 123.1, 119.5, 111.3, 56.47, , 35.3, 31.3. **HRMS** (ESI, positive ion): M^+ = 616.3180 (calculated 616.3211 for $[C_{44}H_{42}NO_2]^+$)

5,6-diphenylbenzo[4,5]oxazolo[3,2-a]quinolin-12-ium trifluoromethanesulfonate (3w):

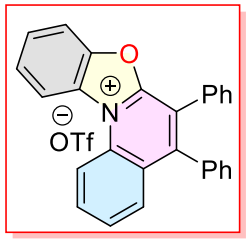

Yield = 80%, 42 mg, ^{1}H NMR (400 MHz, CD_3CN) δ 9.15 (d, *J* = 8.7 Hz, 1H), 9.00 – 8.94 (m, 1H), 8.36 (t, *J* = 7.4 Hz, 1H), 8.07 (d, *J* = 8.4 Hz, 1H), 8.04 – 7.94 (m, 4H), 7.52 – 7.41 (m, 8H), 7.35 (d, *J* = 7.0 Hz, 2H). **^{13}C NMR** (126 MHz, CD_3CN) δ 157.4, 155.6, 148.9, 135.7, 134.5, 133.6, 131.7, 131.5, 131.2, 131.0, 130.8, 130.3, 130.3, 129.5, 129.4, 129.2, 128.7, 127.1, 123.5, 118.6, 118.5, 114.6. **HRMS** (ESI, positive ion): M^+ = 372.1362 (calculated 372.1383 for $[C_{27}H_{18}NO]^+$)

3-methoxy-5,6-diphenylbenzo[4,5]oxazolo[3,2-a]quinolin-12-ium

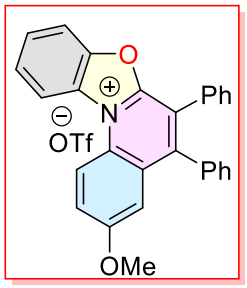

trifluoromethanesulfonate (3x): Yield = 83%, 47 mg, **^{1}H NMR** (400 MHz, CD_3CN) δ 9.05 (d, *J* = 9.5 Hz, 1H), 8.92 (m, 1H), 8.06 – 7.90 (m, 4H), 7.49 – 7.40 (m, 8H), 7.35 (m, 2H), 7.26 (s, 1H), 3.82 (s, 3H). **^{13}C NMR** (126 MHz, CD_3CN) δ 160.1, 156.0, 154.3, 148.8, 134.4, 131.5, 131.3, 131.0, 130.5, 130.2, 130.1, 129.3, 128.9, 128.8, 128.5, 128.1, 125.3, 123.5, 123.0, 120.4, 120.0, 114.4, 111.0, 56.5. **HRMS** (ESI, positive ion): M^+ = 402.1501 (calculated 402.1489 for $[C_{28}H_{20}NO_2]^+$)

9. Mechanistic studies

(a) Synthesis of the cyclometalated Rh(III) intermediate complex 4

To an oven-dried Schlenk tube, **1a** (0.05 mmol), Cs_2CO_3 (1.5 equiv.), $[RhCp^*Cl_2]_2$ (0.5 equiv.) was loaded and then the tube was kept under vacuum for 5 minutes. After that, the tube was filled with N_2 gas. To the reaction mixture, dry and degassed DCE (3.0 mL) was added under the

Schlenk technique and the reaction mixture was left with stirring at a reflux condition of 110 ^{o}C. After 24 h, the whole reaction mixture was passed through a short *C*elite pad which was thereafter washed with DCM (30 mL). The combined filtrate was concentrated under reduced pressure. The solid part was re-precipitated thrice using DCM/Diethyl ether solvent combination to obtain the desired complex **4**. **^{1}H NMR** (400 MHz, $CDCl_3$) δ 7.75 (d, *J* = 7.3 Hz, 1H), 7.33 (d, *J* = 7.7 Hz, 1H), 7.09 (t, *J* = 7.0 Hz, 1H), 7.01 (t, *J* = 7.5 Hz, 1H), 2.48 (s, 3H), 2.36 (s, 3H), 1.78 (s, 15H). **^{13}C NMR** (126 MHz, $CDCl_3$) δ 205.9 (d, $J_{Rh\text{-}C(NOHC)}$ = 61.5 Hz), 160.7 (d, $J_{Rh\text{-}C(Ph)}$ = 33.6 Hz), 148.5, 144.1, 137.8, 125.9, 122.6, 120.8, 112.8, 99.1, 10.2, 9.7, 9.6. **HRMS** (ESI, positive ion): M^+ = 410.0988 (calculated 410.0991for $[C_{21}H_{25}NORh]^+$)

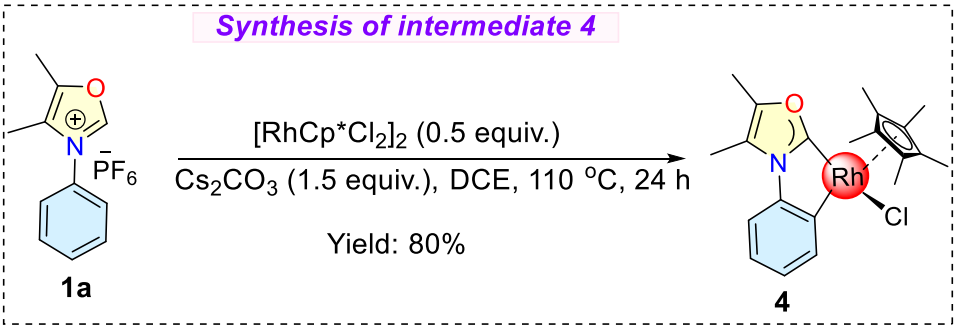

Scheme S8: Synthesis of the complex **4**

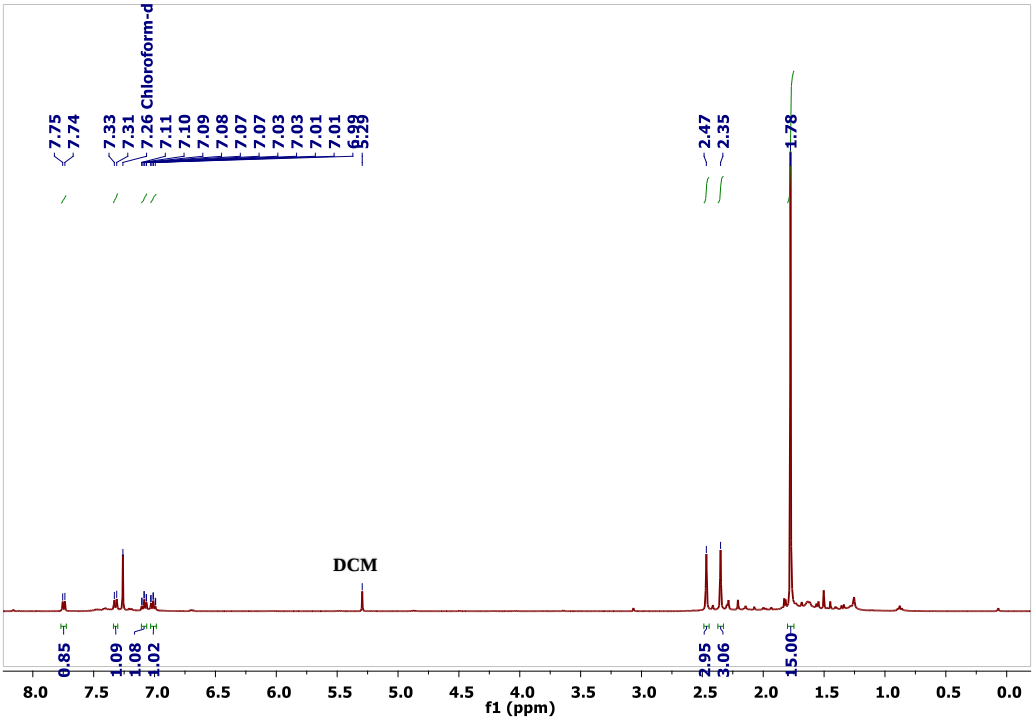

Figure S1: ^{1}H NMR spectrum of complex **4** (500 MHz, $CDCl_3$)

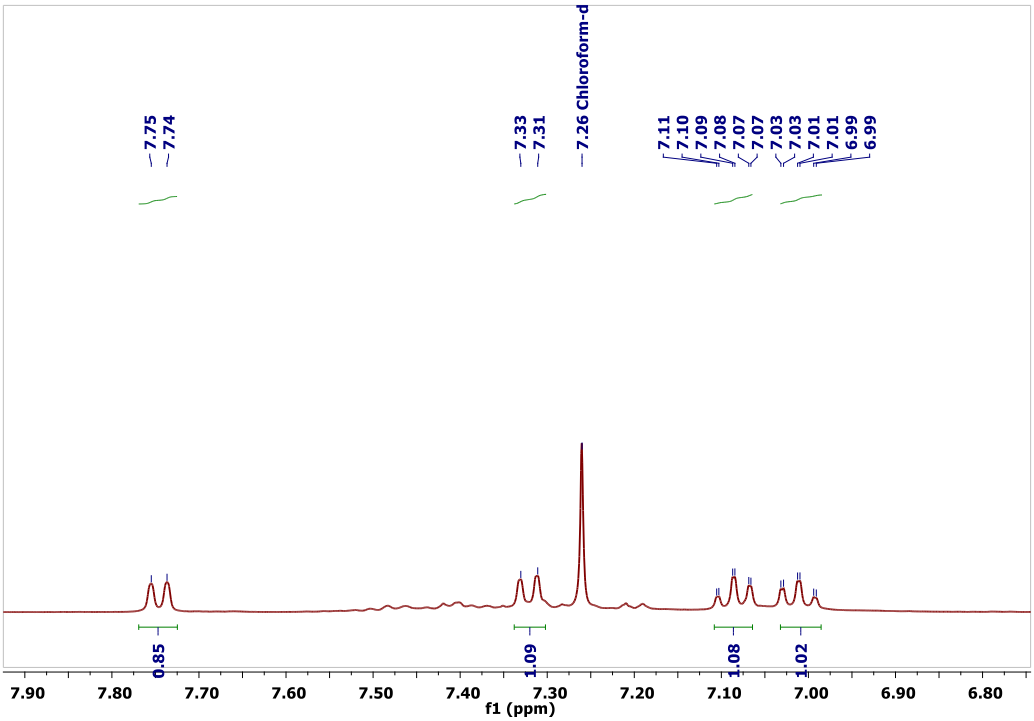

Figure S2: Extended ^{1}H NMR spectrum of complex **4** (500 MHz, $CDCl_3$)

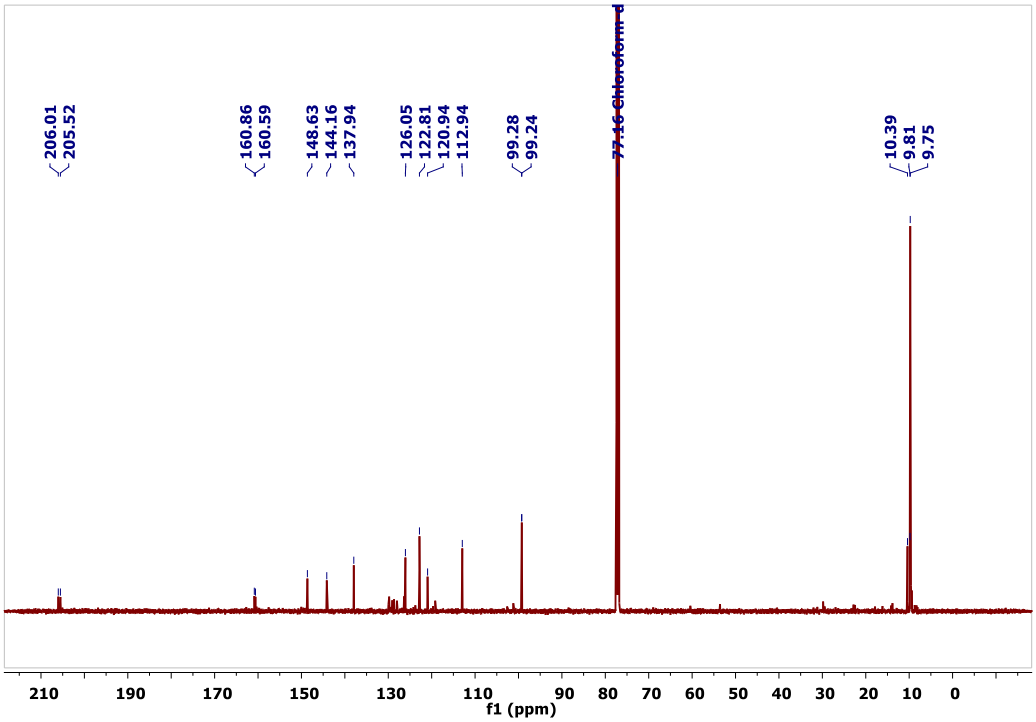

Figure S3: $^{13}C\{^{1}H\}$ NMR spectrum of complex **4** (126 MHz, $CDCl_3$)

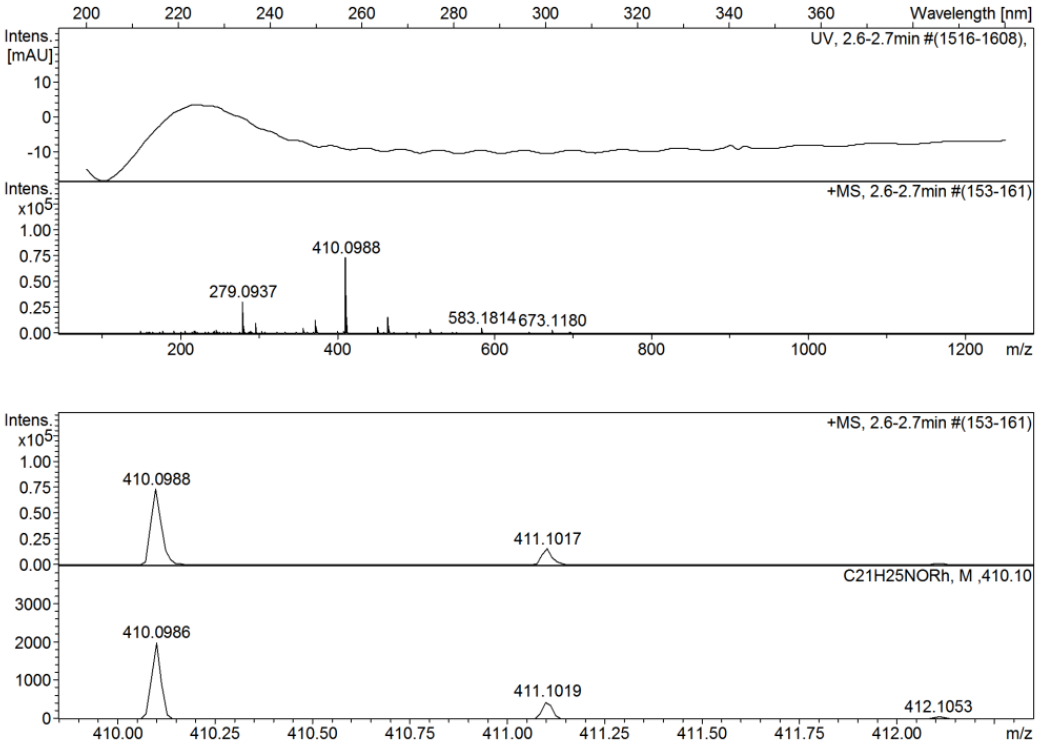

Figure S4: ESI-HRMS (positive ion mode) spectrum of complex **4**

(b) SC-XRD data analysis for complex 4

The structure of this complex was characterized by a single-crystal X-ray diffraction study. A suitable single crystal of **4** was grown by the layering of a dichloromethane solution of **4** with hexane at room temperature. The details of the crystal data are provided in the CIF file.

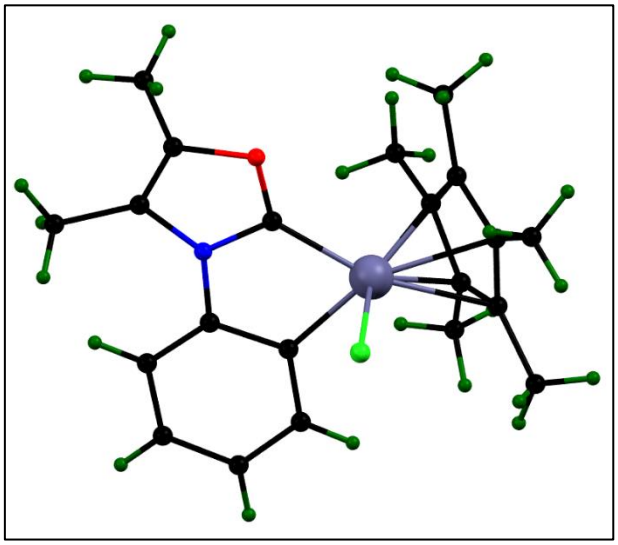

Figure S5: Molecular structure of **4** (50% probability level)

(c) Reaction catalyzed by Rh (III) complex 4

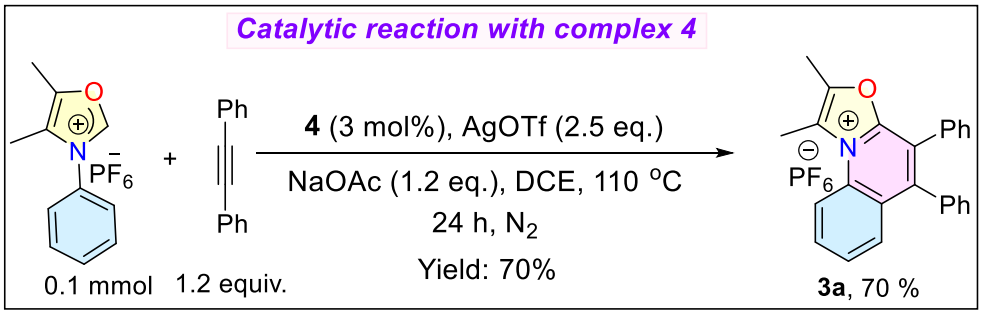

Scheme S9: Catalytic reaction with complex **4**

This chemical reaction took place in an oven-dried Schlenk tube that had been loaded with the following substances: compound **4** (2 mg, 3 mol%), AgOTf (64 mg, 2.5 mmol), and **1a** (0.1 mmol) and diphenyl acetylene (0.021 mmol). After being in a vacuum for five minutes, the tube was filled with N_2 gas. Using the Schlenk procedure, dry and degassed DCE (2.0 mL) were added to the mixture. The reaction mixture was then allowed to stir at 110 ^oC in the dark. The entire reaction mixture was run through a short *C*elite pad and rinsed with dichloromethane (40 ml). Under low pressure, the mixed filtrate was concentrated. The desired product (70% yield) was achieved by separating it by silica gel column chromatography and eluting as a $CHCl_3$/MeOH solvent mixture.

(d) Stoichiometric reaction of Rh (III) complex 4

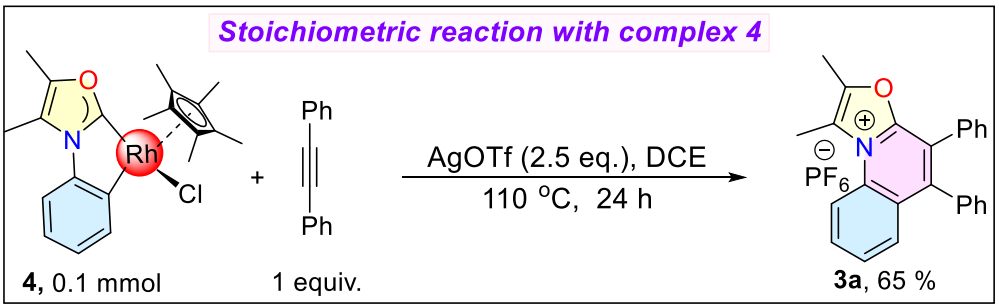

Scheme S10: Stoichiometric reaction with Rh (III) complex **4.**

In an oven-dried Schlenk tube, complex **4** (0.021 mmol) AgOTf (1.2 equivalent) and diphenyl acetylene (0.021 mmol) were added. Then the tube was vacuumed for 5 minutes and filled with N_2 gas. The mixture was then treated with dry and degassed DCM (2.0 mL) in an N_2 atmosphere and the reaction mixture was stirred for 24 hours at 110 °C under dark conditions. After 24 hours, the entire reaction mixture was passed through a short Celite pad and washed with dichloromethane (30 mL). The mixed filtrate was then concentrated under reduced pressure. The desired product (65% yield) was achieved by separating it by silica gel column chromatography and eluting as a $CHCl_3$/MeOH solvent mixture.

(e) Plausible reaction mechanism

We proposed the following catalytic cycle. In the presence of **1a**, NaOAc, and $[Cp^*RhIIICl_2]_2$, the five-membered cyclometalated complex **4** formed. Then, the alkyne coordinate occurs and generates intermediate **I** after halide abstraction from **4** by AgOTf. After that, the coordinated alkyne is inserted into the Rh–C_{aryl} bond of **I** to produce the seven-membered rhodacycle intermediate **I′**. Following reductive elimination from **I′**, the annulated product **3a** and a Cp*RhI species **I′′** are produced, which are oxidized by AgOTf to Cp*RhIII for additional C–H activation of **1a** to continue the catalytic cycle.

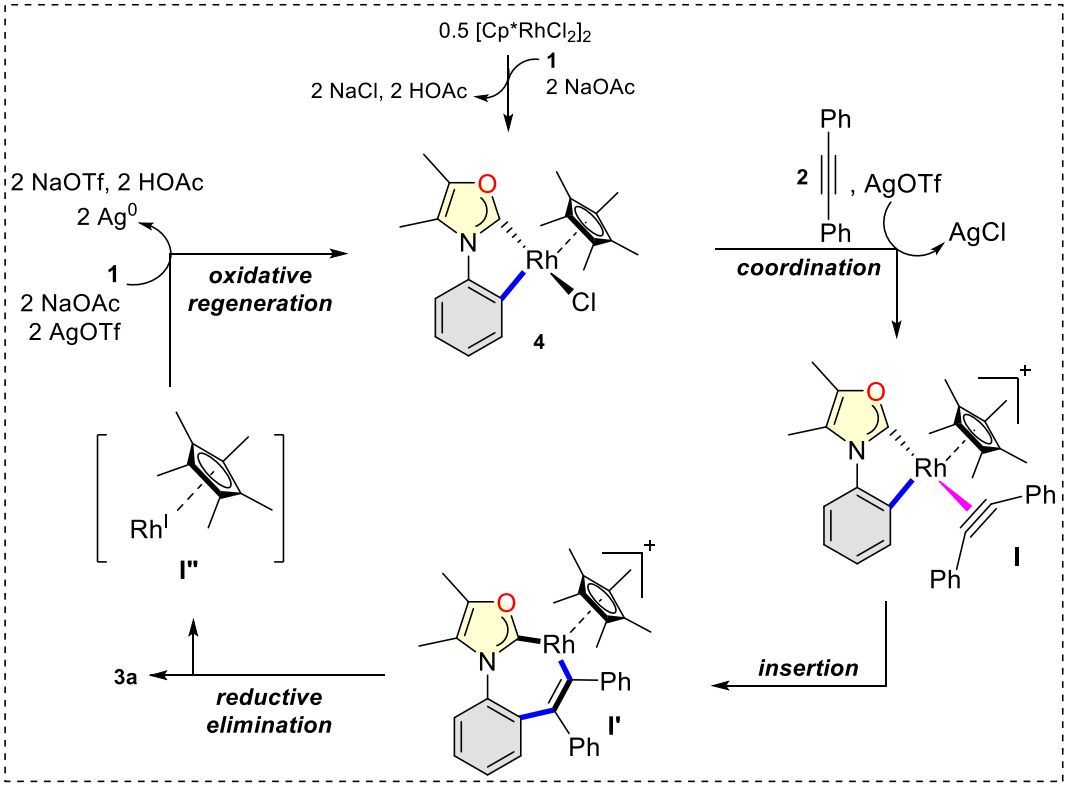

Scheme 11: Plusable reaction mechanism

10. Fluorescence and UV-visible studies

At room temperature, the UV-visible absorption spectra were obtained using a Cary 100 UV-Vis spectrophotometer and 1.0 cm quartz cuvettes. Fluorescence emission experiments were carried out with a Jobin Yvon Horiba Model Fluorolog-3-21. Sample solutions of 10 μM were introduced in 2 mL acetonitrile solution and the excitation wavelength was adjusted to 340 nm to record the emission spectra.

(a) Spectroscopic data of oxazolo[3,2-a]quinolin-based AIEgens in solution and solid state

Entry	λ_{abs}(nm)	Extinction coefficient ($M^{-1}cm^{-1}$)	λ_{em} (nm)	Stokes shift (nm)	Φ (%) solution	Φ (%) solid
3k	343	20856	445	102	5	15.29
3p	344	17495	463	119	4.6	18.25
3t	345	30937	473	128	6	26.39
3r	339	27555	428	89	3.7	5.12
3o	341	23891	439	98	-	-
3u	338	40216	430	92	-	-

Table S10: Spectroscopy data for selected cationic compounds in acetonitrile solution (10 μM). Extinction coefficient measure at lower energy transition.

(b) UV-Vis and emission spectra of selected oxazolo[3,2-a]quinolin-based AIEgens in solution

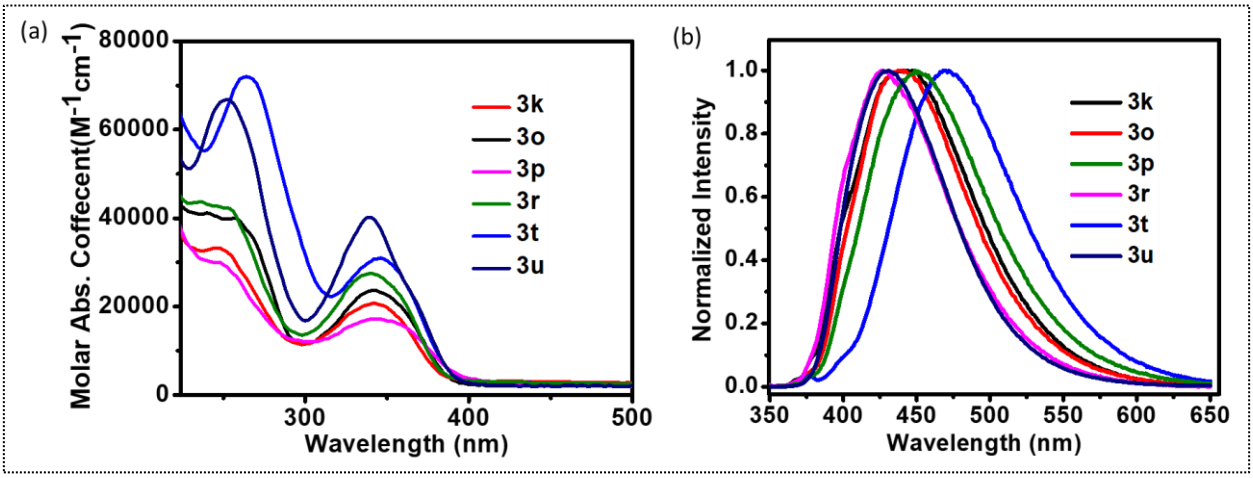

Figure S6: (a) UV-Vis and (b) emission spectra of selected cationic compounds in acetonitrile (10 μM).

(c) Aggregation-induced emission properties of 3p and 3r

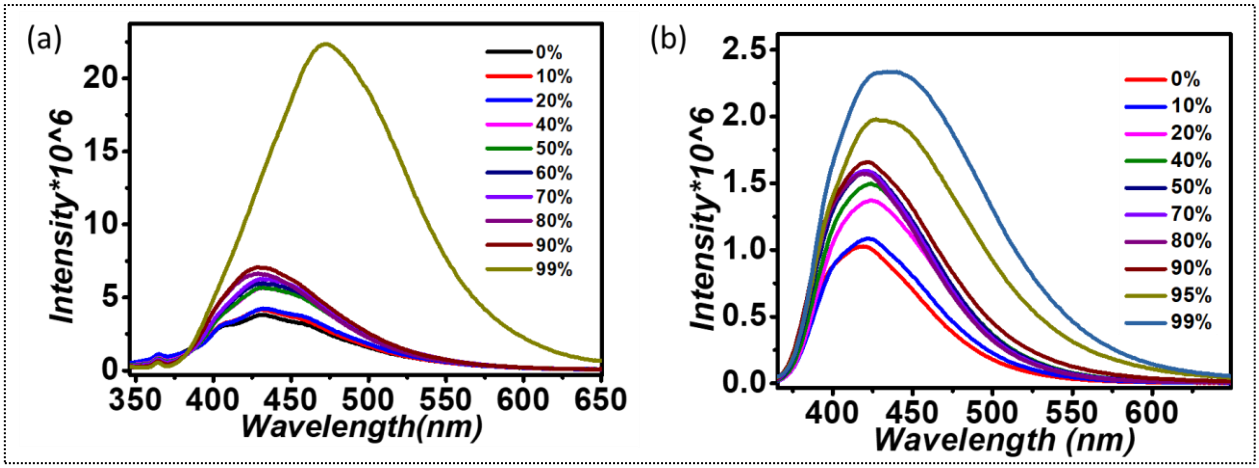

Figure S7: (a) and (b) AIE profile of **3p** and **3r** respectively, in various THF/hexane solvent mixtures.

11. Computational studies

For all of the theoretical studies, the software Gaussian 09 was used. Density functional theory (DFT) simulations were carried out using the 6-31G (d) basis set for H, C, and N atoms, as well as the B3LYP exchange-correlation functional. The optimized structure was determined for solvent phase simulations. Frequency calculations were performed to ensure that the optimized structures corresponded to genuine minima. The optimized ground state geometries were discovered to have no imaginary frequency. Images of the highest occupied molecular orbital (HOMO) and lowest unoccupied molecular orbital (LUMO) were acquired from the optimized geometry to investigate electronic distributions and the energy gap between them.

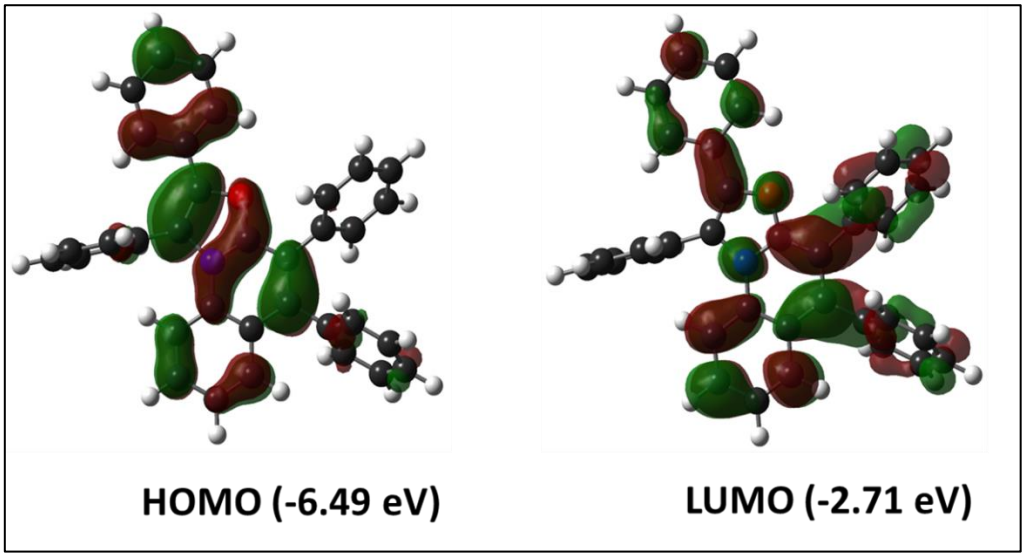

Figure S8: Kohn-Sham frontier orbital representation and MO energies of **3k**

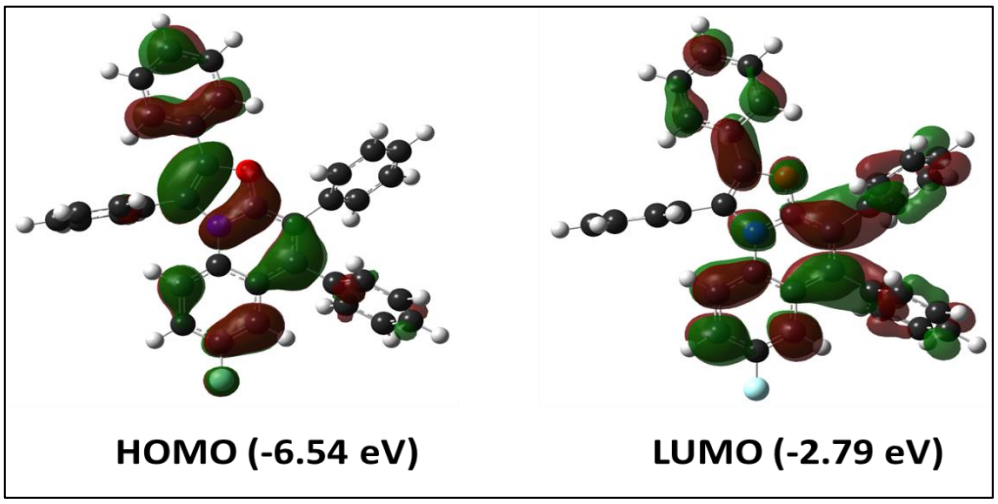

Figure S9: Kohn-Sham frontier orbital representation and MO energies of **3p**

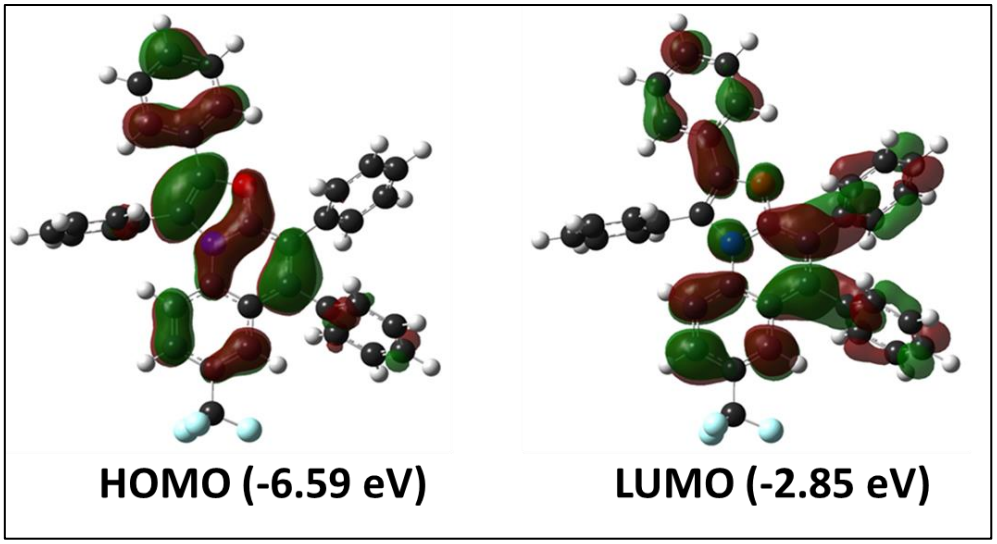

Figure S10: Kohn-Sham frontier orbital representation and MO energies of **3t**

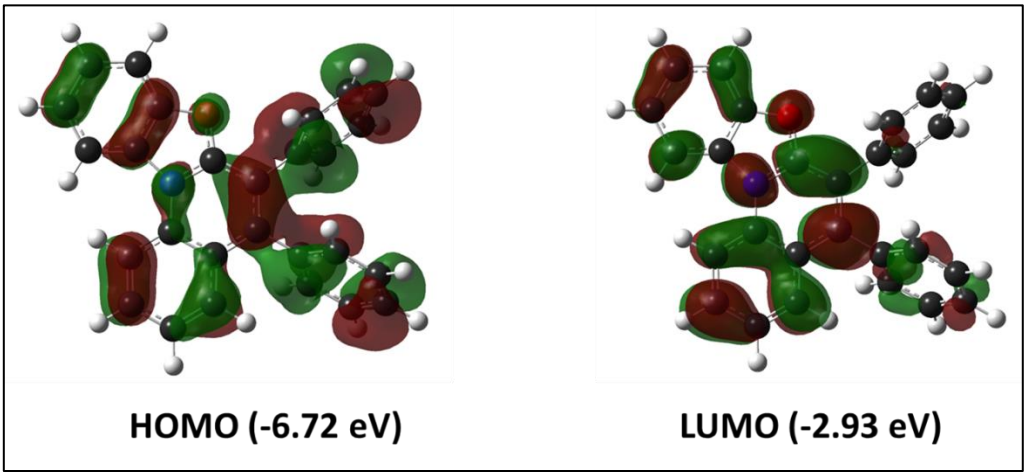

Figure S11: Kohn-Sham frontier orbital representation and MO energies of **3w**

Table S2: Energy of FMOs calculated at 6-31g(d,p) level of theory (CPCM, acetonitrile)

#	HOMO (eV)	LUMO (eV)	E_g
3k	-6.49	-2.71	3.78
3p	-6.54	-2.79	3.75
3t	-6.59	-2.85	3.74
3w	-6.72	-2.93	3.79

The x, y, and z coordinates for the optimized structures of **3k**, **3p**, **3t** and **3w** are as below.

3k

Symbolic Z-matrix:
Charge = 1 Multiplicity = 1

O	-1.7448	2.08102	-0.0548
N	-2.25022	-0.05401	-0.00686
C	0.13217	0.55247	0.01873
C	-1.24424	0.85034	0.00097
C	-1.95888	-1.42608	0.03609
C	0.46502	-0.79462	0.02575
C	-0.57953	-1.79411	0.05023
C	1.10018	1.687	-0.02069
C	-3.67502	0.58748	-0.08419
C	1.10474	2.6468	1.00259
H	0.41418	2.55212	1.83486
C	1.99689	1.82124	-1.09104
H	1.99236	1.08998	-1.89233
C	2.88899	2.89216	-1.12973
H	3.57687	2.98738	-1.96415
C	-3.23657	2.17178	-0.1125
C	1.89632	-1.21543	0.04093
C	2.89523	3.83931	-0.1032
C	-0.27401	-3.17656	0.12904
H	0.76491	-3.47643	0.16515
C	-2.96352	-2.40694	0.07923
H	-4.00605	-2.13632	0.07324
C	2.00157	3.71434	0.96228
H	2.00133	4.4465	1.76375
C	2.45449	-1.89142	-1.05547
H	1.84094	-2.10816	-1.92462
C	-2.616	-3.74473	0.13945
H	-3.40033	-4.49304	0.17355
C	-1.26686	-4.13317	0.16883
C	2.70031	-0.93551	1.15592

H	2.27523	-0.41644	2.00889
C	3.79667	-2.2717	-1.03797
H	4.21991	-2.78552	-1.89542
C	4.0383	-1.32856	1.17386
H	4.64892	-1.11332	2.04522
C	4.59018	-1.99381	0.07694
C	-5.27954	-0.08281	-0.14019
C	-6.17786	-0.39907	1.03687
C	-6.06422	-0.4695	-1.37561
C	-7.46392	-0.93693	0.99228
H	-5.71491	-0.1601	2.00527
C	-7.35104	-1.00661	-1.42044
H	-5.51262	-0.28539	-2.30887
C	-8.05088	-1.24048	-0.23677
H	-8.01558	-1.12155	1.92548
H	-7.81336	-1.24573	-2.38922
H	-9.06492	-1.6645	-0.27168
C	-4.10723	3.65286	-0.19046
C	-4.63233	4.47659	0.97425
C	-4.51601	4.41795	-1.43842
C	-5.33891	5.67742	0.91129
H	-4.40033	4.02545	1.9499
C	-5.22194	5.61965	-1.50154
H	-4.19181	3.92161	-2.36452
C	-5.63353	6.24936	-0.32697
H	-5.66364	6.17376	1.8373
H	-5.45398	6.07016	-2.47759
H	-6.19061	7.1962	-0.37637
H	-1.00789	-5.16958	0.2295
H	4.03964	3.7341	0.82862
H	4.82086	-1.04223	-1.28749

3p

Symbolic Z-matrix:
Charge = 1 Multiplicity = 1

O	0.70514	1.39098	-0.02782
N	0.61366	-0.79902	-0.05449
C	-1.51456	0.42976	-0.05023
C	-0.11044	0.34138	-0.05851
C	-0.03815	-2.04305	-0.07508
C	-2.20048	-0.77725	-0.03902
C	-1.46589	-2.02211	-0.06815
C	-2.13528	1.78566	0.00102

C	1.99195	-0.43333	-0.01647
C	-1.90692	2.70878	-1.03062
H	-1.29569	2.42742	-1.8826
C	-2.92838	2.16181	1.09516
H	-3.10043	1.45837	1.90293
C	-3.49069	3.43662	1.14986
H	-4.10077	3.71758	2.0027
C	2.01012	0.932	-0.0023
C	-3.69195	-0.7922	-0.02632
C	-3.26663	4.34859	0.11604
C	-2.13585	-3.27061	-0.12765
H	-3.21756	-3.27776	-0.14886
C	0.66444	-3.2588	-0.11445
H	1.74212	-3.27129	-0.12038
C	-2.47413	3.98208	-0.97352
H	-2.29691	4.6853	-1.78126
C	-4.393	-1.29231	1.08244
H	-3.8458	-1.66974	1.94085
C	-0.03483	-4.45188	-0.15413
H	0.51598	-5.38574	-0.18581
C	-1.43936	-4.46046	-0.16613
C	-4.40953	-0.29942	-1.12655
H	-3.87477	0.08561	-1.98879
C	-5.78804	-1.29056	1.0912
H	-6.31957	-1.67064	1.95799
C	-5.80399	-0.3114	-1.11826
H	-6.34877	0.0651	-1.97843
C	-6.49601	-0.80321	-0.00934
C	3.13382	-1.37405	0.01382
C	3.74043	-1.78511	-1.18362
C	3.63515	-1.83036	1.24317
C	4.83031	-2.65456	-1.14847
H	3.35617	-1.42529	-2.13259
C	4.72534	-2.69972	1.2701
H	3.1701	-1.5052	2.16823
C	5.32146	-3.11335	0.0763
H	5.29567	-2.97105	-2.07633
H	5.10928	-3.05128	2.2223
H	6.17012	-3.78971	0.10052
C	3.0436	1.96206	0.0326
C	4.41215	1.63674	0.07896
C	2.66127	3.3174	0.01987
C	5.36916	2.64718	0.11149
H	4.73039	0.60275	0.09013
C	3.62714	4.31918	0.05309

H	1.61158	3.58369	-0.01701
C	4.98339	3.98955	0.0989
H	6.42105	2.38256	0.14713
H	3.31782	5.35936	0.04274
H	5.73445	4.77272	0.12447
H	-3.70606	5.34035	0.16028
H	-7.58158	-0.80679	-0.00288
F	-2.10896	-5.63127	-0.22387

3t

Symbolic Z-matrix:
Charge = 1 Multiplicity = 1

O	1.83077	1.40367	-0.0491
F	-4.08833	-4.28306	-1.33914
F	-4.04385	-4.55069	0.81558
F	-5.1436	-2.87831	-0.05034
N	0.73576	-0.49502	-0.02477
C	2.70439	-2.17241	0.05716
C	2.7789	0.39432	-0.00766
C	2.12992	-0.80938	0.00829
C	4.16951	0.83092	0.01035
C	6.54624	0.36427	0.10885
H	7.35758	-0.35338	0.17346
C	5.23152	-0.08975	0.09316
H	5.03484	-1.15237	0.14736
C	6.82379	1.73138	0.04355
H	7.85188	2.07886	0.05647
C	-0.49911	3.07341	-0.02536
C	-1.02785	3.80222	1.0498
H	-1.51496	3.2819	1.86775
C	4.4563	2.20873	-0.0537
H	3.64847	2.92859	-0.11545
C	2.9296	-2.7993	1.29342
H	2.66683	-2.28717	2.214
C	5.77531	2.64976	-0.03715
H	5.98431	3.71337	-0.08688
C	-1.67245	-0.61308	-0.00775
C	-2.77636	-2.78492	-0.08594
C	3.05974	-2.83024	-1.13144
H	2.89739	-2.34209	-2.08751
C	-3.08223	1.50236	0.04966
C	-0.58268	1.58427	-0.04419
C	-0.30424	5.86762	0.02018

H	-0.23155	6.95045	0.03748
C	0.13424	3.75742	-1.0741
H	0.54305	3.20361	-1.91431
C	0.61983	0.8533	-0.05654
C	3.83762	-4.72759	0.15065
H	4.27735	-5.71923	0.18691
C	-0.3593	-2.69921	-0.04605
H	0.59062	-3.2091	-0.05271
C	-3.49503	2.32375	-1.01087
H	-2.84359	2.46875	-1.86645
C	-0.41828	-1.29347	-0.02092
C	-2.84466	-1.40964	-0.05779
H	-3.80925	-0.92228	-0.08133
C	3.4931	-4.07418	1.33621
H	3.66654	-4.55425	2.29388
C	-1.52748	-3.43315	-0.07138
H	-1.47959	-4.51653	-0.0892
C	-4.03035	-3.62476	-0.16436
C	-0.92811	5.19193	1.07053
H	-1.33764	5.74674	1.90862
C	-1.75316	0.83256	0.00693
C	3.62283	-4.10505	-1.08121
H	3.89676	-4.60926	-2.00229
C	-4.74151	2.94518	-0.97255
H	-5.05584	3.56843	-1.80358
C	-3.93523	1.32457	1.1519
H	-3.62158	0.70003	1.9834
C	0.22528	5.14853	-1.05244
H	0.70668	5.66904	-1.87433
C	-5.58135	2.76947	0.12887
H	-6.54931	3.25949	0.15807
C	-5.17424	1.96254	1.1926
H	-5.82052	1.82646	2.05382

3w

Symbolic Z-matrix:

Charge = 1 Multiplicity = 1

O	5.2565	-0.9303	10.12
N	5.3263	1.1144	9.2326
C	5.0951	0.9423	11.6738
C	5.0564	0.0164	12.846
C	5.0969	2.3084	11.7684
C	5.1913	0.3929	10.3794

C	5.1067	4.667	8.2329
H	5.1204	5.2047	7.448
C	4.9835	5.2772	9.474
H	4.8991	6.2212	9.5256
C	5.1823	2.9895	13.0956
C	4.0791	3.2103	13.9235
H	3.2241	2.8952	13.655
C	5.0935	3.1214	10.5635
C	5.2108	2.5188	9.2915
C	5.2106	3.3007	8.1159
H	5.2809	2.8931	7.2604
C	5.443	4.34	15.5518
H	5.5346	4.7989	16.3798
C	6.2232	-0.6311	13.2815
H	7.0316	-0.5233	12.7926
C	4.9819	4.5295	10.6272
H	4.9049	4.9614	11.4707
C	5.5271	0.1973	8.1589
C	3.8809	-0.1597	13.5758
H	3.0798	0.262	13.2901
C	4.2092	3.8824	15.1301
H	3.4425	4.0302	15.6706
C	6.4311	3.4524	13.5224
H	7.2	3.3167	12.982
C	6.2061	-1.4209	14.4141
H	6.9989	-1.8598	14.6998
C	3.8759	-0.9536	14.7222
H	3.0723	-1.0635	15.2179
C	5.4493	-1.0645	8.739
C	6.5435	4.1123	14.7411
H	7.3974	4.4164	15.0234
C	5.8104	0.3097	6.7922
H	5.907	1.1562	6.3722
C	5.0249	-1.5765	15.1387
H	5.0154	-2.1137	15.9219
C	5.5532	-2.2522	8.0401
H	5.462	-3.0992	8.4619
C	5.8017	-2.1253	6.6769
H	5.8742	-2.9061	6.1416
C	5.944	-0.8744	6.0813
H	6.1407	-0.8285	5.1518

12. Cyclic voltammetric studies and measurements

Cyclic voltammetry (CV) and differential pulse voltammetry (DPV) experiments were performed on three-electrode systems, where Pt disk (1.0 mm diameter) acts as a working electrode, Pt wire as a counter electrode, and Ag/AgCl as a reference electrode. The experiments were carried out in dry acetonitrile after proper degassing with nitrogen gas. 0.1 M solution of $[Bu_4N^+]$ PF_6^- in dry acetonitrile was used as a supporting electrolyte. Ferrocene ($E_{1/2}$, Fc^+/Fc = 0.44 V as Ag/AgCl) was used as an external calibration standard for all the measurements. The scan rate of 100 mV/s was used for all the experiments.

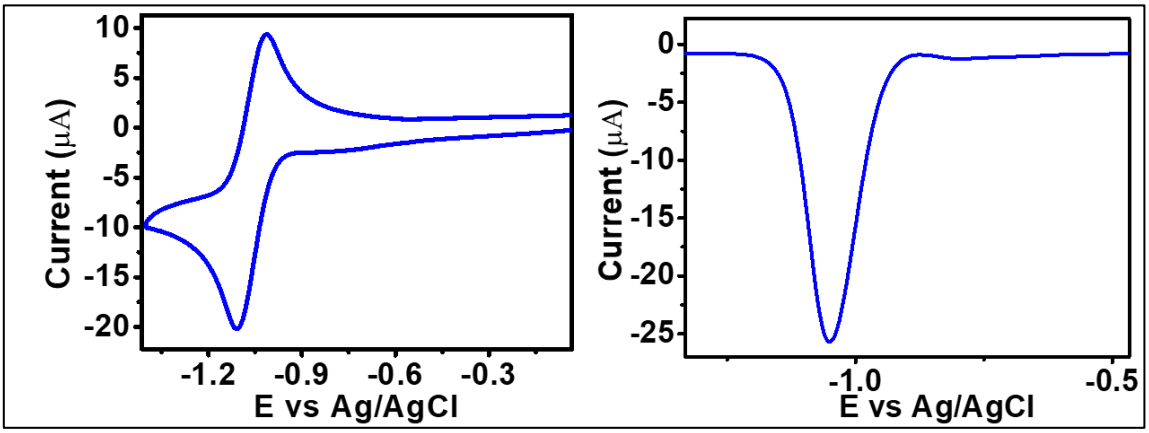

Figure S12: Cyclic voltammogram and DPV measured of **3k** in DCM with 0.1 M $^nBu_4NPF_6$ with a scan rate of 100 mV/s.

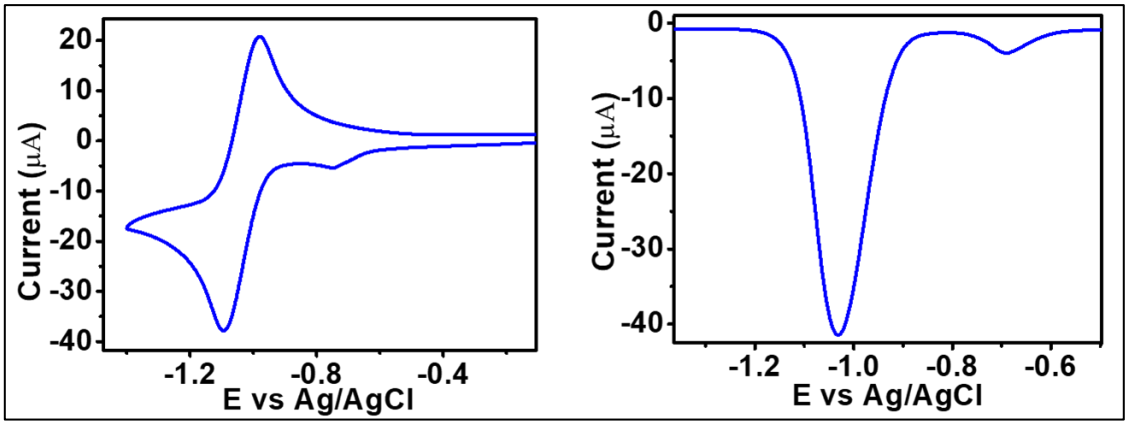

Figure S13: Cyclic voltammogram and DPV measured of **3p** in DCM with 0.1 M $^nBu_4NPF_6$ with a scan rate of 100 mV/s.

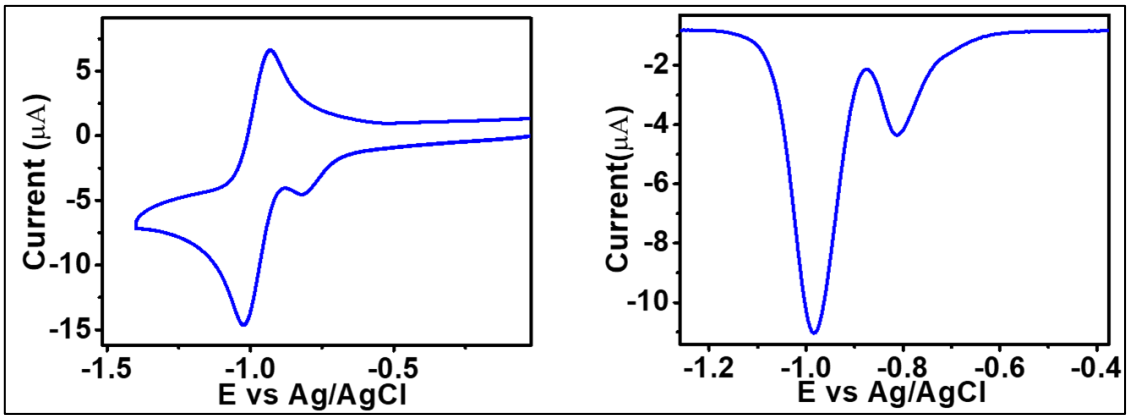

Figure S14: Cyclic voltammogram and DPV measured **3t** in DCM with 0.1 M $^{n}Bu_4NPF_6$ with a scan rate of 100 mV/s.

13. Generation and analysis of the $3t^R$ radical species

(A) Generation of $3t^R$ radical species

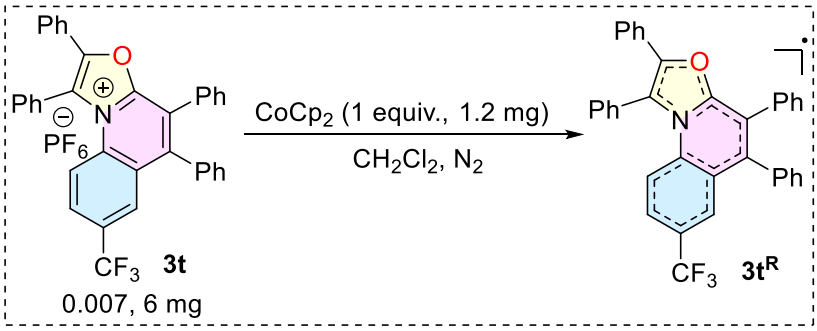

Scheme S12: Synthetic scheme for generation $\mathbf{3t^R}$ radical

The experiment was carried out inside the glove box. The compound **3t** (6 mg, 0.007 mmol) and cobaltocene (1.2 mg, 0.008 mmol) were loaded in a 5 mL vial. Then dry 2.0 mL dichloromethane was added to the vial and the reaction mixture was stirred at room temperature for one minute. The color change was observed from colorless to yellowish. After that 20 μL of the reaction mixture was transferred to a quartz cuvette by taking 2 mL dichloromethane and the absorption spectra were recorded, along with the appearance of a broad absorption band in the visible region with maxima (λ_{max}) at 426 nm (for $\mathbf{3t^R}$).

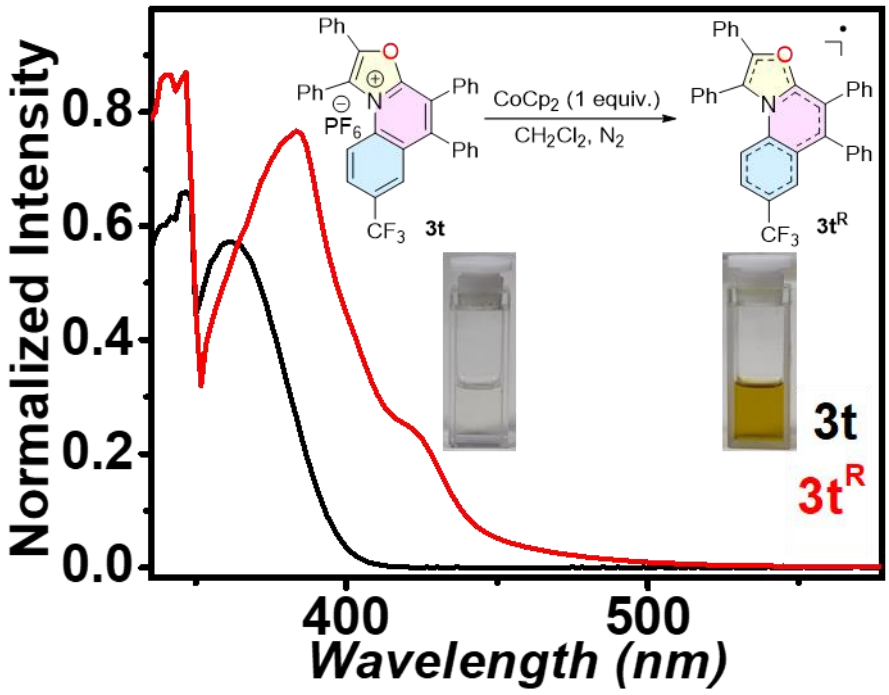

Figure S15: UV-Vis spectra of **3t^{R}** in dichloromethane (DCM) at room temperature

(B) Analysis of the 3t^{R} radical species

The compound **3t** (6 mg, 0.007 mmol, 1 equiv.) and cobaltocene (1.2 mg, 0.008 mmol, 1.0 equiv.) were taken in an EPR tube under inert condition (inside glovebox) and then 0.7 mL dry CH_2Cl_2 was added to it. Then the brown solution was immediately subjected to electron paramagnetic resonance (EPR) spectroscopic analysis at 120 K.

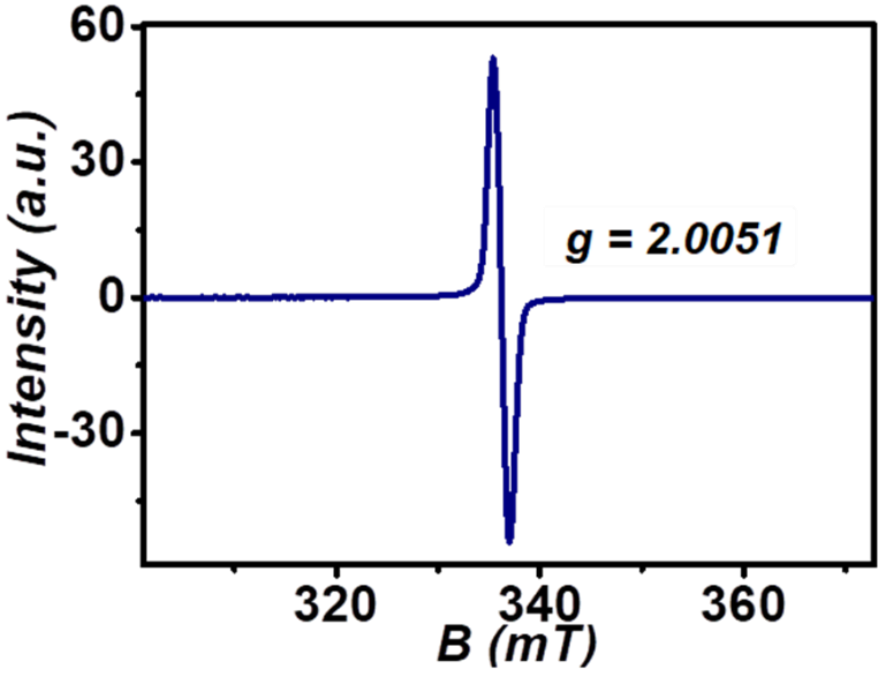

Figure S16: EPR spectrum of the radical **3t^{R}** in dry CH_2Cl_2.

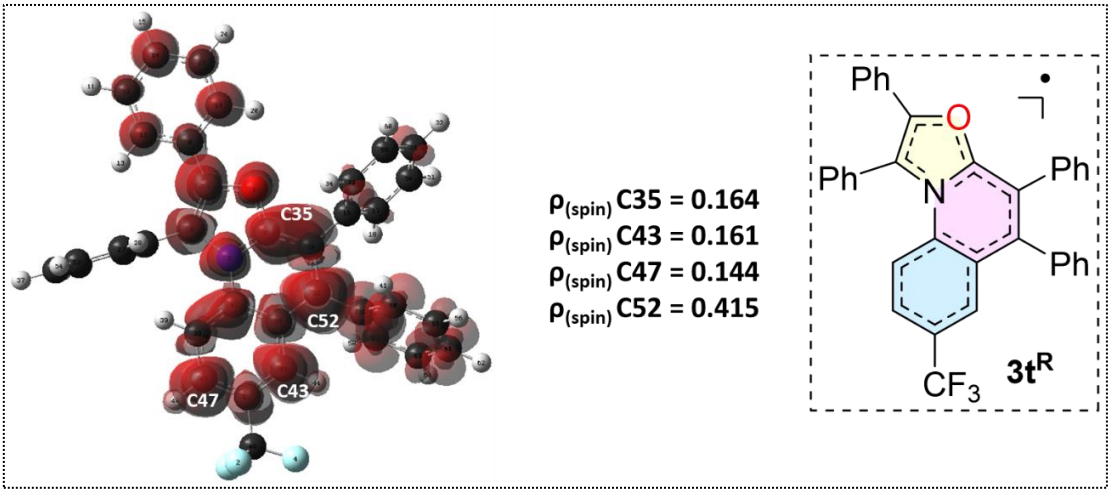

Figure S17: Spin density plot of the proposed radical **3t^{R}** at ub3lyp/6-31g(d,p)level of theory.
*Note: The calculated spin density ($\rho_{(spin)}$) was largely distributed over C35, C43, C47, and C52 atoms of **3t^{R}**.*

Note: *All of these cationic compounds exhibit a highly reversible single-electron reduction process within a mild potential range of −0.9 V to −1.1 V vs Ag/AgCl. For this reason, the one-electron chemical reduction of **3t** by cobaltocene ($CoCp_2$; $E_{1/2}$ = –1.33 V vs Fc^{+}/Fc) produced the radical species **3t^{R}**, causing the solution to change from colorless to yellowish, accompanied by a broad absorption band at 426 nm in the visible region. The Electron Paramagnetic Resonance (EPR) spectra of the yellowish solution confirmed the presence of the **3t^{R}** radical with an isotropic g value of 2.0051. We did not observe significant coupling in the EPR with nearby nitrogen and oxygen atoms in the EPR spectra, indicating extensive electron delocalization of the single electron. The calculated spin density was distributed over the backbone and largely distributed over C35, C43, C47, and C52 of **3t^{R}**.*

14. Single Crystal X-Ray data analysis

Table S3: Crystal data and structure refinement for **3k**

Identification code	2365213
Empirical formula	$C_{35}H_{24}F_6NOP$
Formula weight	619.52
Temperature/K	140.00
Crystal system	monoclinic
Space group	$P2_1/c$
a/Å	13.9378(6)
b/Å	9.0106(4)
c/Å	22.5804(10)
α/°	90
β/°	98.884(2)
γ/°	90

Volume/Å^3	2801.8(2)
Z	4
ρ_{calc}g/cm^3	1.469
μ/mm^{-1}	1.500
F(000)	1272.0
Crystal size/mm^3	0.31 × 0.21 × 0.08
Radiation	CuKα (λ = 1.54178)
2Θ range for data collection/°	6.418 to 148.982
Index ranges	-17 ≤ h ≤ 17, -11 ≤ k ≤ 11, -27 ≤ l ≤ 28
Reflections collected	42104
Independent reflections	5542 [R_{int} = 0.0509, R_{sigma} = 0.0282]
Data/restraints/parameters	5542/0/397
Goodness-of-fit on F^2	1.033
Final R indexes [I>=2σ (I)]	R_1 = 0.0389, wR_2 = 0.0948
Final R indexes [all data]	R_1 = 0.0428, wR_2 = 0.0972
Largest diff. peak/hole / e Å^{-3}	0.39/-0.25

Table S4: Crystal data and structure refinement for **3t**

Identification code	2365214
Empirical formula	$C_{36.5}H_{24}ClF_9NOP$
Formula weight	729.99
Temperature/K	140.0
Crystal system	monoclinic
Space group	$P2_1/c$
a/Å	14.5509(16)
b/Å	15.3261(17)
c/Å	15.5887(17)
α/°	90
β/°	109.068(4)
γ/°	90
Volume/Å^3	3285.7(6)
Z	4
ρ_{calc}g/cm^3	1.476
μ/mm^{-1}	0.248
F(000)	1484.0
Crystal size/mm^3	0.27 × 0.15 × 0.07
Radiation	MoKα (λ = 0.71073)
2Θ range for data collection/°	4.258 to 60.104
Index ranges	-20 ≤ h ≤ 20, -21 ≤ k ≤ 21, -21 ≤ l ≤ 21
Reflections collected	90788
Independent reflections	9571 [R_{int} = 0.1743, R_{sigma} = 0.1090]
Data/restraints/parameters	9571/0/433
Goodness-of-fit on F^2	1.008
Final R indexes [I>=2σ (I)]	R_1 = 0.0603, wR_2 = 0.1493
Final R indexes [all data]	R_1 = 0.1260, wR_2 = 0.1896
Largest diff. peak/hole / e Å^{-3}	0.41/-0.45

Table S6: Crystal data and structure refinement for **3c**

Identification code	2365215
Empirical formula	$C_{54.1}H_{46.9}F_{12}N_2O_4P_2$
Formula weight	1078.97
Temperature/K	140.00
Crystal system	tetragonal
Space group	$I4_1/a$
a/Å	32.0534(18)
b/Å	32.0534(18)
c/Å	19.7407(19)
α/°	90
β/°	90
γ/°	90
Volume/Å^3	20282(3)
Z	16
ρ_{calc}g/cm^3	1.413
μ/mm^{-1}	0.178
F(000)	8888.0
Crystal size/mm^3	0.22 × 0.18 × 0.05
Radiation	MoKα (λ = 0.71073)
2Θ range for data collection/°	3.512 to 50.23
Index ranges	$-38 \leq h \leq 37$, $-37 \leq k \leq 38$, $-23 \leq l \leq 23$
Reflections collected	53681
Independent reflections	9001 [R_{int} = 0.1796, R_{sigma} = 0.1203]
Data/restraints/parameters	9001/44/683
Goodness-of-fit on F^2	1.019
Final R indexes [I>=2σ (I)]	R_1 = 0.0793, wR_2 = 0.1963
Final R indexes [all data]	R_1 = 0.1544, wR_2 = 0.2538
Largest diff. peak/hole / e Å^{-3}	0.95/-0.55

Table S8: Crystal data and structure refinement for **3w**

Identification code	2365211
Empirical formula	$C_{56}H_{36}F_6N_2O_8S_2$
Formula weight	1042.99
Temperature/K	140.0
Crystal system	triclinic
Space group	P-1
a/Å	8.064(9)
b/Å	17.31(3)
c/Å	18.08(3)
α/°	105.90(6)
β/°	96.56(4)
γ/°	94.52(3)
Volume/Å^3	2395(6)
Z	2
ρ_{calc}g/cm^3	1.446
μ/mm^{-1}	0.195
F(000)	1072.0

Crystal size/mm^3	0.22 × 0.13 × 0.07
Radiation	MoKα (λ = 0.71073)
2Θ range for data collection/°	4.734 to 52.516
Index ranges	-10 ≤ h ≤ 10, -21 ≤ k ≤ 21, -22 ≤ l ≤ 22
Reflections collected	27176
Independent reflections	9594 [R_{int} = 0.1257, R_{sigma} = 0.1547]
Data/restraints/parameters	9594/0/667
Goodness-of-fit on F^2	0.997
Final R indexes [I>=2σ (I)]	R_1 = 0.0697, wR_2 = 0.1363
Final R indexes [all data]	R_1 = 0.1487, wR_2 = 0.1753
Largest diff. peak/hole / e Å^{-3}	0.33/-0.34

Table S9: Crystal data and structure refinement for **4**

Identification code	2365212
Empirical formula	$C_{21}H_{25}ClNORh$
Formula weight	445.78
Temperature/K	140.0
Crystal system	monoclinic
Space group	$P2_1/n$
a/Å	8.8209(14)
b/Å	15.115(2)
c/Å	14.830(2)
α/°	90
β/°	93.286(7)
γ/°	90
Volume/Å^3	1974.1(5)
Z	4
ρ_{calc}g/cm^3	1.500
μ/mm^{-1}	1.009
F(000)	912.0
Crystal size/mm^3	0.28 × 0.12 × 0.08
Radiation	MoKα (λ = 0.71073)
2Θ range for data collection/°	6.128 to 60.142
Index ranges	-12 ≤ h ≤ 12, -21 ≤ k ≤ 21, -20 ≤ l ≤ 20
Reflections collected	44500
Independent reflections	5752 [R_{int} = 0.0979, R_{sigma} = 0.0534]
Data/restraints/parameters	5752/15/252
Goodness-of-fit on F^2	1.140
Final R indexes [I>=2σ (I)]	R_1 = 0.0724, wR_2 = 0.1535
Final R indexes [all data]	R_1 = 0.0865, wR_2 = 0.1601
Largest diff. peak/hole / e Å^{-3}	1.41/-1.55

Crystal packing arrangements and non-covalent interactions of the cationic compounds

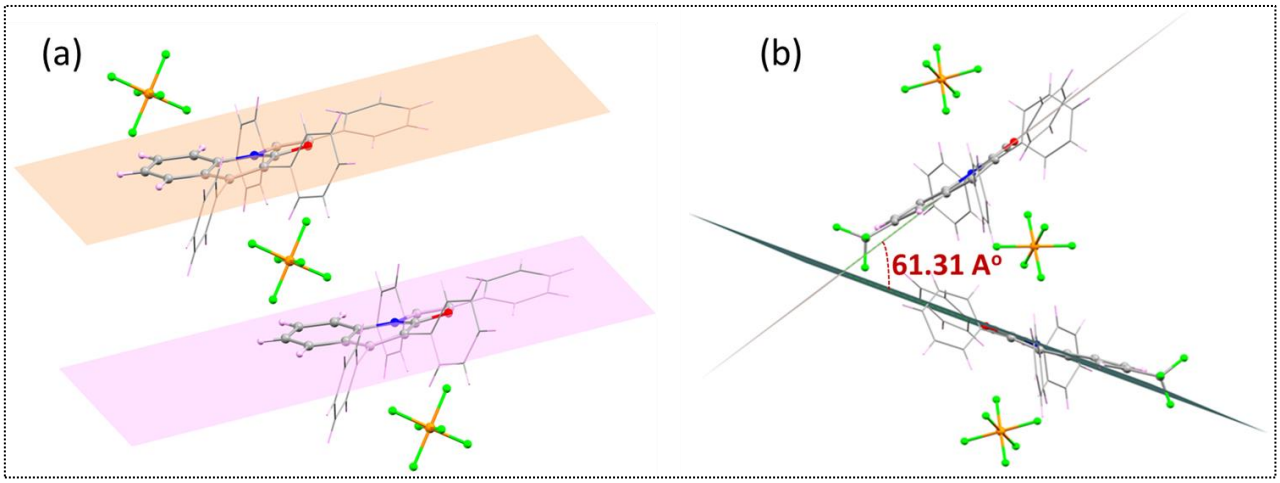

Figure S18: (a) Represents the parallel crystal packing arrangement in the presence of PF_6 anions anion of **3k**. (b) Represents crystal packing arrangement in the presence of PF_6 anions, showing the flanking PF_6 anions forced the vertically positioned oxazolium cores to deviate significantly from the parallel arrangement between the two molecules forming the dihedral angle of the **3t**.

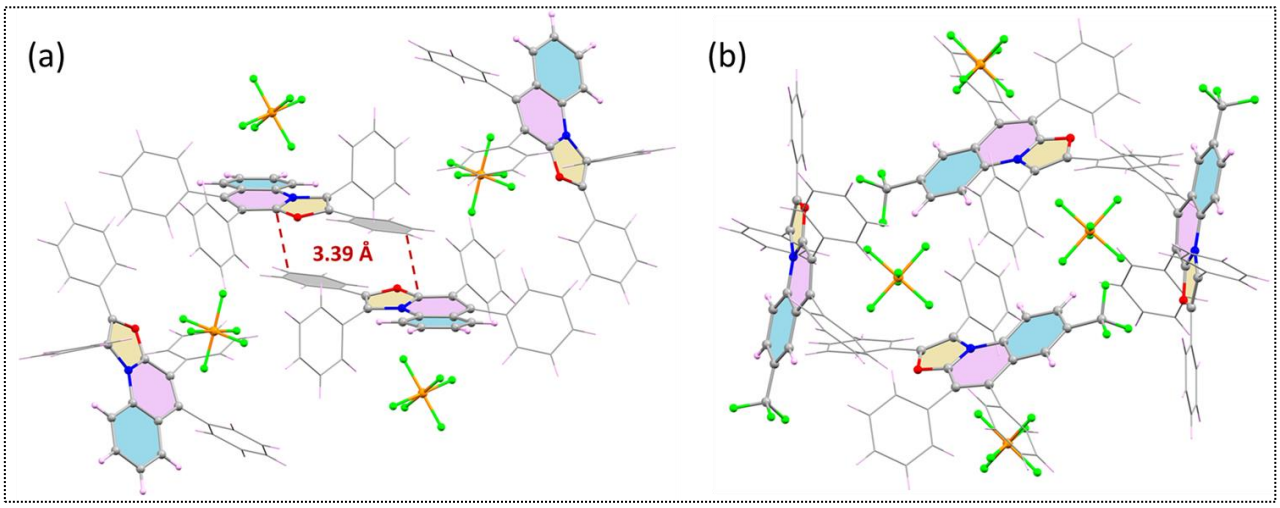

Figure S19: (a) Represents intermolecular non-covalent interaction in the crystal packing of **3k**, showing strong intermolecular π··π interaction with the neighboring molecules. (b) Represents negligible intermolecular π··π interaction with the neighboring molecules.

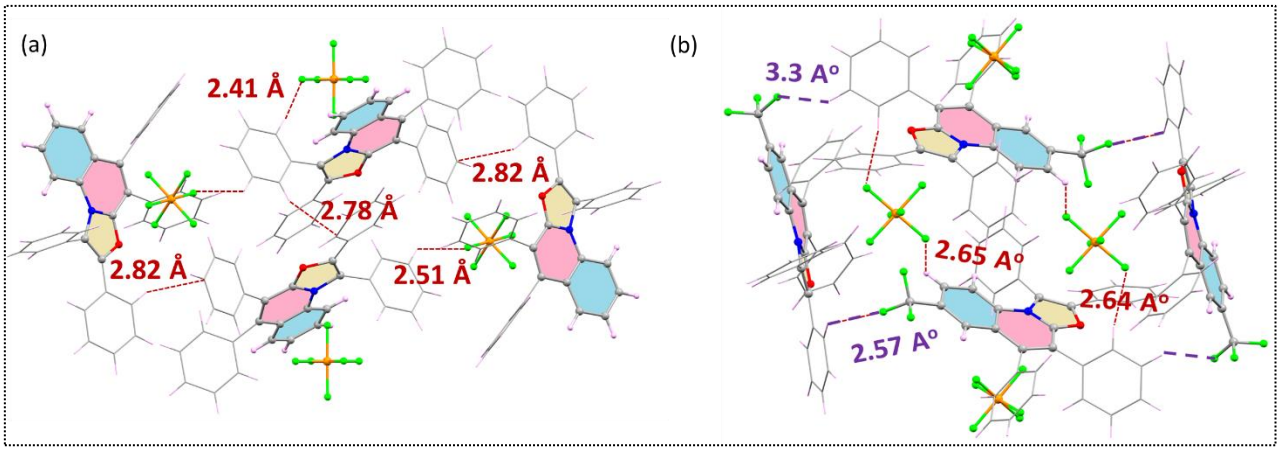

Figure S20: (a) Represent the non-covalent C···C−H, anion···C–H interaction of **3k** and (b) Represent the non-covalent C···C−H, anion···C–H and F···C–H interactions between the fluorine atoms of hexafluorophosphate anion with the phenyl ring.

*Note: In the crystal packing of both molecules, multiple noncovalent interactions are observed, including C···C−H, F···C–H, C−H···π, and anion···C–H/π interactions. The peripheral phenyl rings in both compounds engage in strong intermolecular C···C−H and F···C–H interactions with neighboring phenyl rings, effectively preventing the rotation of the phenyl rings within the molecule. Similarly, the counter anions strongly interact with the phenyl rings, further restricting their rotation. These interactions reduce non-radiative pathways by decreasing the efficiencies of internal conversion and vibrational relaxation. However, the crystal packing structure reveals distinct arrangements for the **3k** and **3t** compounds. The **3k** compound displays strong intermolecular π···π interactions with distances around 3.39 Å, which facilitates non-radiative pathways by transferring energy to neighboring molecules in the aggregated state, resulting in reduced emissive properties in the solid state.*[S4, S5 ,S6]

15. Powder XRD data analysis

Microcrystals of **3t** were obtained through the slow evaporation of its dichloromethane (DCM) solution. The aggregates of **3t** were obtained by filtration of its suspension in a THF/hexane mixture (5/95%). The PXRD pattern of the microcrystals showed multiple sharp and intense diffraction peaks which closely matched with the XRD spectrum of the aggregates, suggesting a similar packing microcrystals and aggregates state.

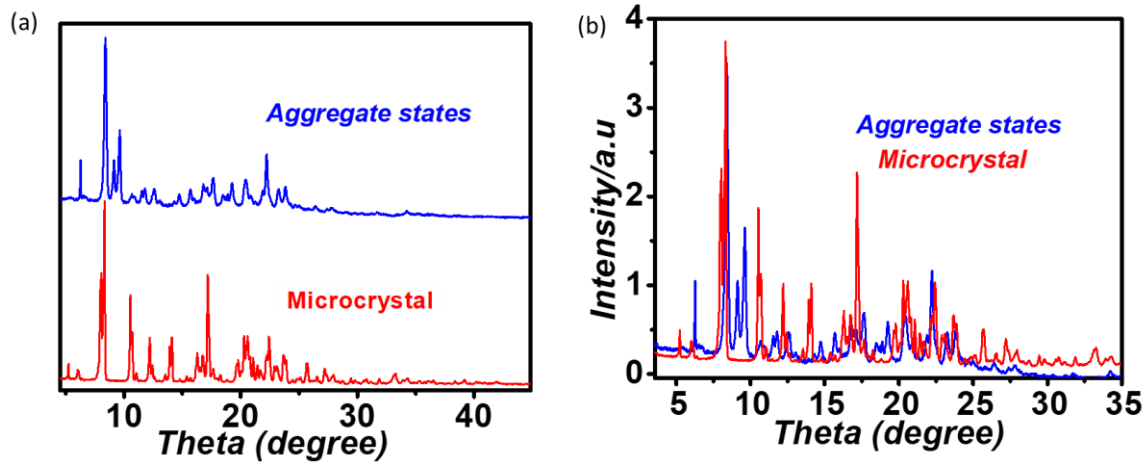

Figure S21: Powder XRD spectrum of single crystals (micro crystals) of **3t** and its aggregate states in THF/hexane mixture with a hexane fraction of 95%.

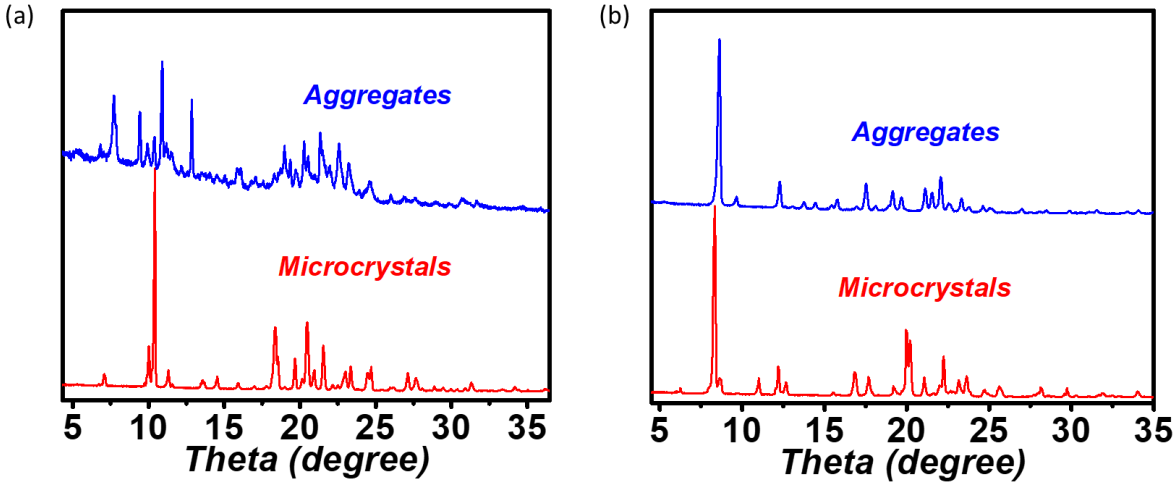

Figure S22: (a) Powder XRD spectrum of microcrystals of **3k** and its aggregate states in THF/hexane mixture with a hexane fraction of 95%. (b) Powder XRD spectrum of microcrystals of **3r** and its aggregate states in THF/hexane mixture with a hexane fraction of 95%.

16. Spectral data for compounds 1a-1n

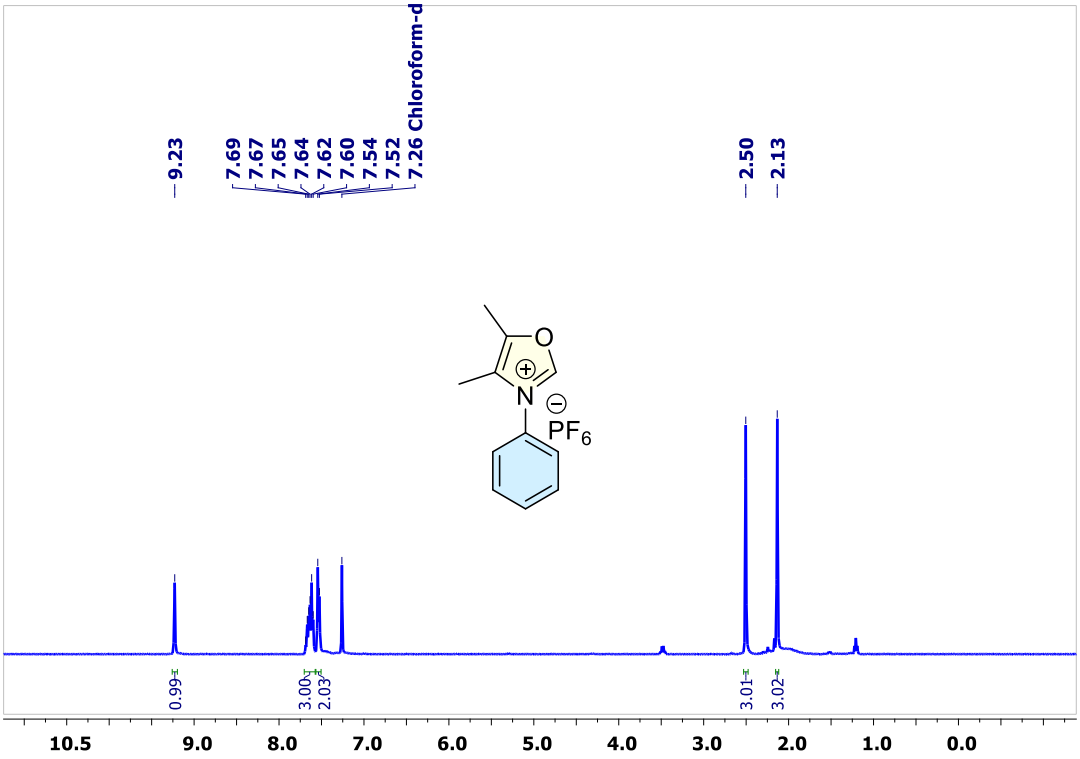

^{1}H NMR spectrum of **1a** (400 MHz, $CDCl_3$)

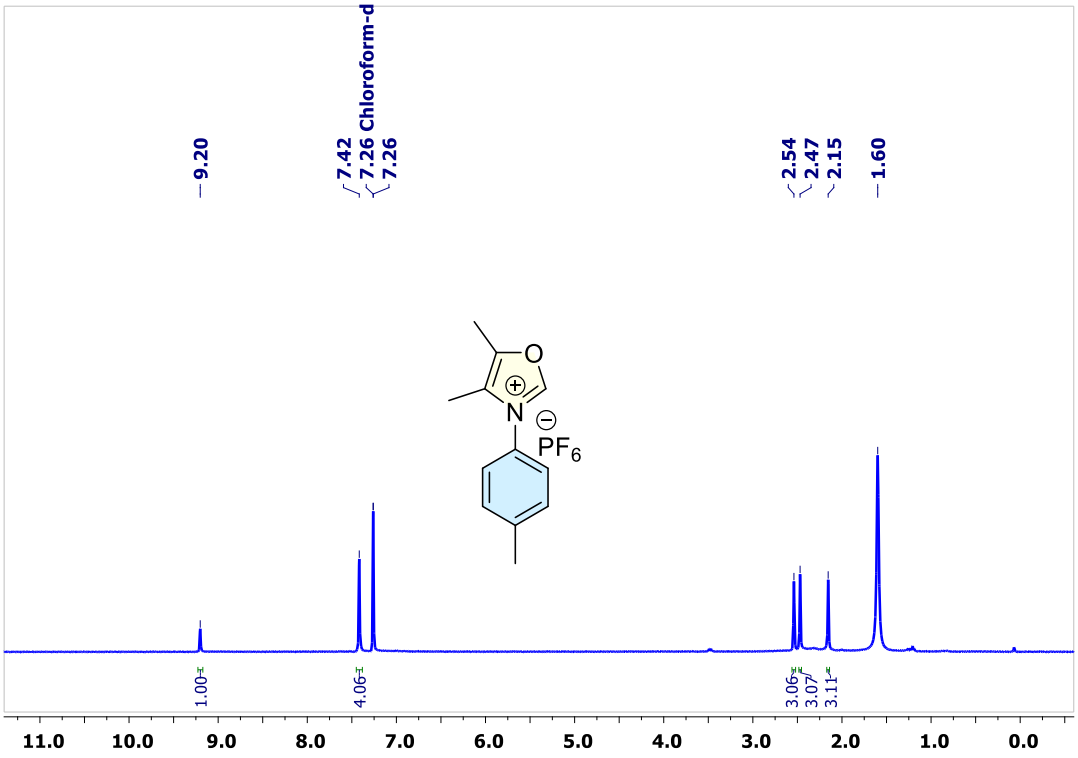

^{1}H NMR spectrum of **1b** (400 MHz, $CDCl_3$)

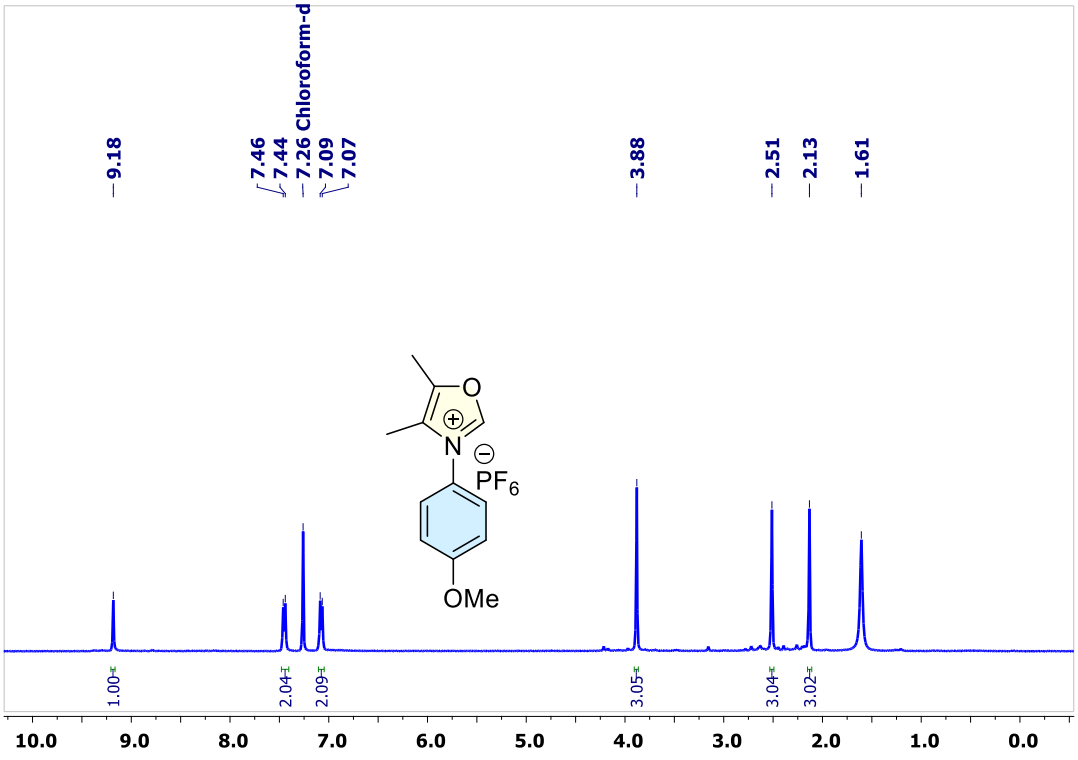

^{1}H NMR spectrum of **1c** (400 MHz, $CDCl_3$)

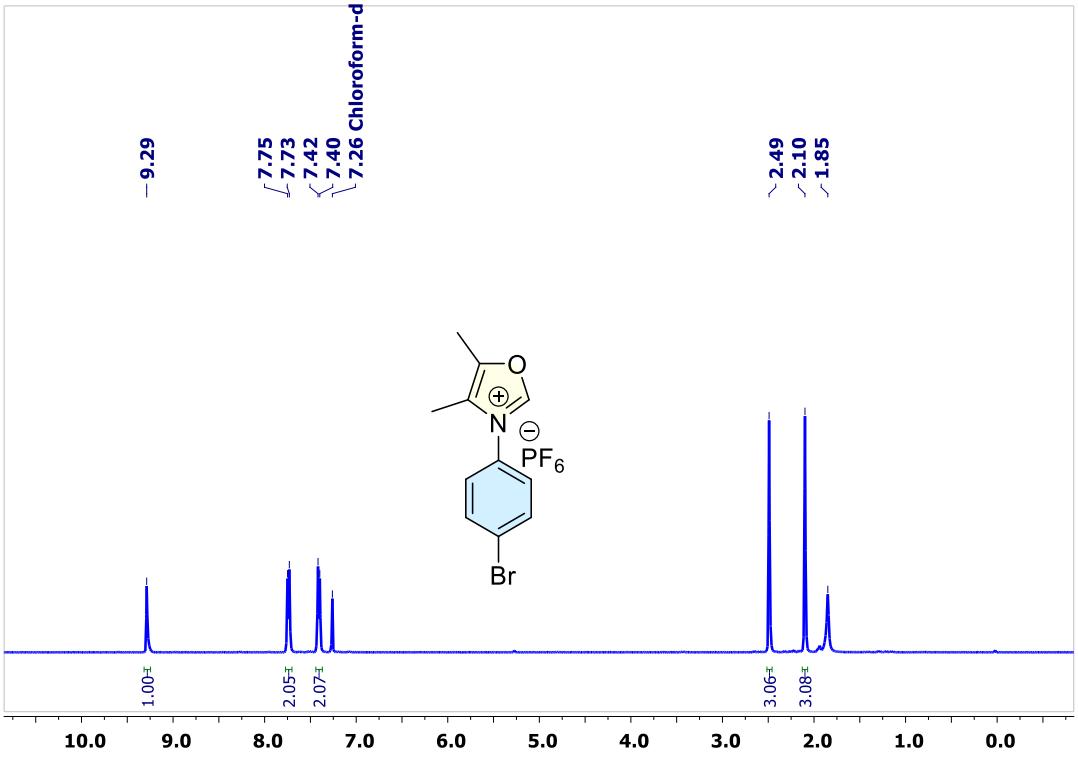

^{1}H NMR spectrum of **1d** (400 MHz, $CDCl_3$)

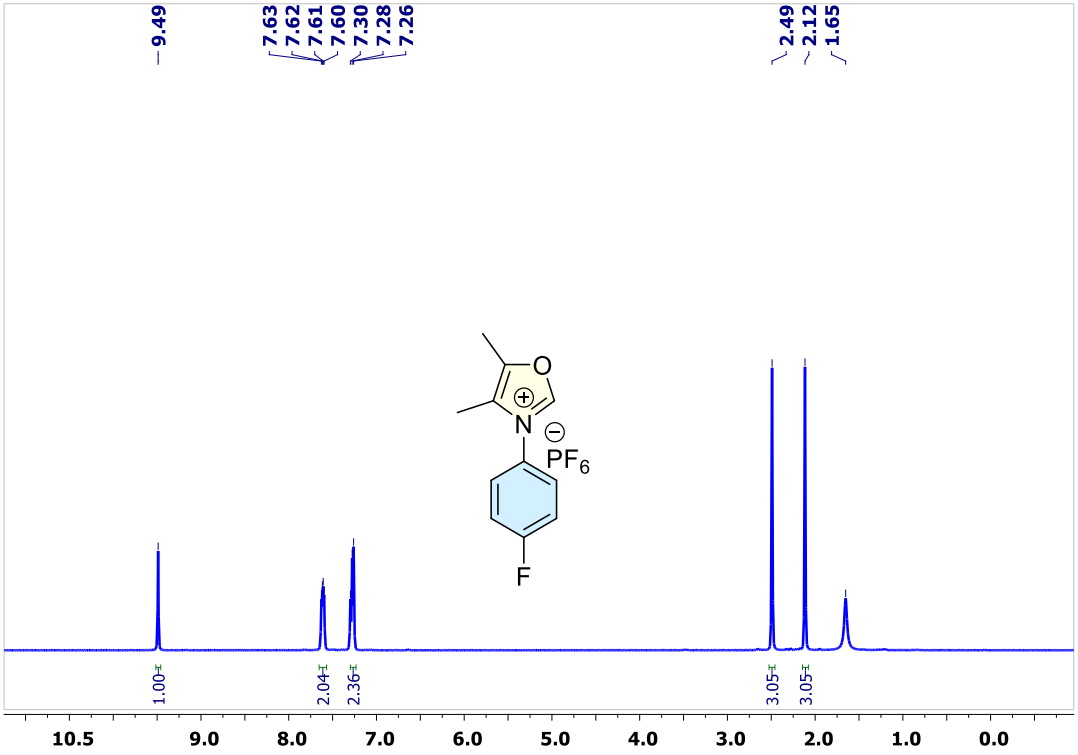

^{1}H NMR spectrum of **1e** (400 MHz, $CDCl_3$)

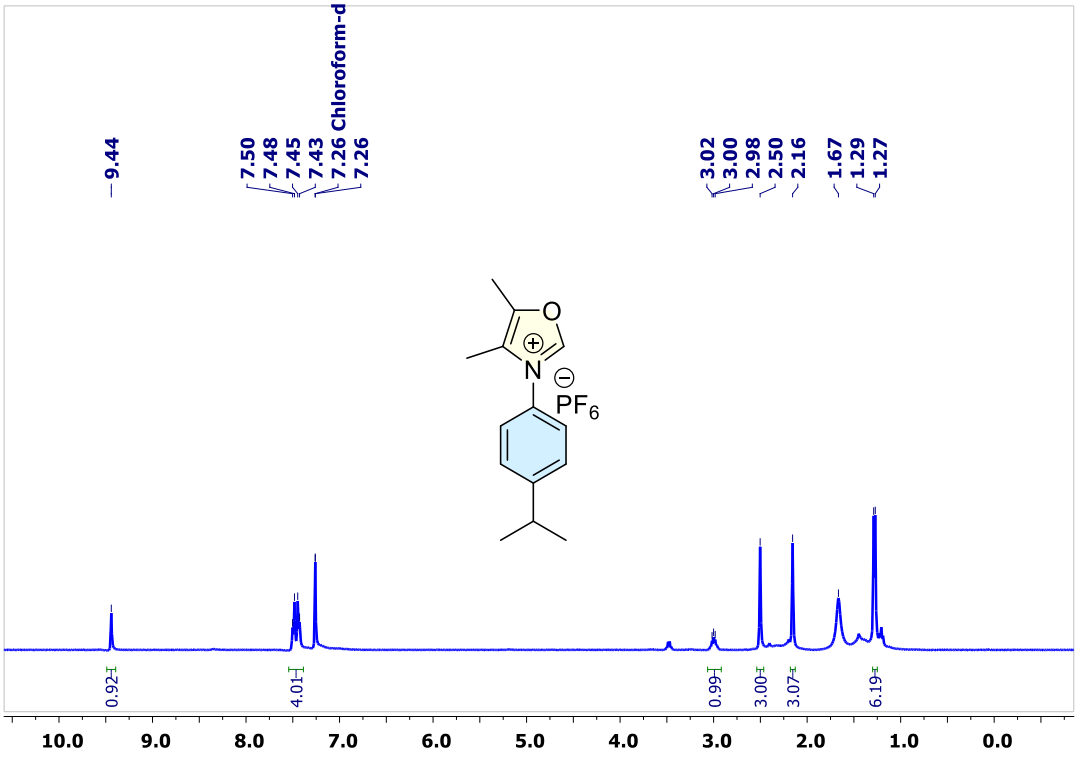

^{1}H NMR spectrum of **1f** (400 MHz, $CDCl_3$)

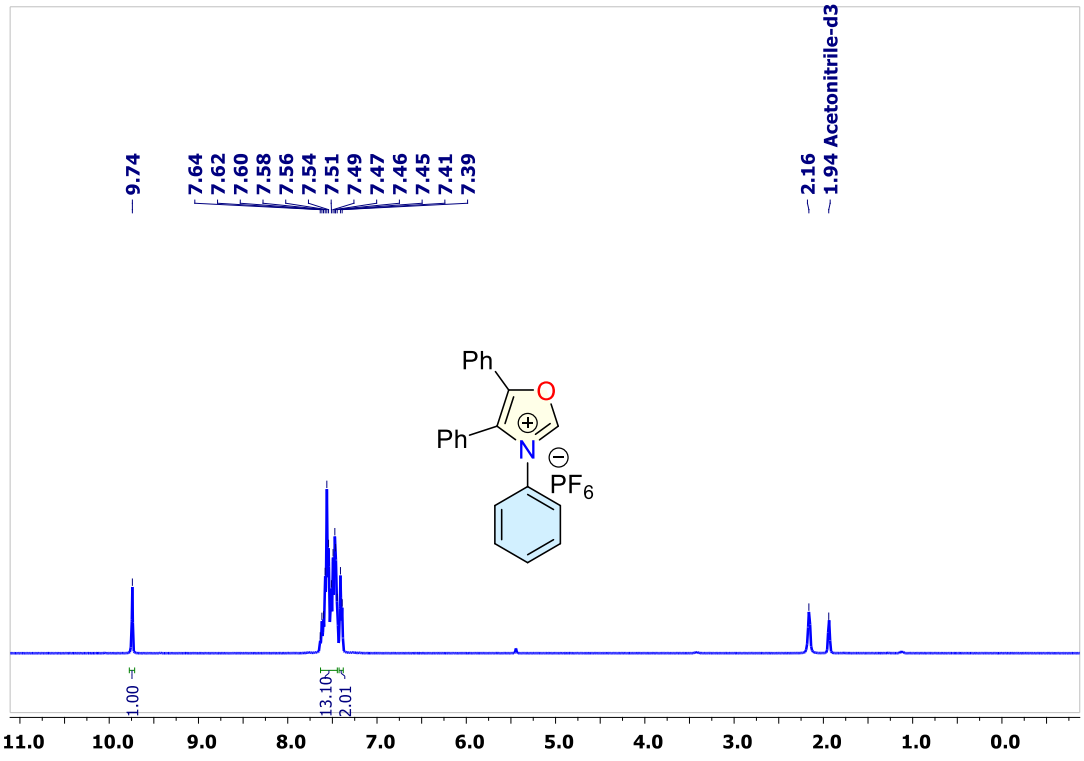

^{1}H NMR spectrum of **1g** (400 MHz, CD_3CN)

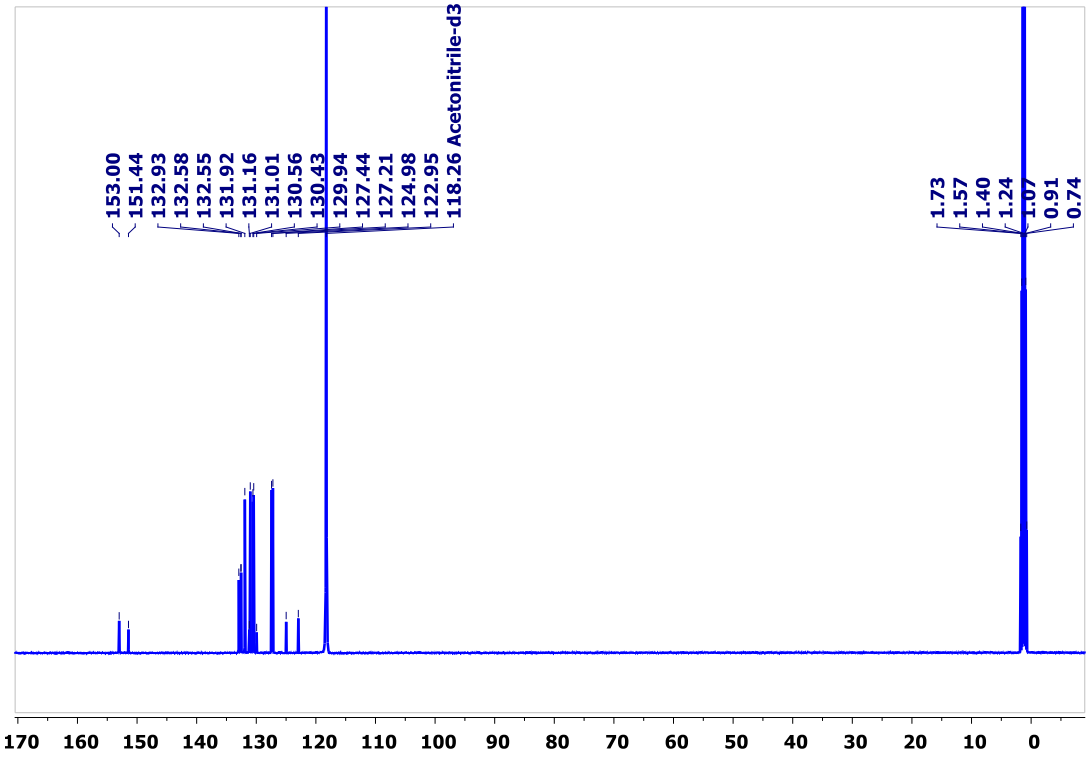

^{13}C{^{1}H} NMR spectrum of **1g** (126 MHz, CD_3CN)

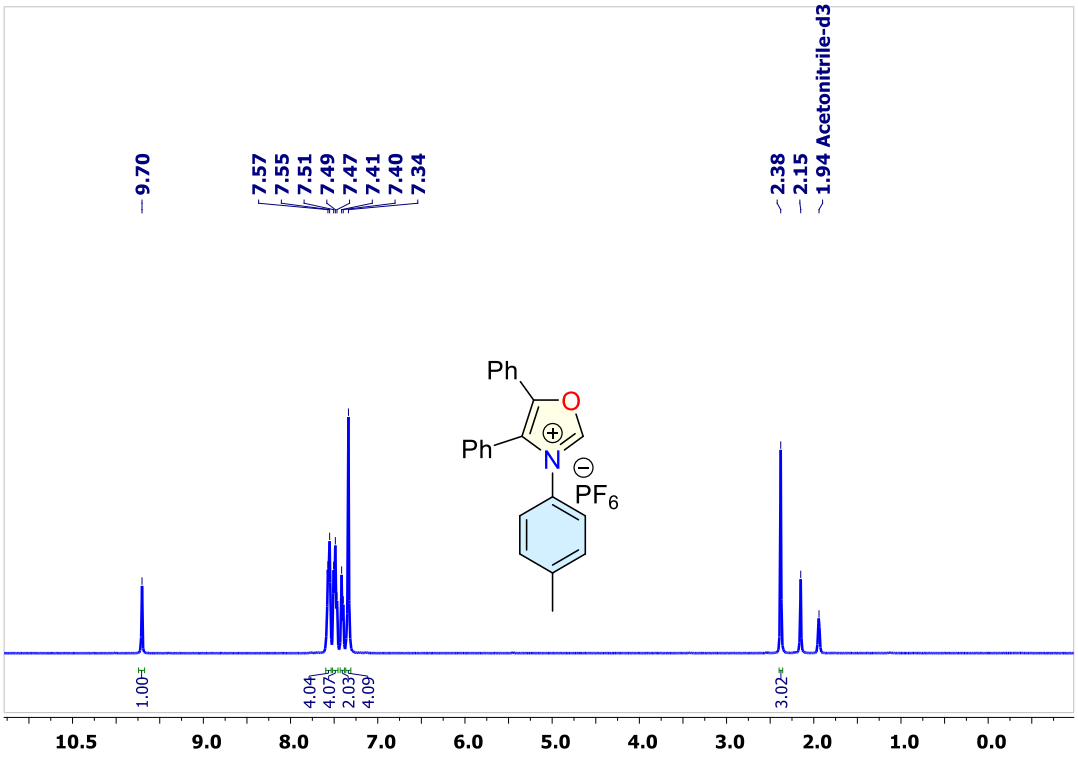

^{1}H NMR spectrum of **1h** (400 MHz, CD_3CN)

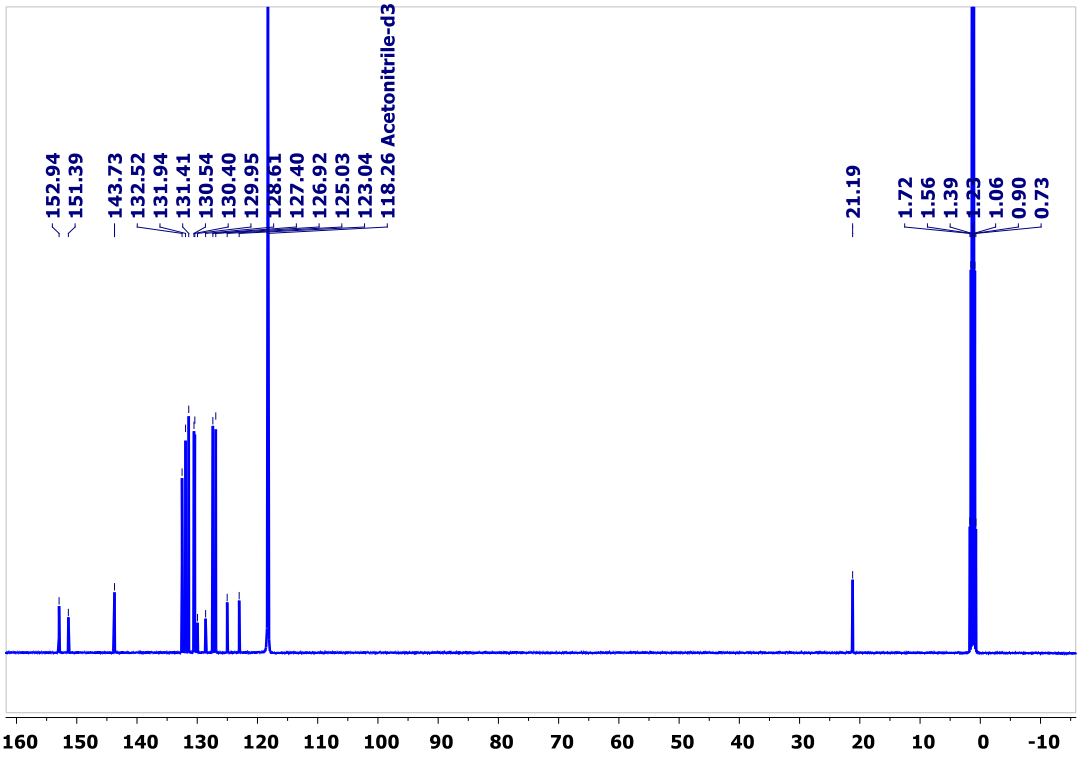

^{13}C{^{1}H} NMR spectrum of **1h** (126 MHz, CD_3CN)

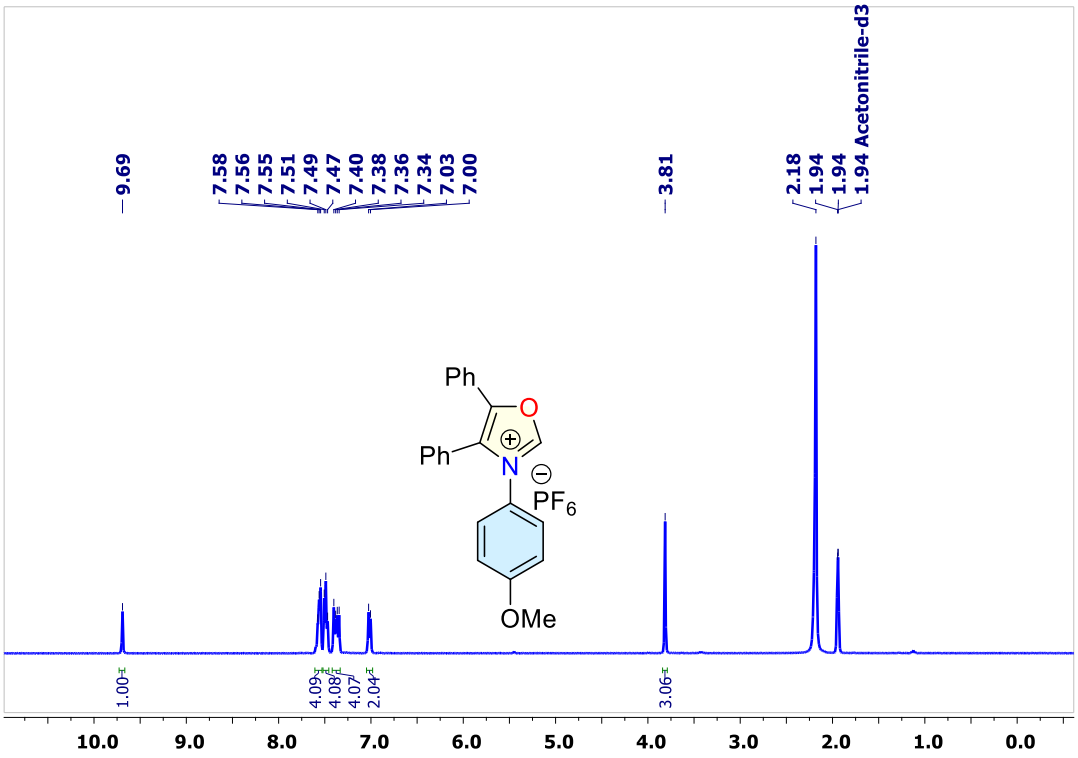

^{1}H NMR spectrum of **1i** (400 MHz, CD_3CN)

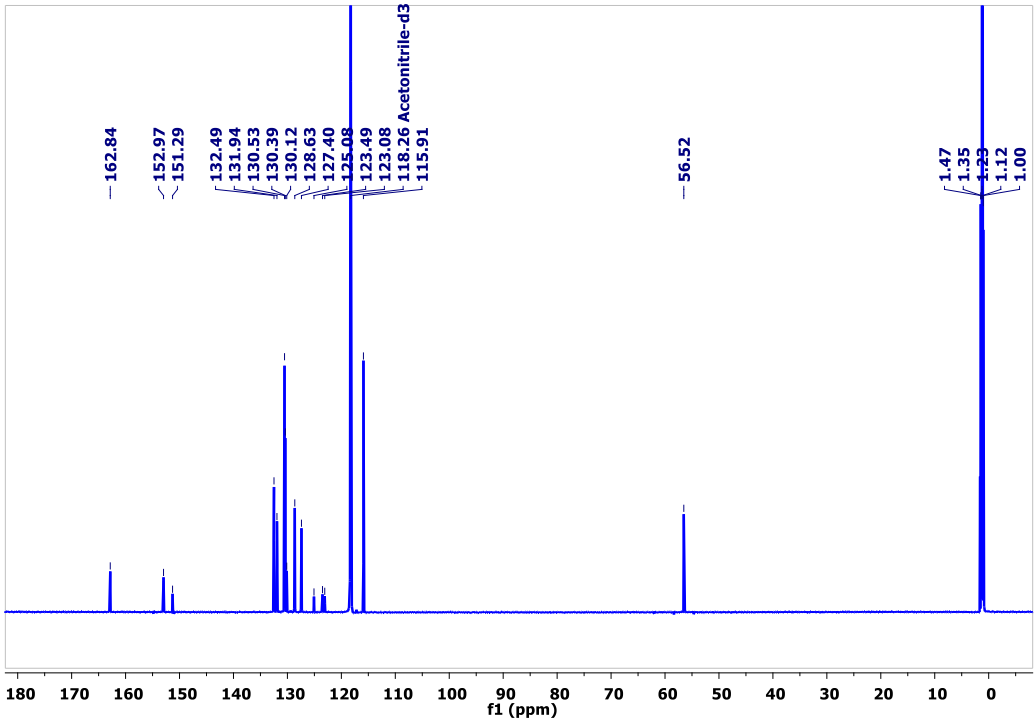

^{13}C{^{1}H} NMR spectrum of **1i** (176 MHz, CD_3CN)

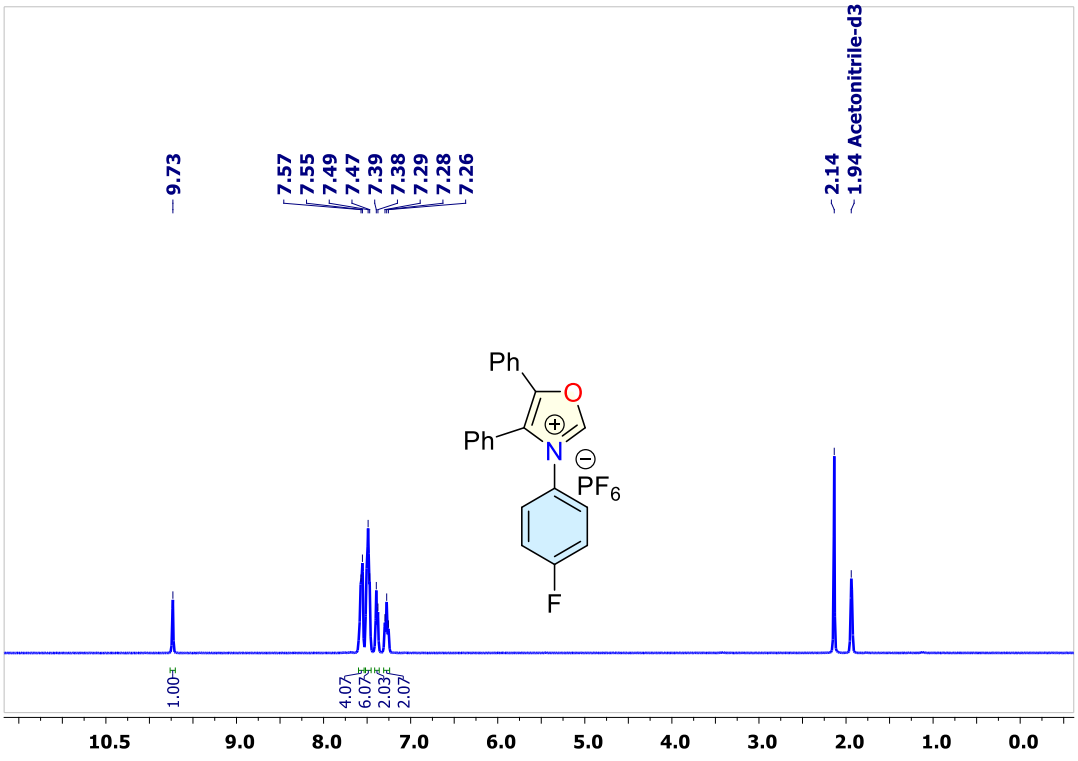

^{1}H NMR spectrum of **1j** (400 MHz, CD_3CN)

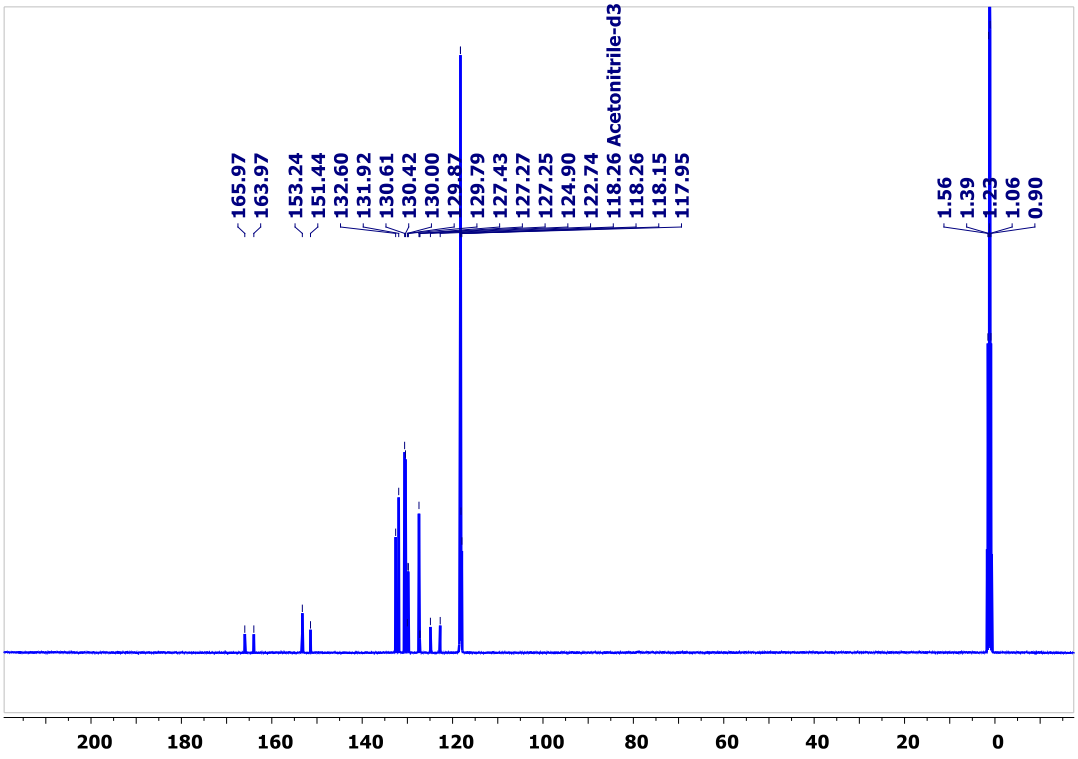

^{13}C{^{1}H} NMR spectrum of **3j** (126 MHz, CD_3CN)

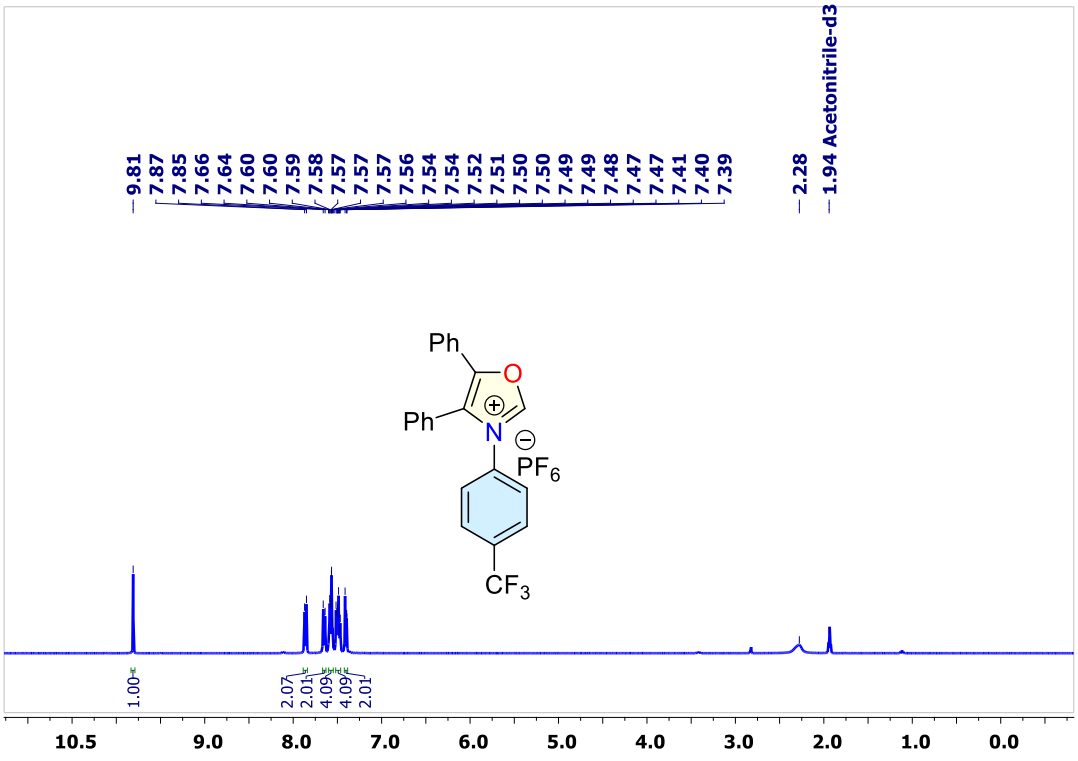

^{1}H NMR spectrum of **1k** (400 MHz, CD_3CN)

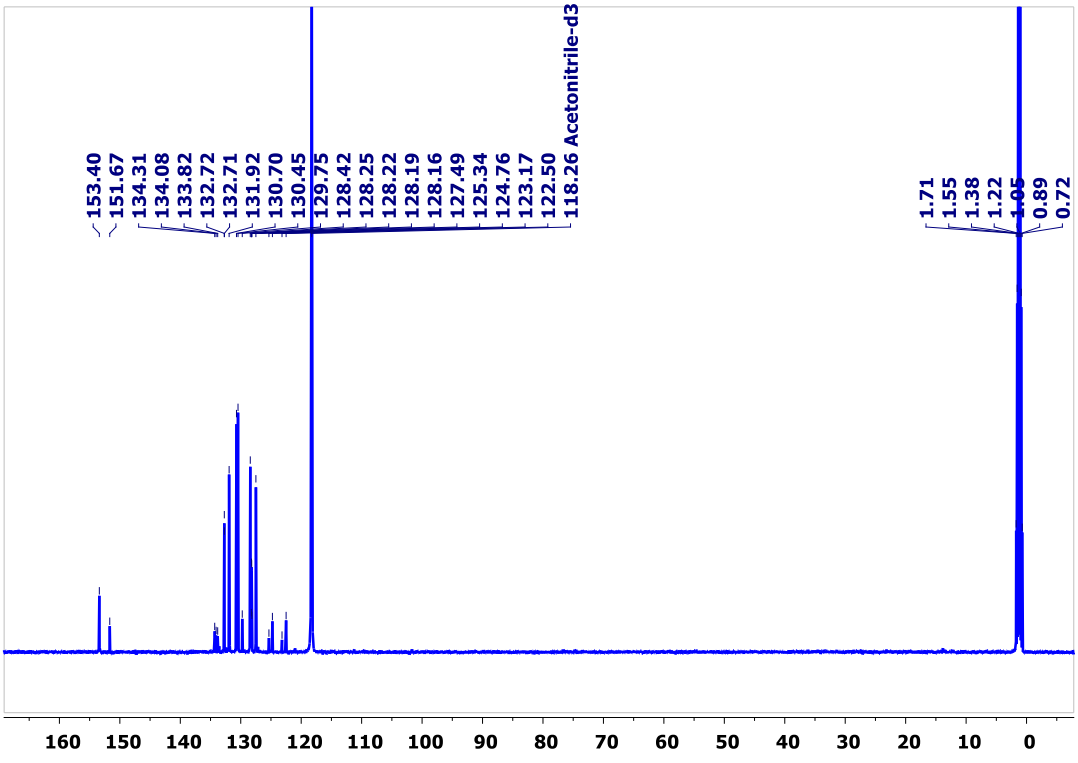

^{13}C{^{1}H} NMR spectrum of **1k** (126 MHz, CD_3CN)

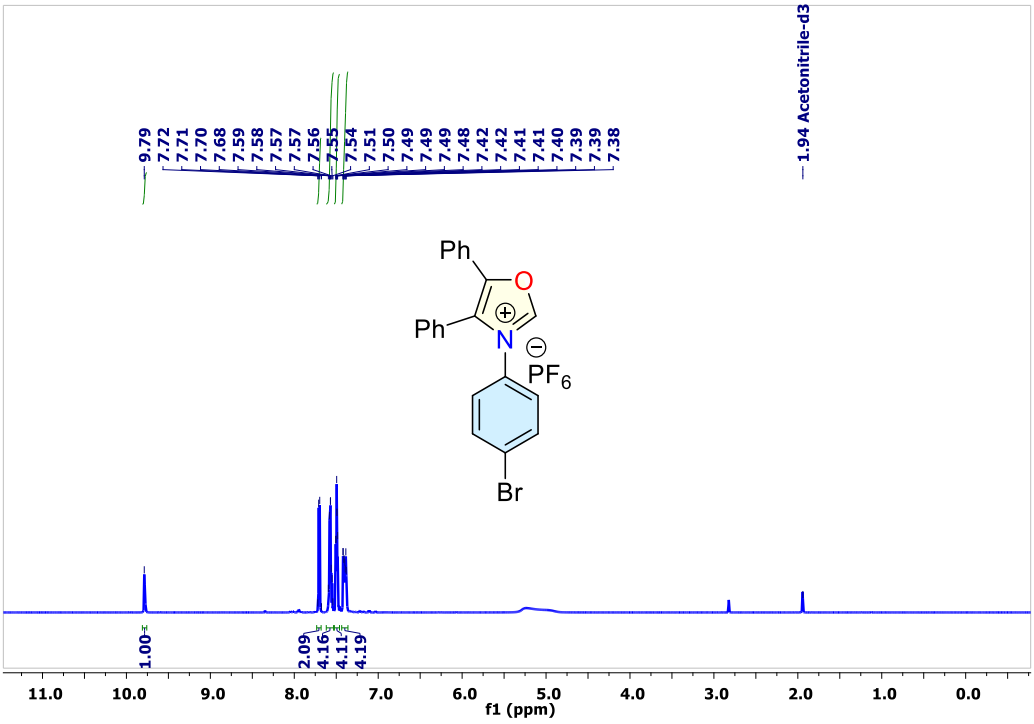

^{1}H NMR spectrum of **1l** (700 MHz, CD_3CN)

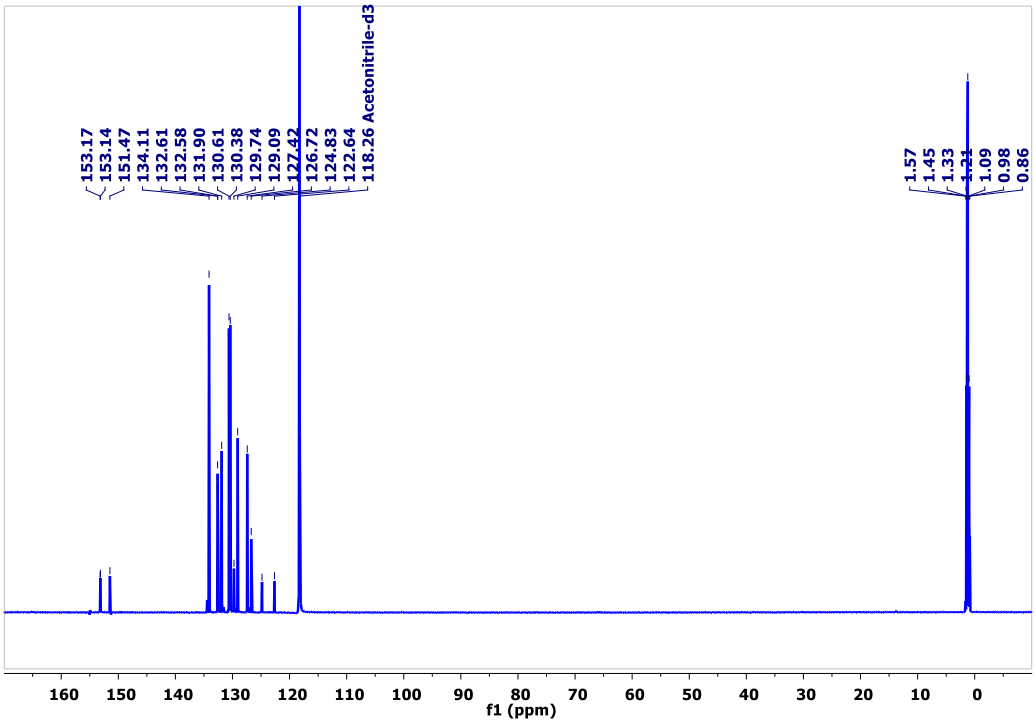

^{13}C{^{1}H} NMR spectrum of **1l** (176 MHz, CD_3CN)

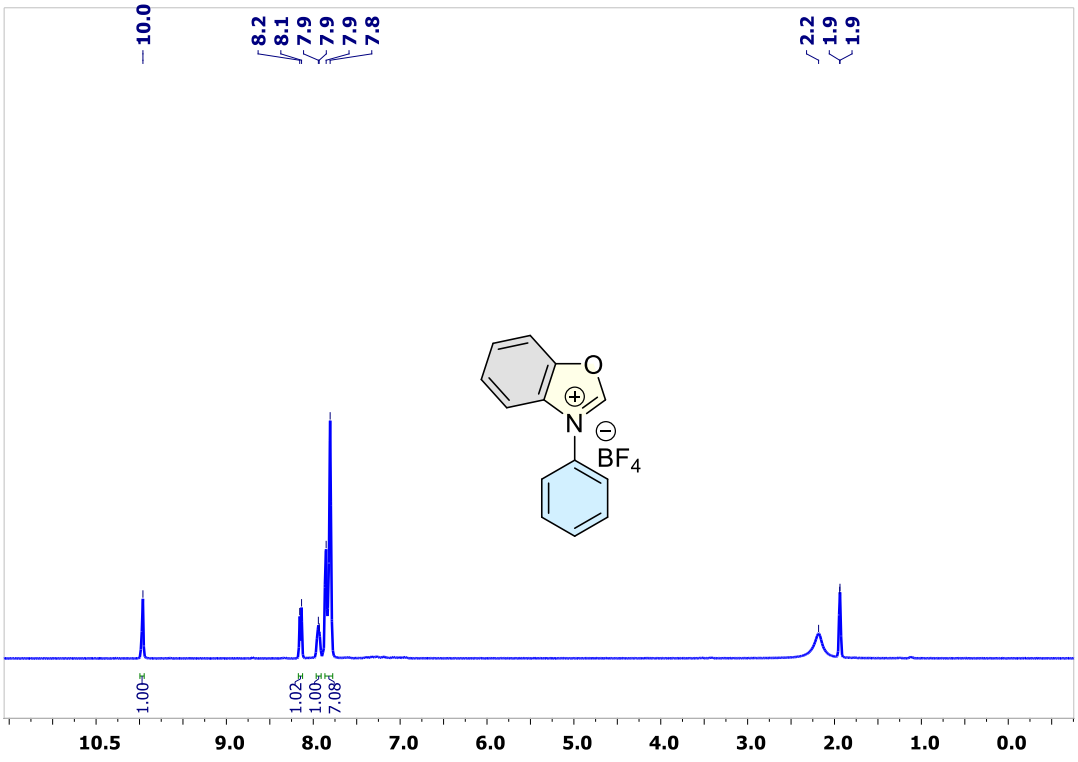

^{1}H NMR spectrum of **1m** (400 MHz, CD_3CN)

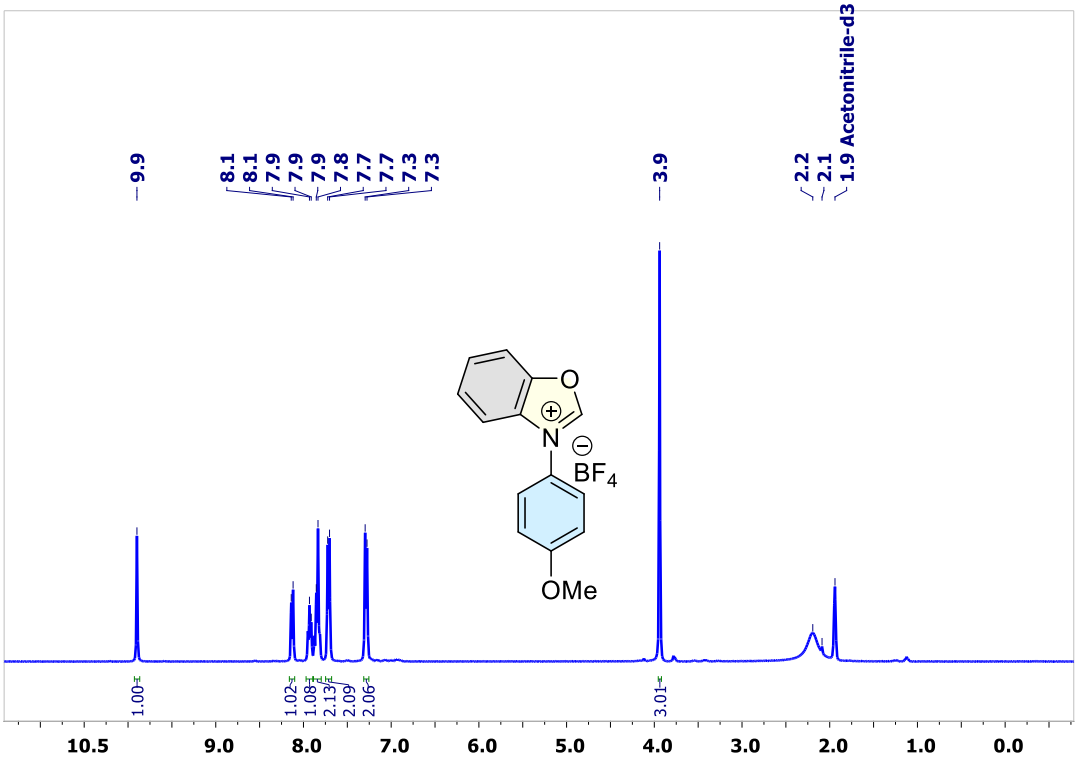

^{1}H NMR spectrum of **1n** (400 MHz, CD_3CN)

17. Spectral data for compounds 3a-3x

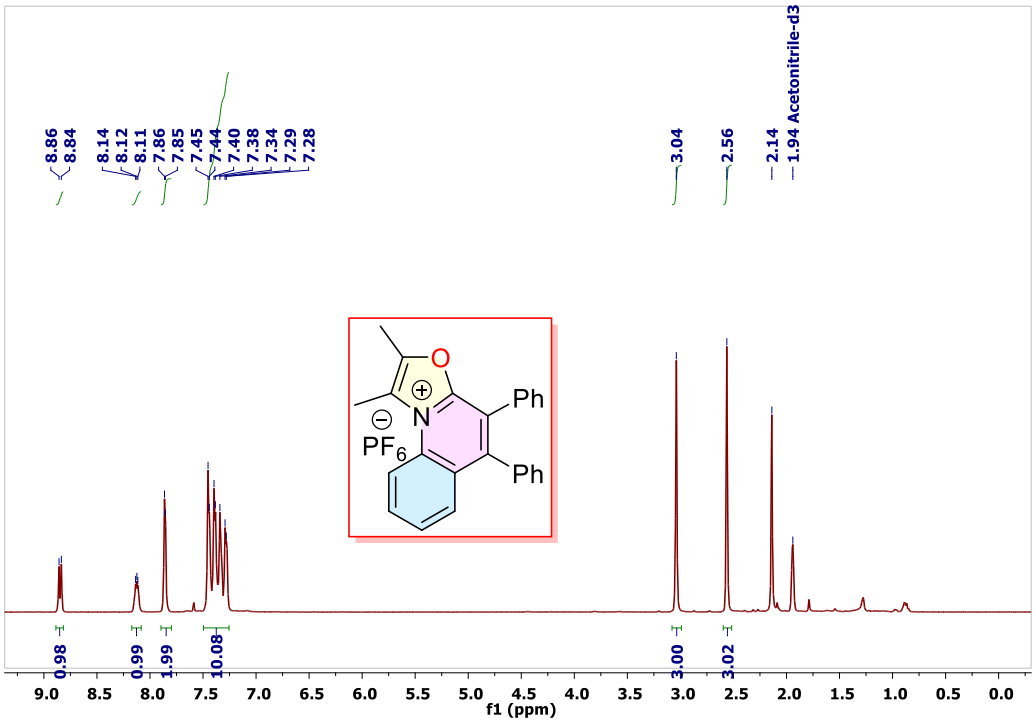

^{1}H NMR spectrum of **3a** (400 MHz, CD_3CN)

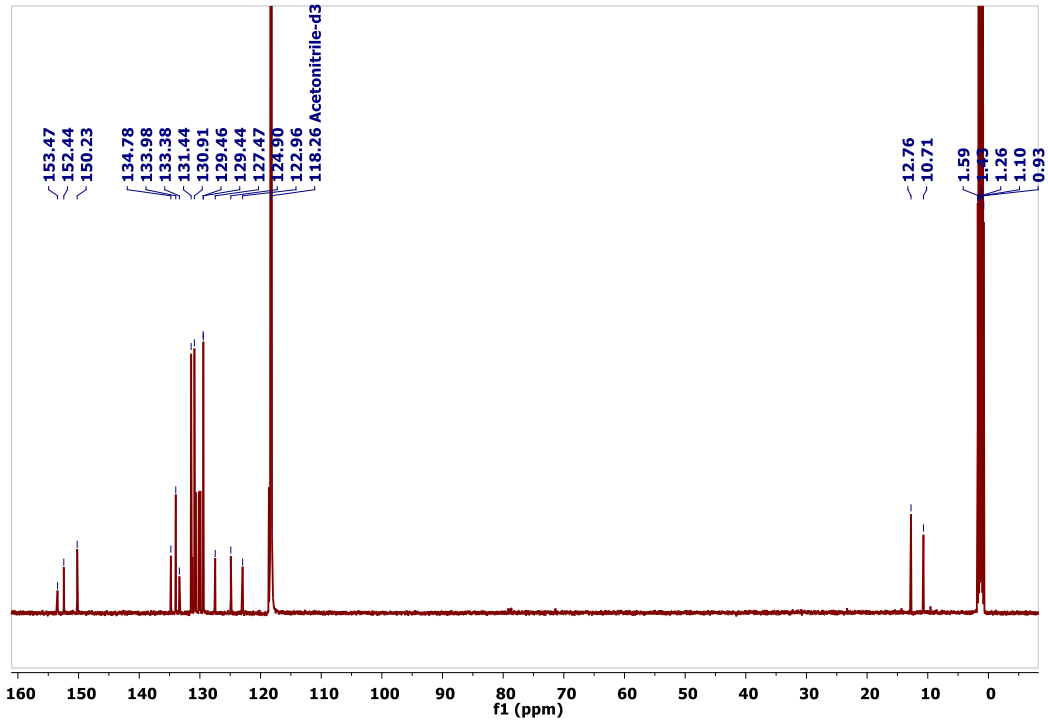

^{13}C{^{1}H} NMR spectrum of **3a** (126 MHz, CD_3CN)

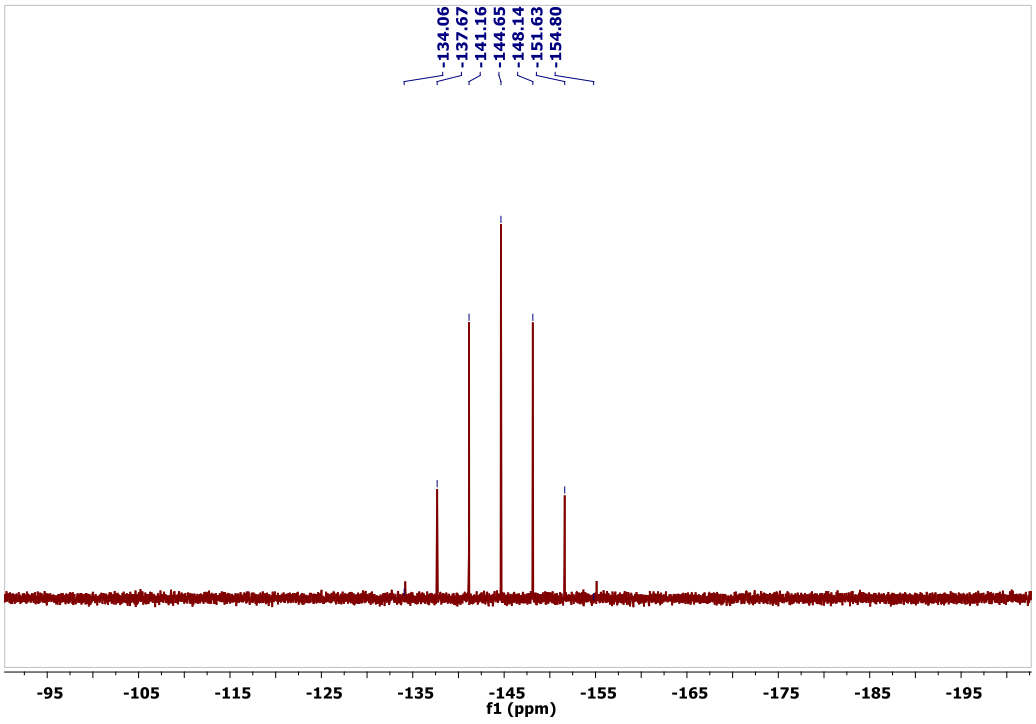

^{31}P NMR spectrum of **3a** (162 MHz, CD_3CN)

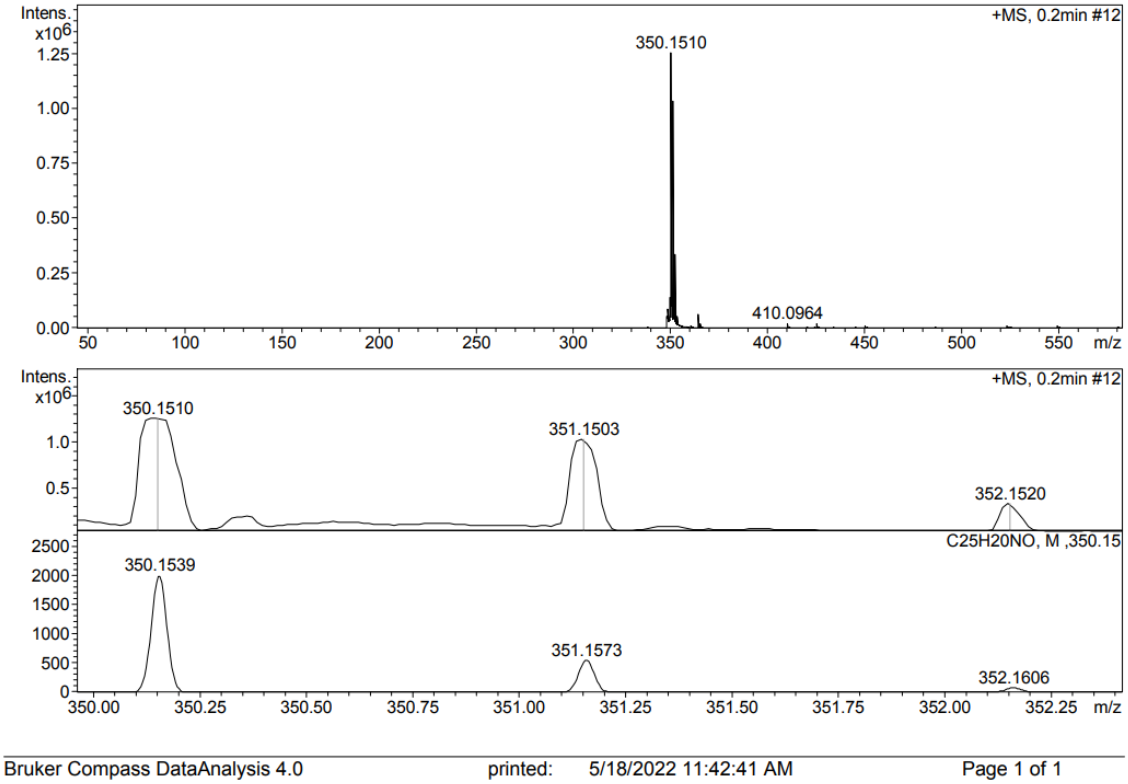

ESI-HRMS (positive ion mode) spectrum of **3a**

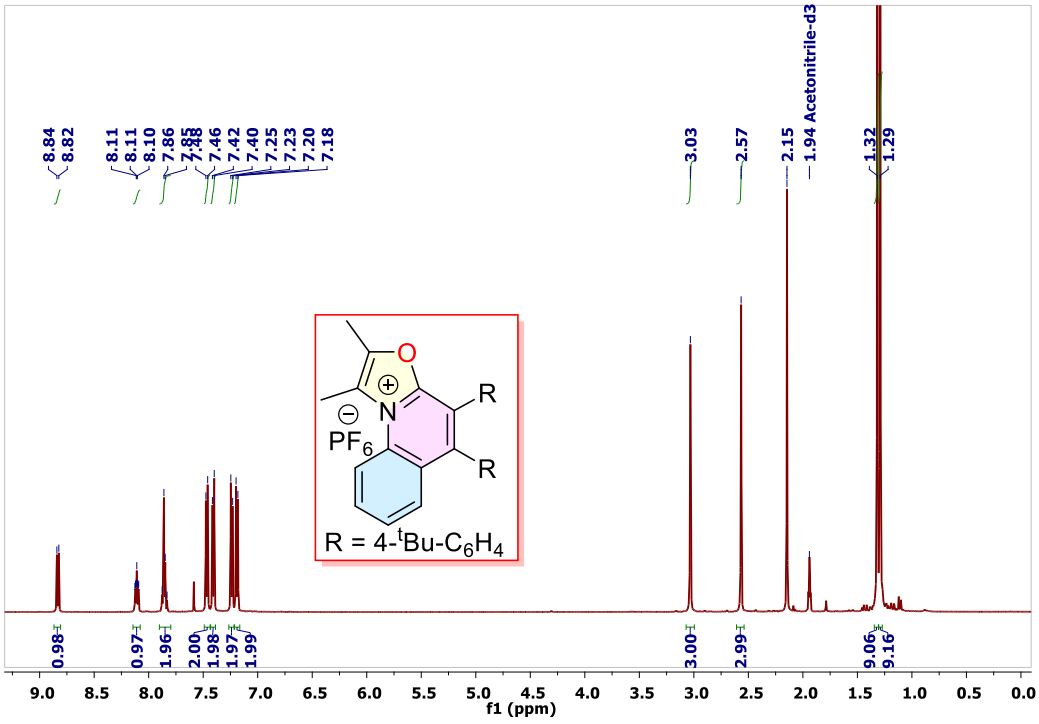

^{1}H NMR spectrum of **3b** (500 MHz, CD_3CN)

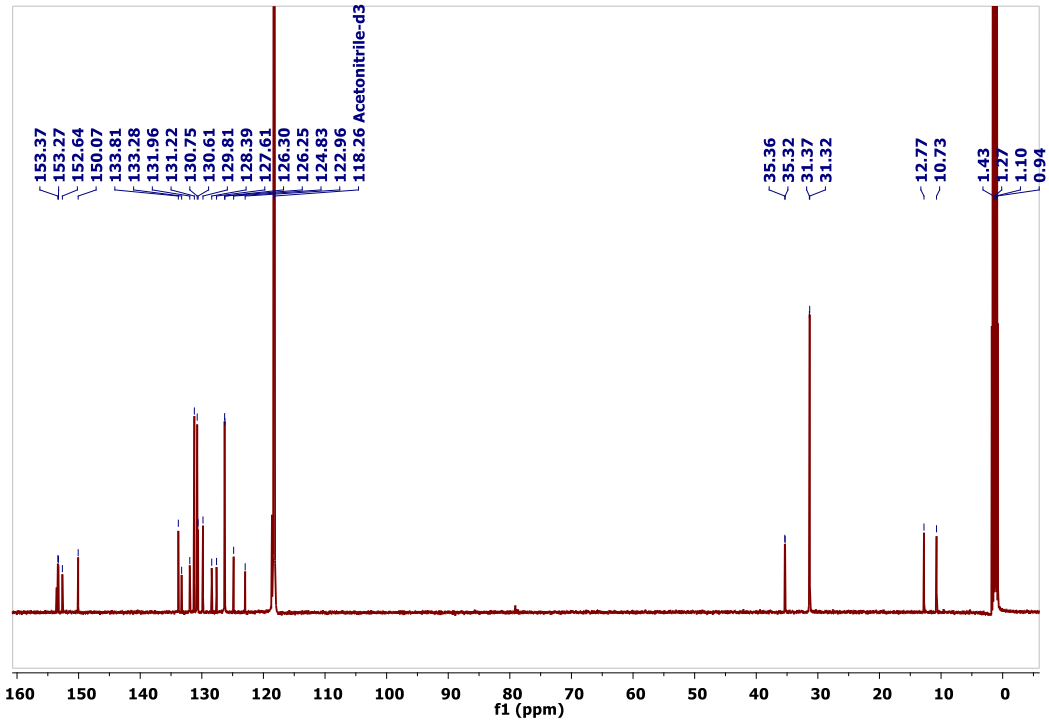

^{13}C{^{1}H} NMR spectrum of **3b** (126 MHz, CD_3CN)

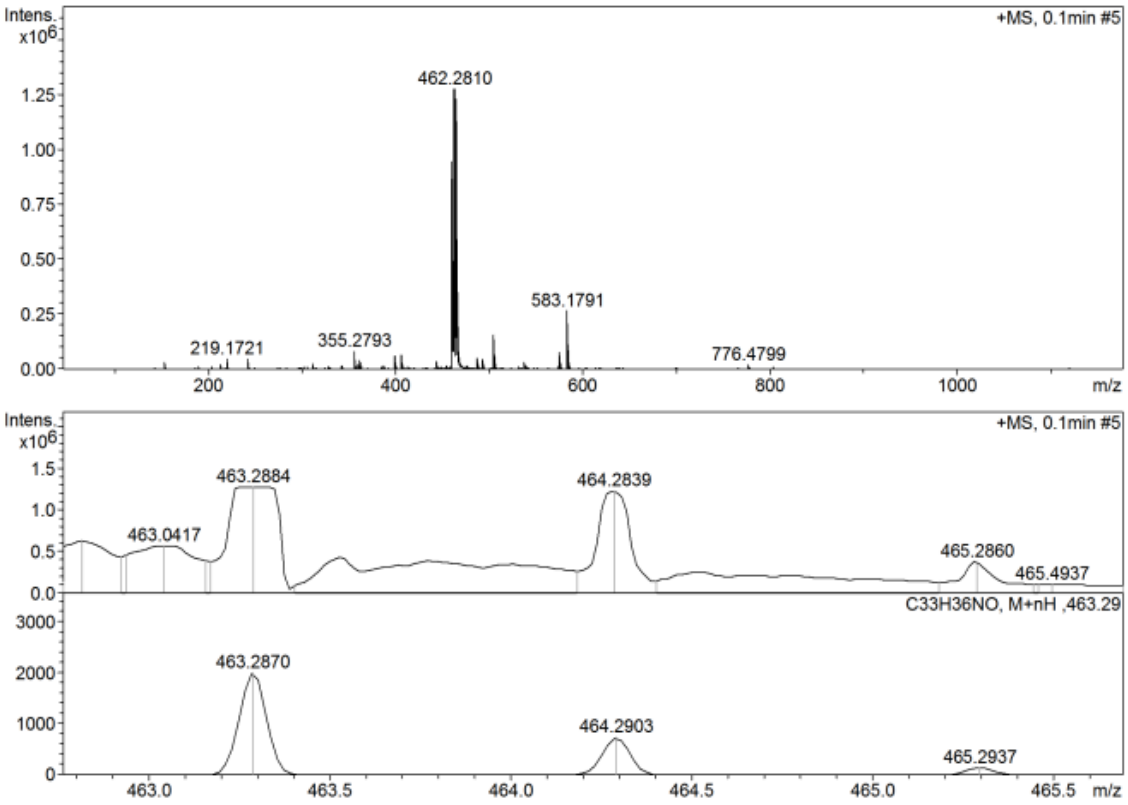

ESI-HRMS (positive ion mode) spectrum of **3b**

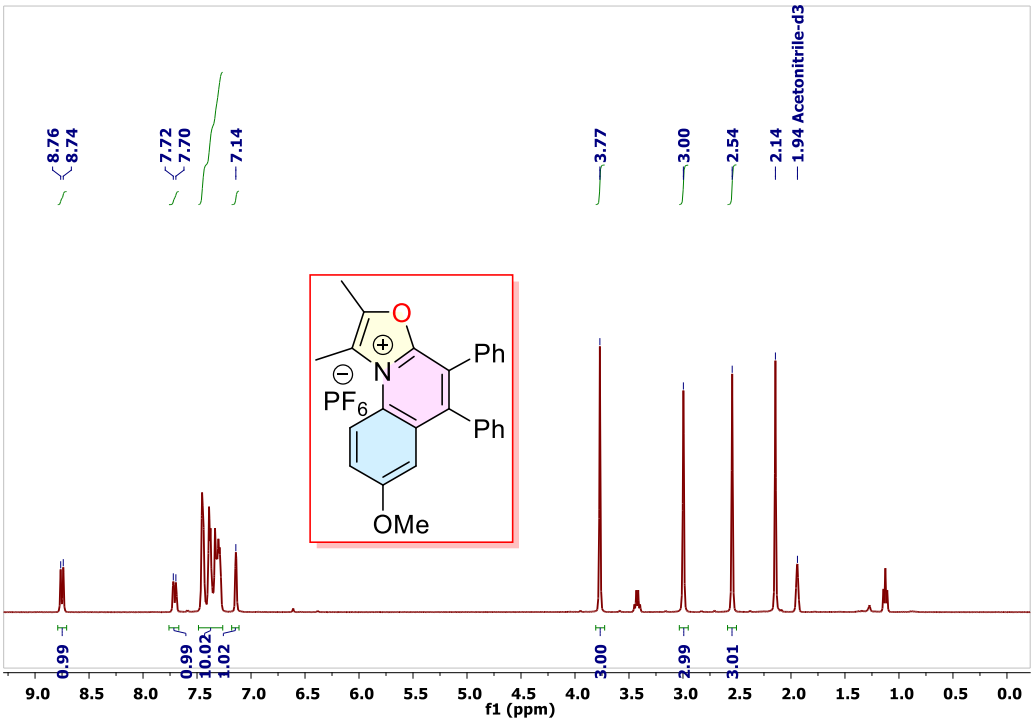

^{1}H NMR spectrum of **3c** (400 MHz, CD_3CN)

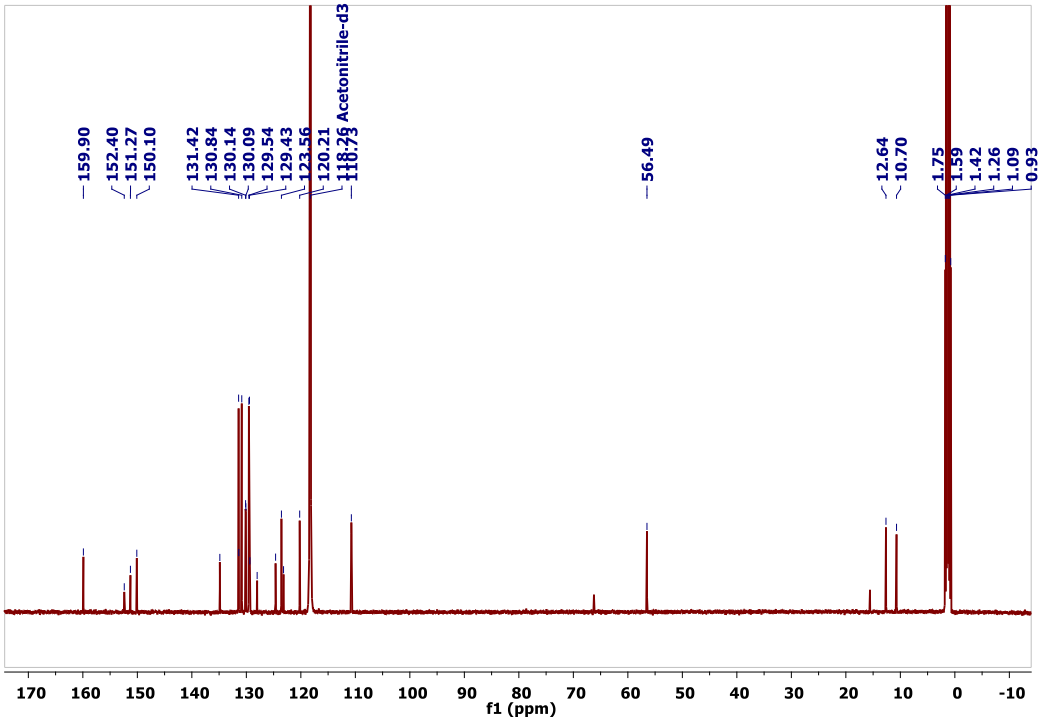

$^{13}C\{^{1}H\}$ NMR spectrum of **3c** (126 MHz, CD_3CN)

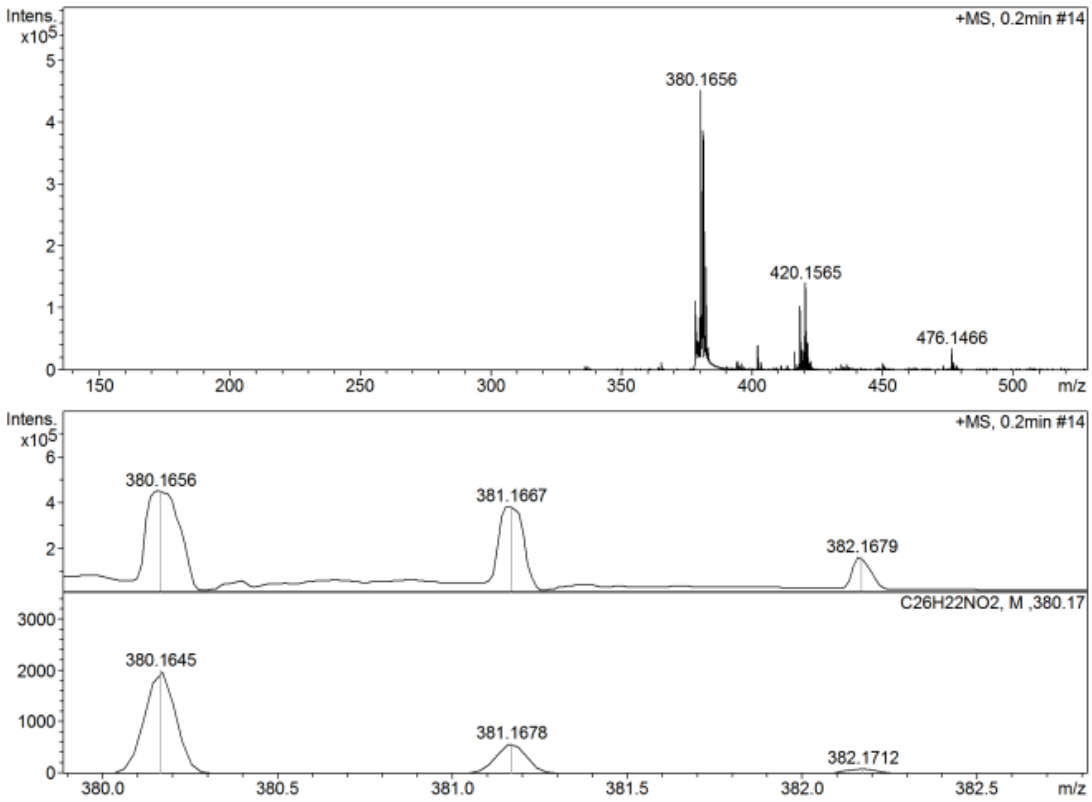

ESI-HRMS (positive ion mode) spectrum of **3c**

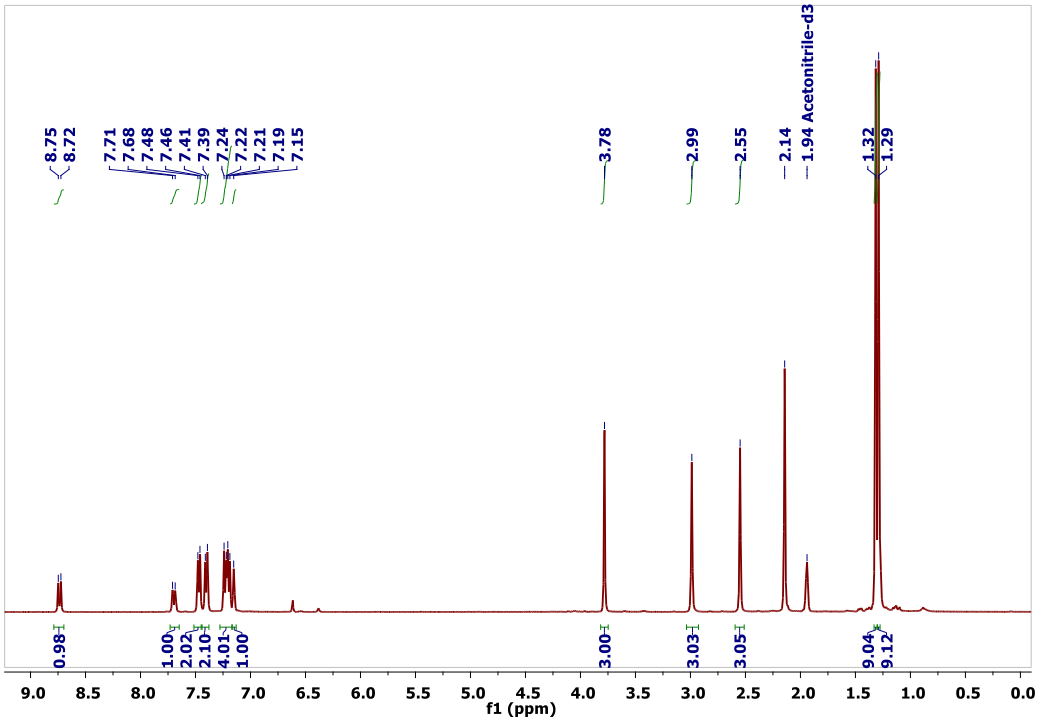

^{1}H NMR spectrum of **3d** (400 MHz, CD_3CN)

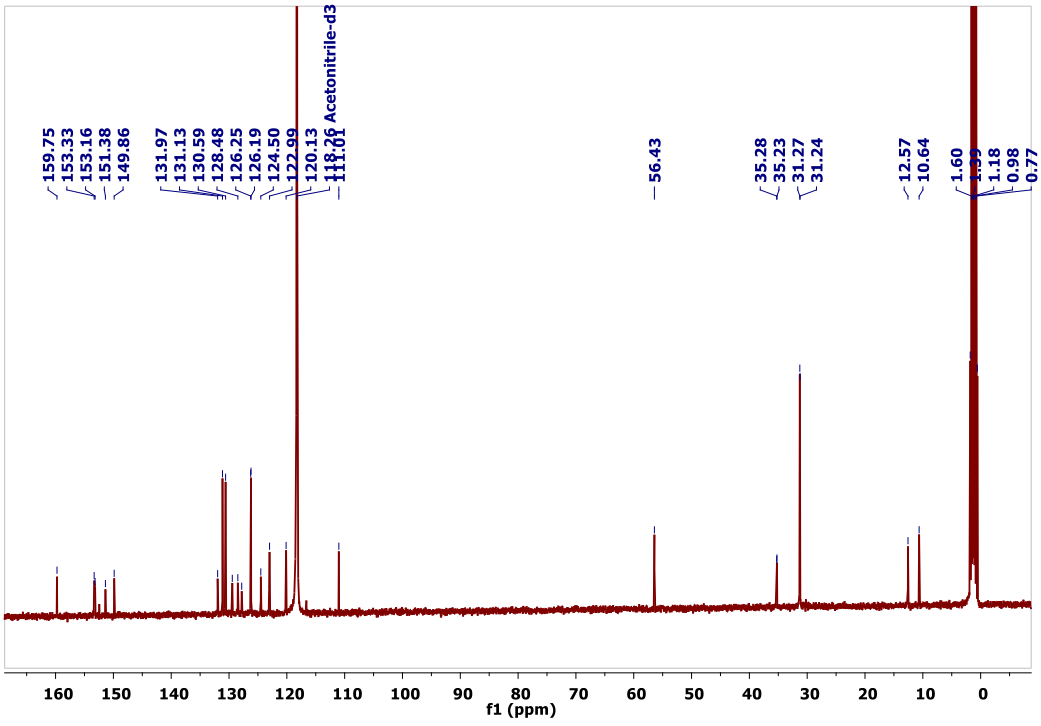

^{13}C{^{1}H} NMR spectrum of **3d** (176 MHz, CD_3CN)

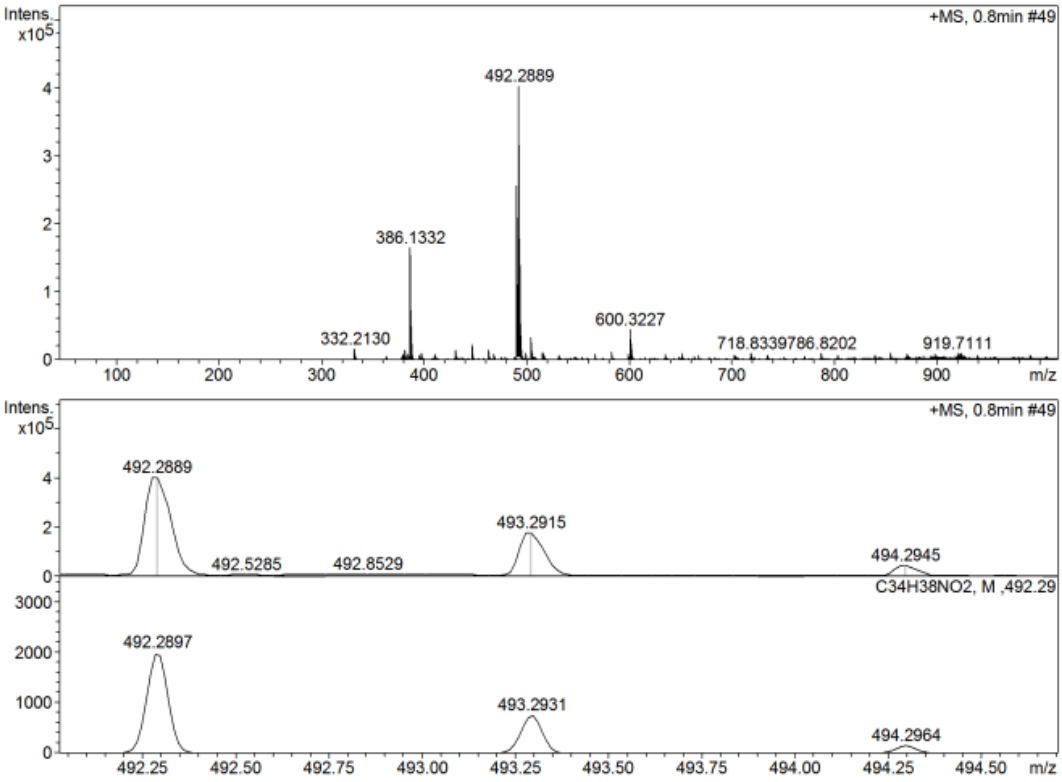

ESI-HRMS (positive ion mode) spectrum of **3d**

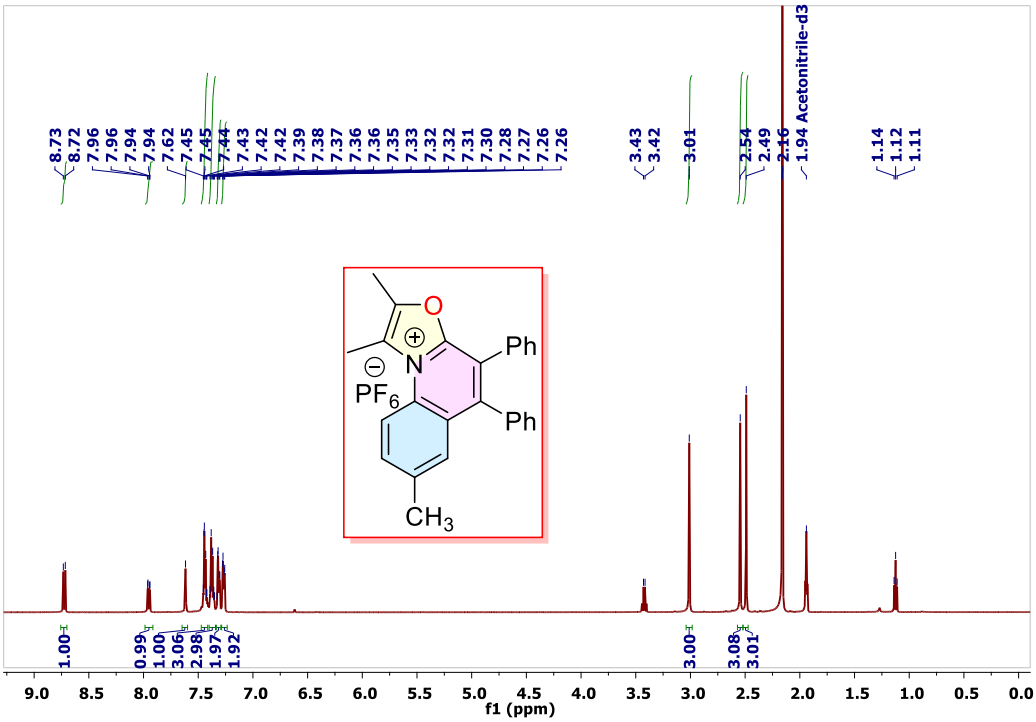

^{1}H NMR spectrum of **3e** (500 MHz, CD_3CN)

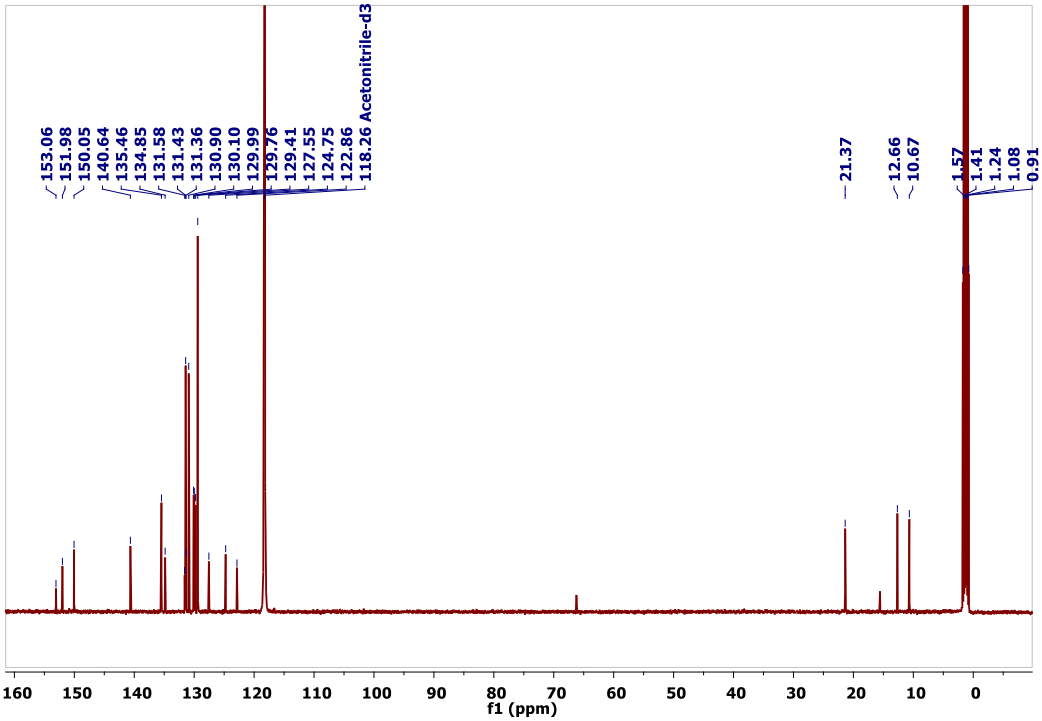

$^{13}C\{1H\}$ NMR spectrum of **3e** (126 MHz, CD_3CN)

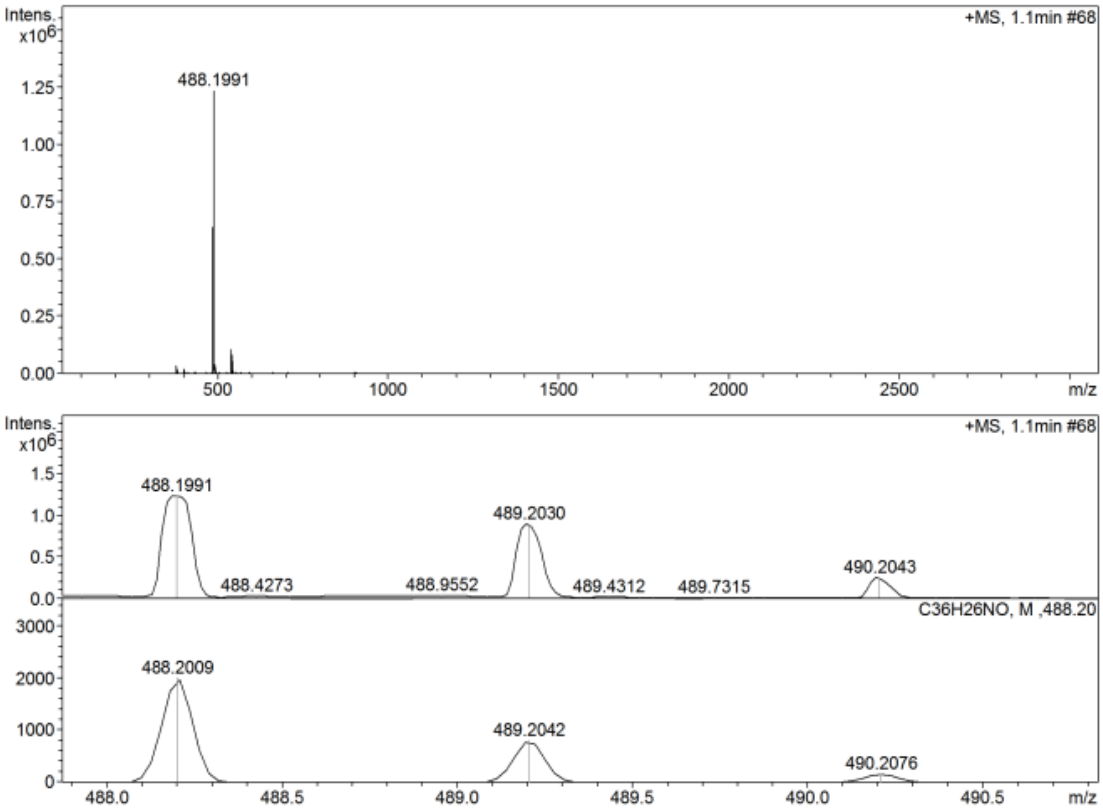

ESI-HRMS (positive ion mode) spectrum of **3e**

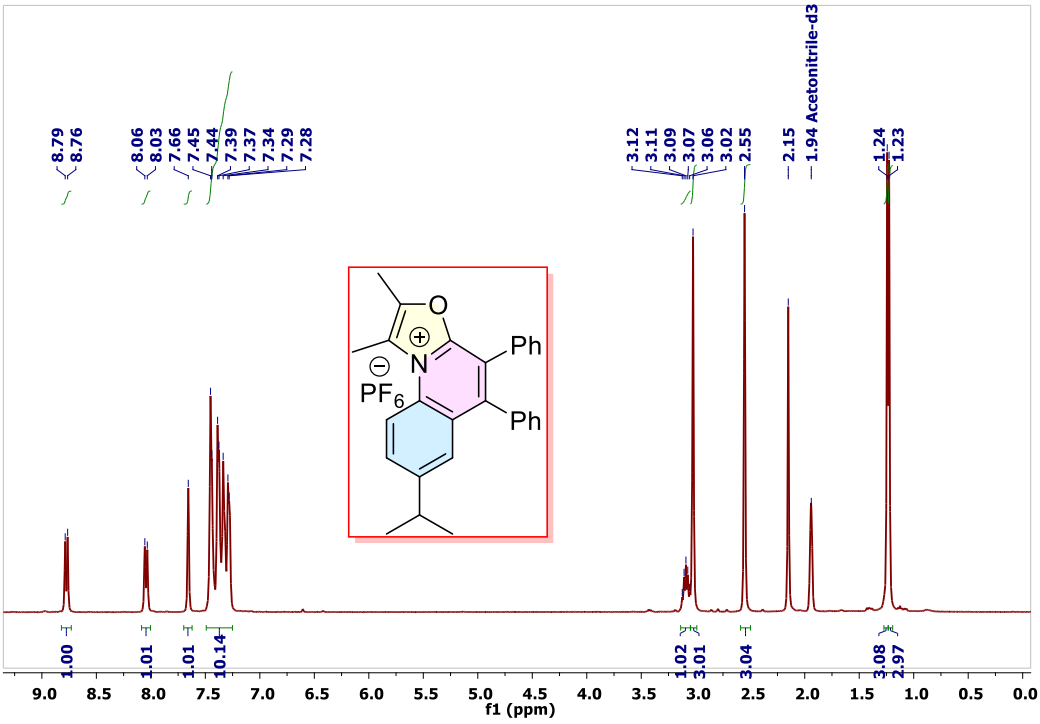

^{1}H NMR spectrum of **3f** (400 MHz, CD_3CN)

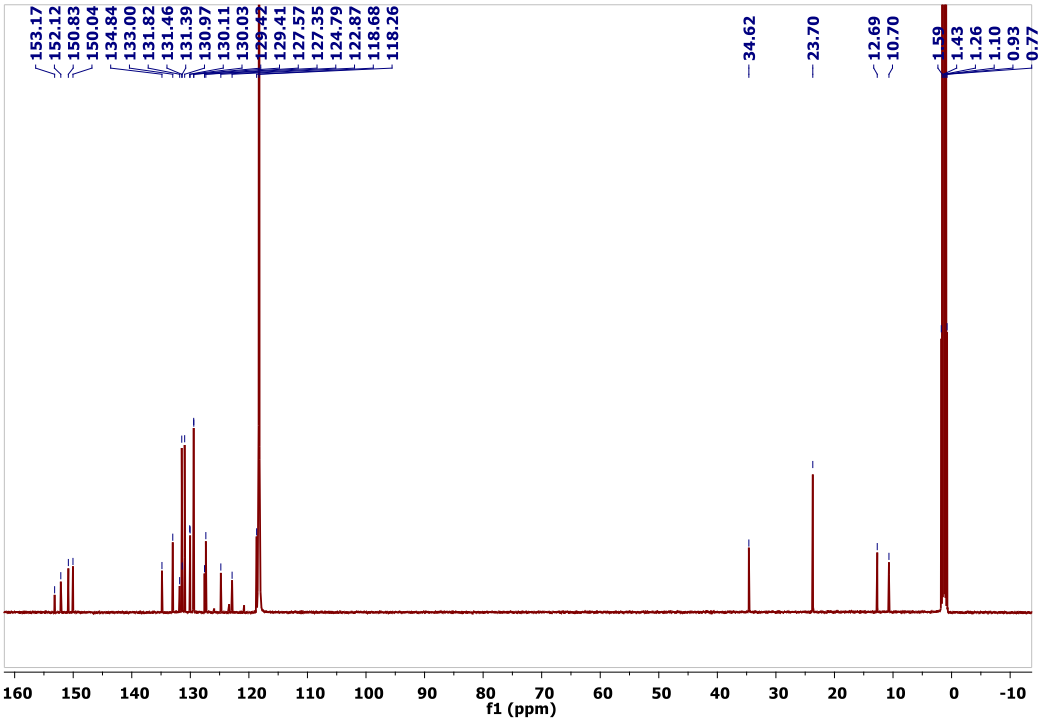

^{13}C{^{1}H} NMR spectrum of **3f** (126 MHz, CD_3CN)

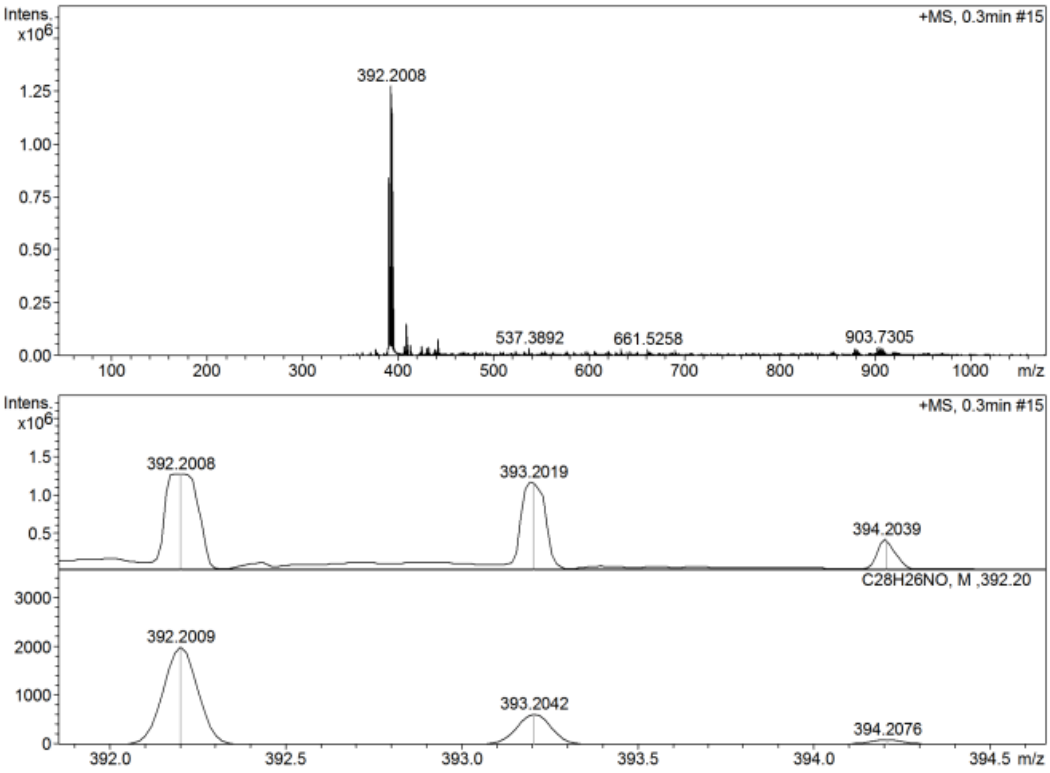

ESI-HRMS (positive ion mode) spectrum of **3f**

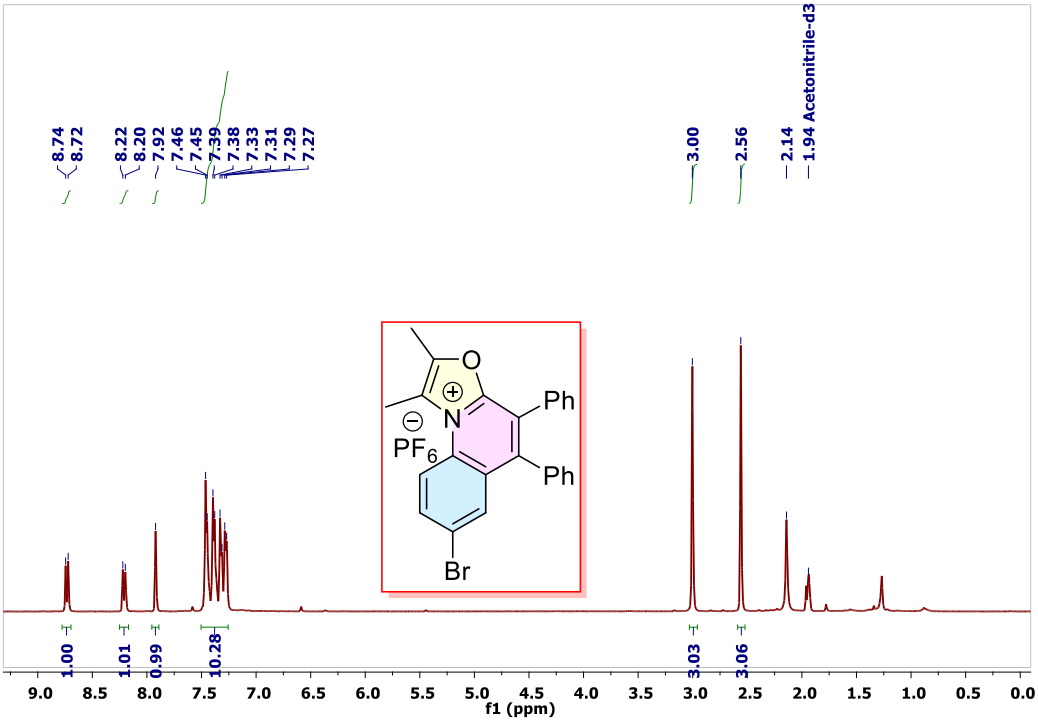

^{1}H NMR spectrum of **3g** (400 MHz, CD_3CN)

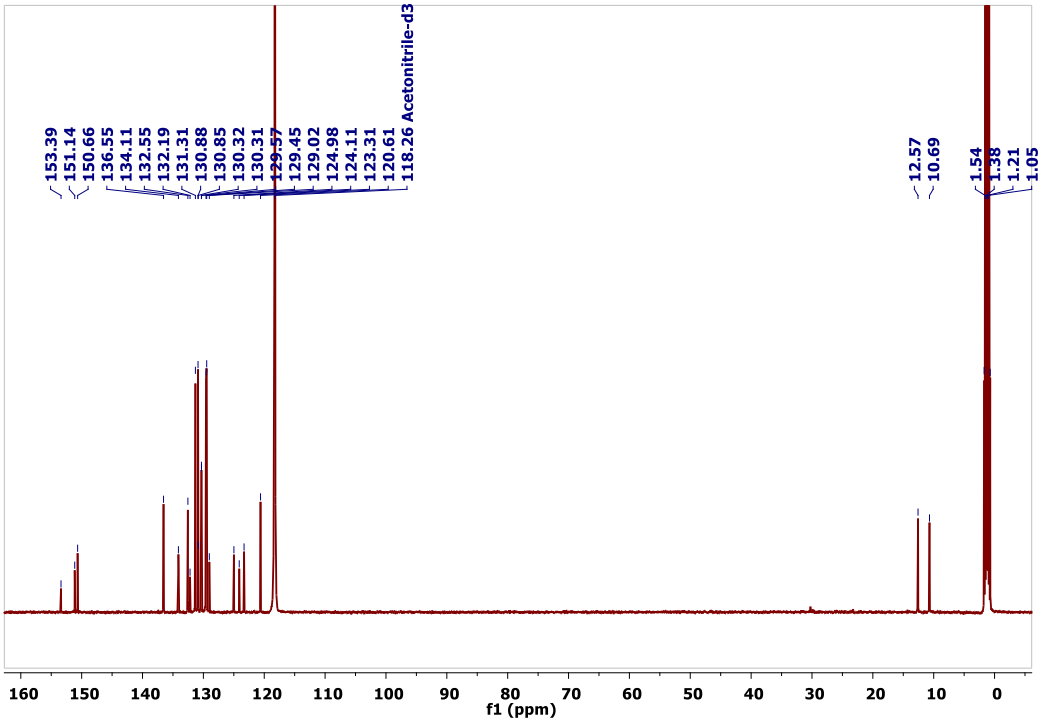

$^{13}C\{1H\}$ NMR spectrum of **3g** (126 MHz, CD_3CN)

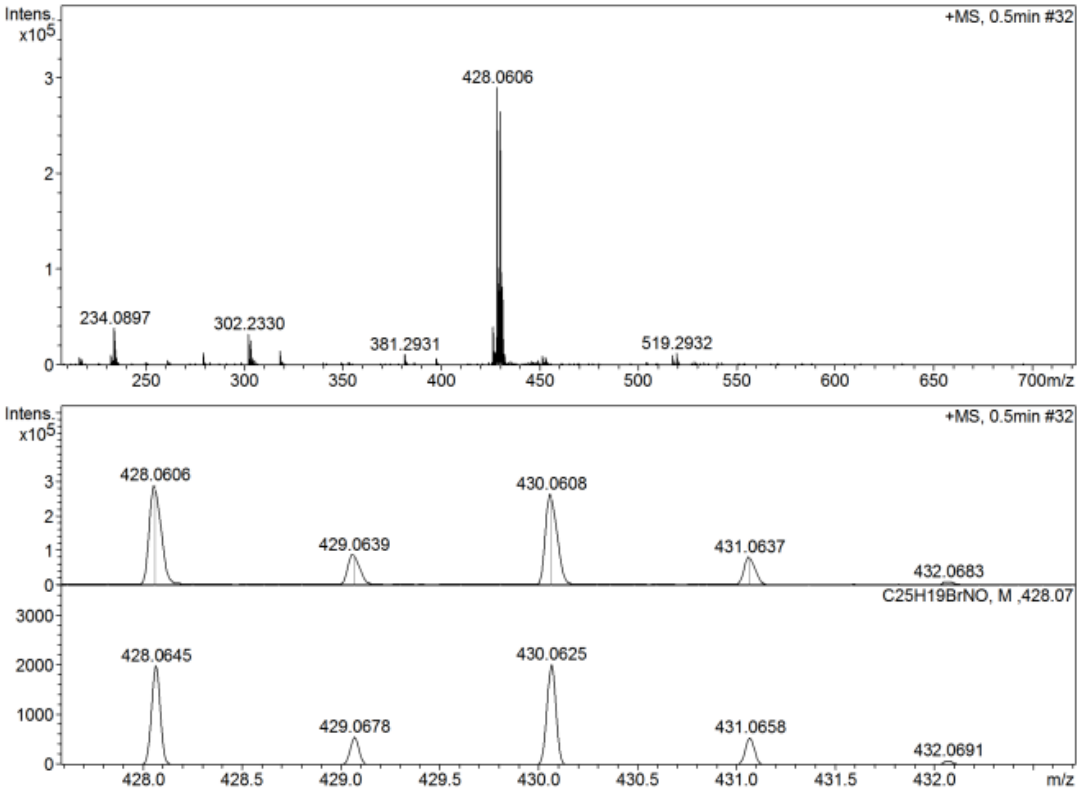

ESI-HRMS (positive ion mode) spectrum of **3g**

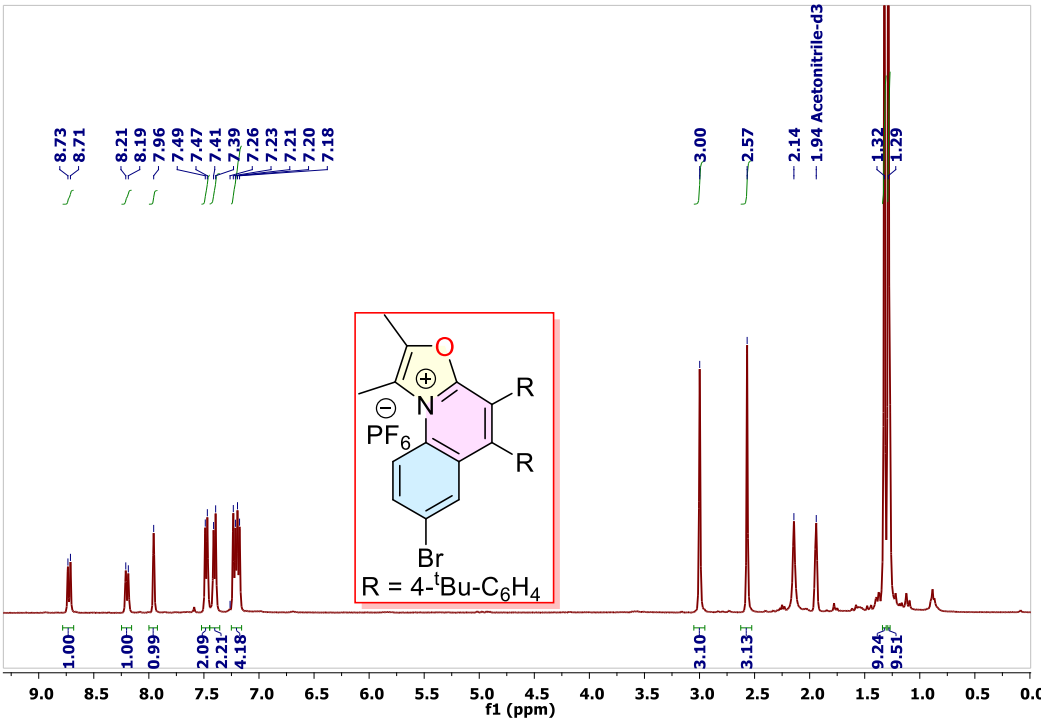

^{1}H NMR spectrum of **3h** (400 MHz, CD_3CN)

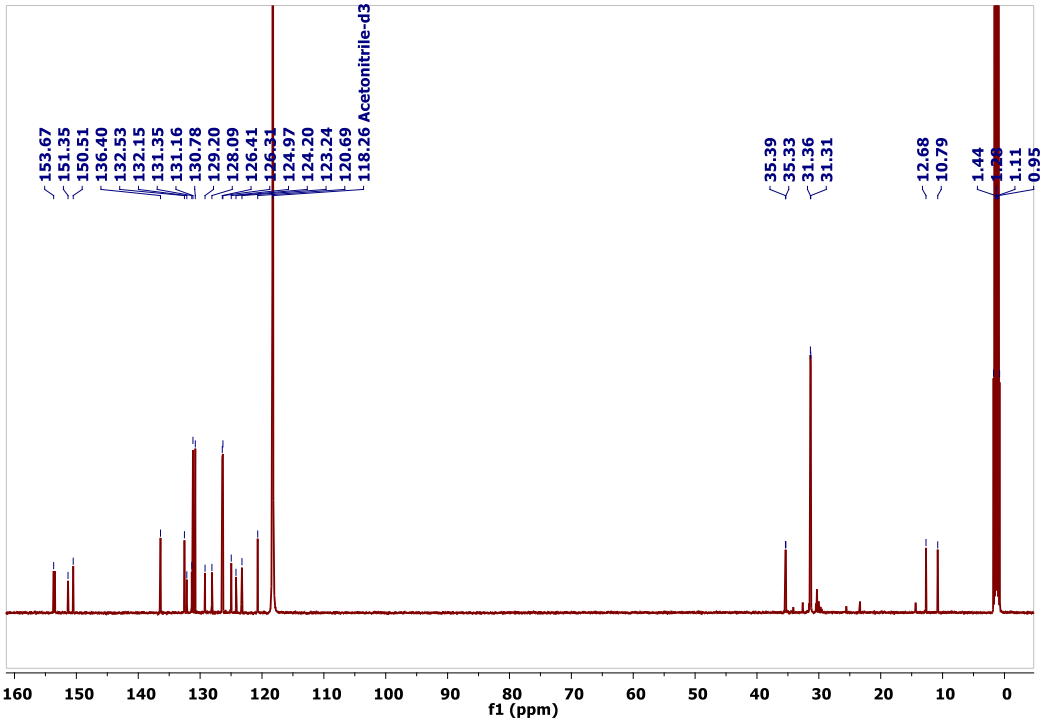

^{13}C{1H} NMR spectrum of **3h** (126 MHz, CD_3CN)

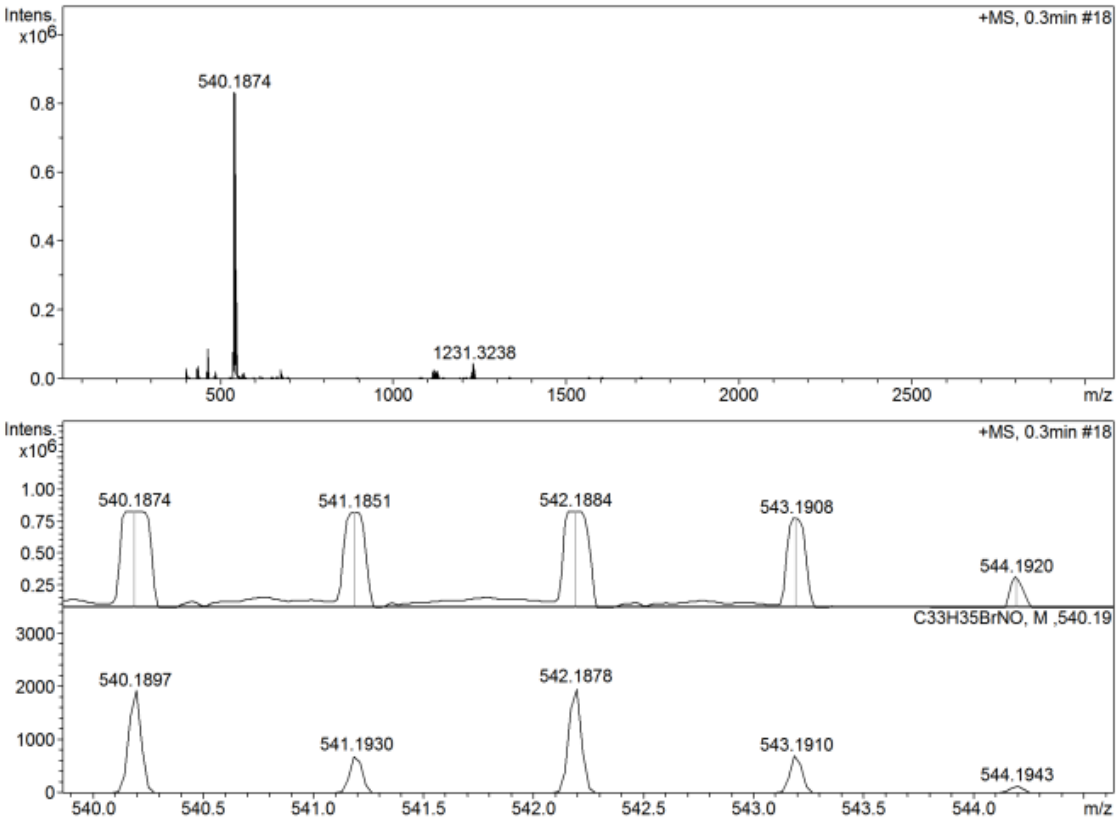

ESI-HRMS (positive ion mode) spectrum of **3h**

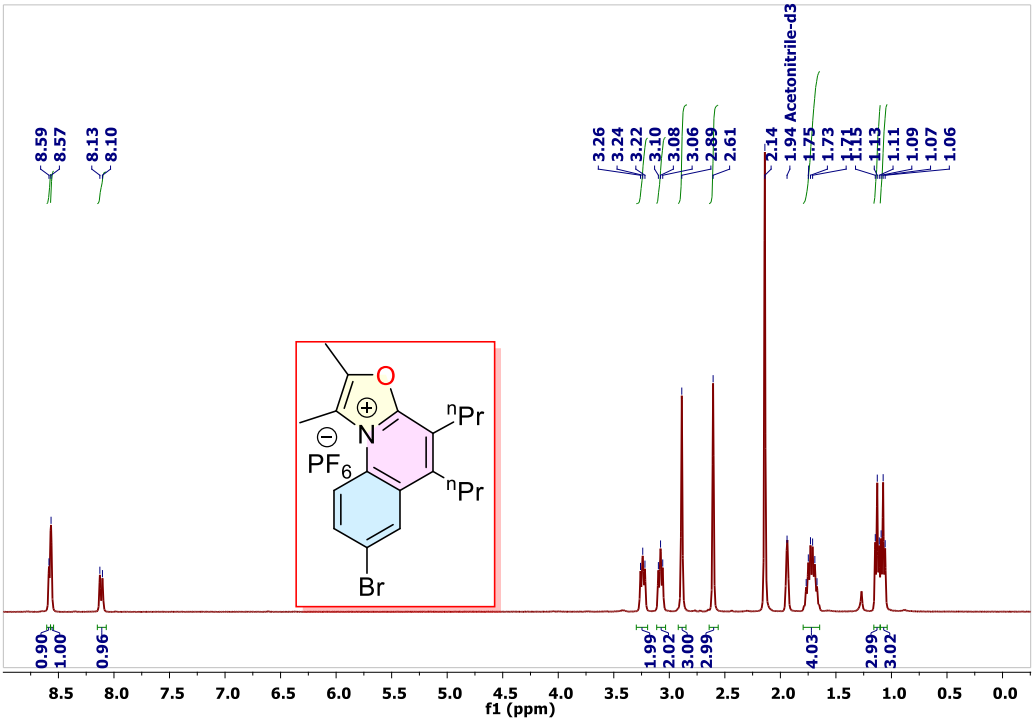

^{1}H NMR spectrum of **3i** (400 MHz, CD_3CN)

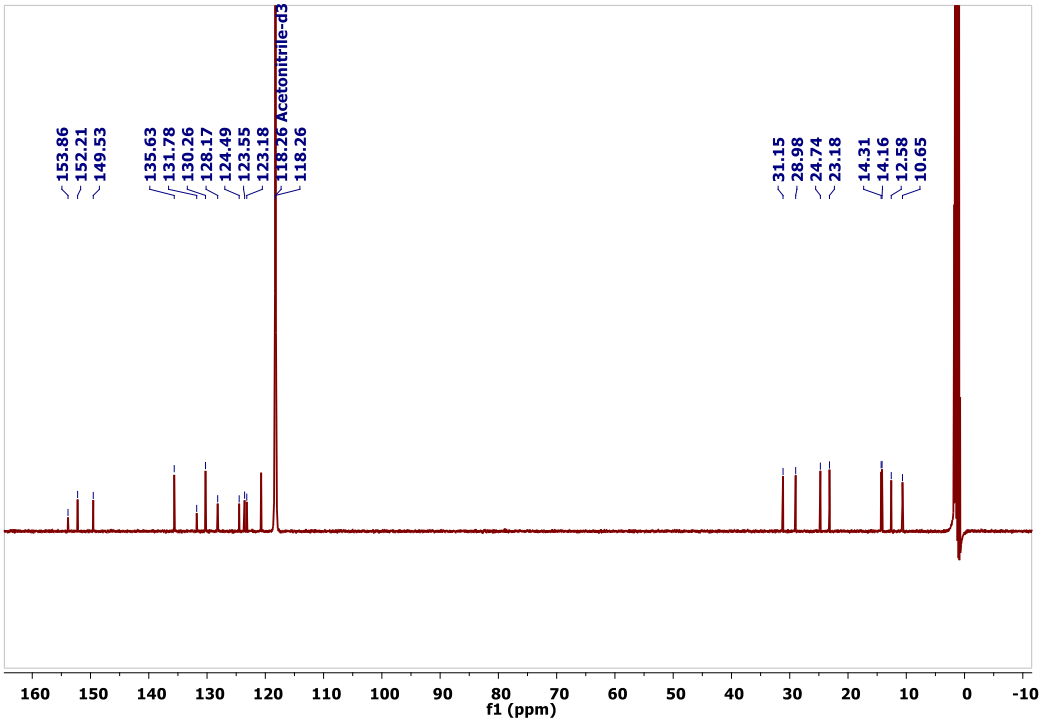

$^{13}C\{^{1}H\}$ NMR spectrum of **3i** (126 MHz, CD_3CN)

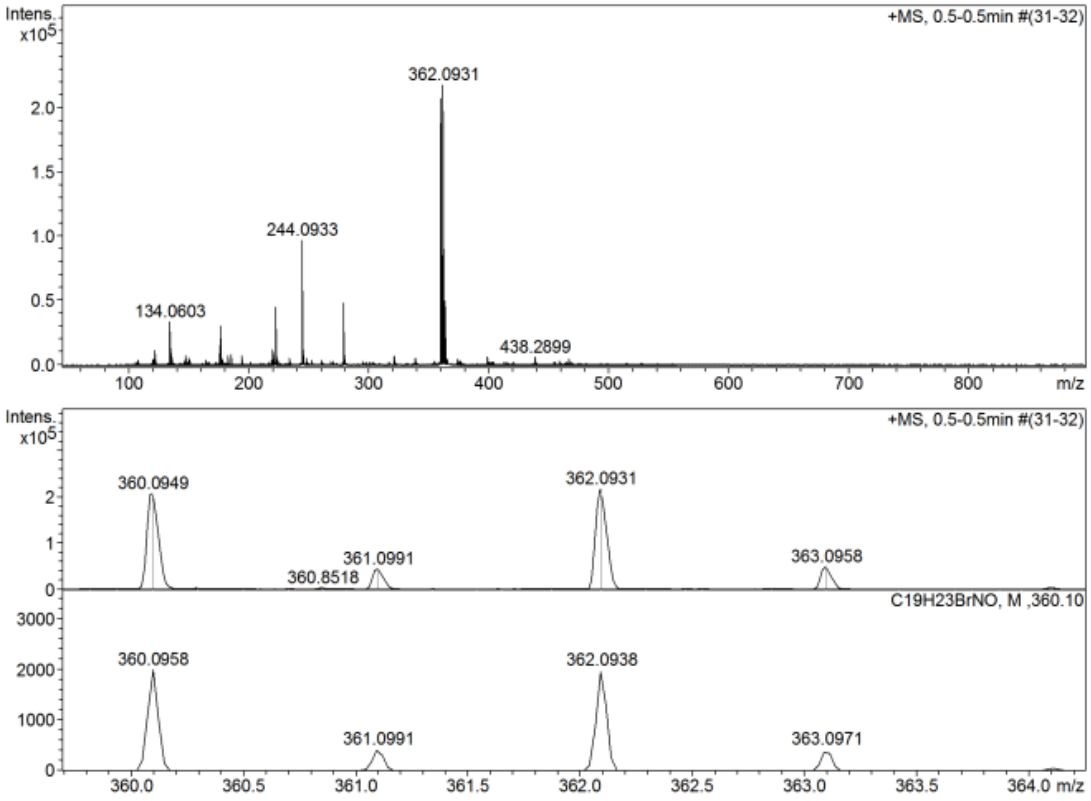

ESI-HRMS (positive ion mode) spectrum of **3i**

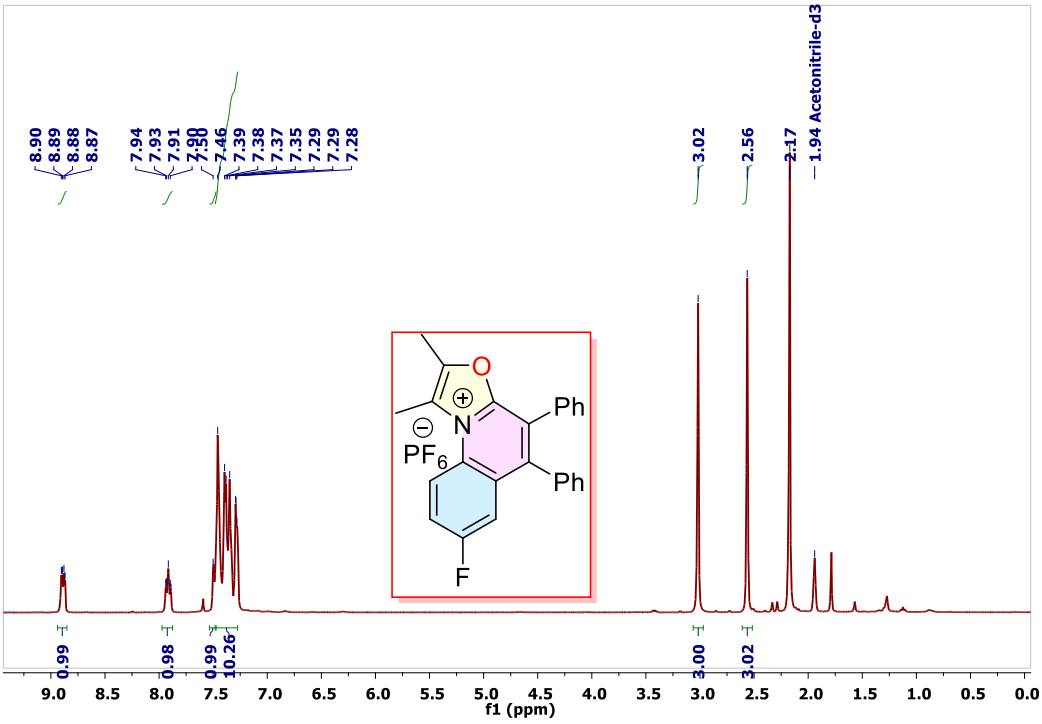

^{1}H NMR spectrum of **3j** (400 MHz, CD_3CN)

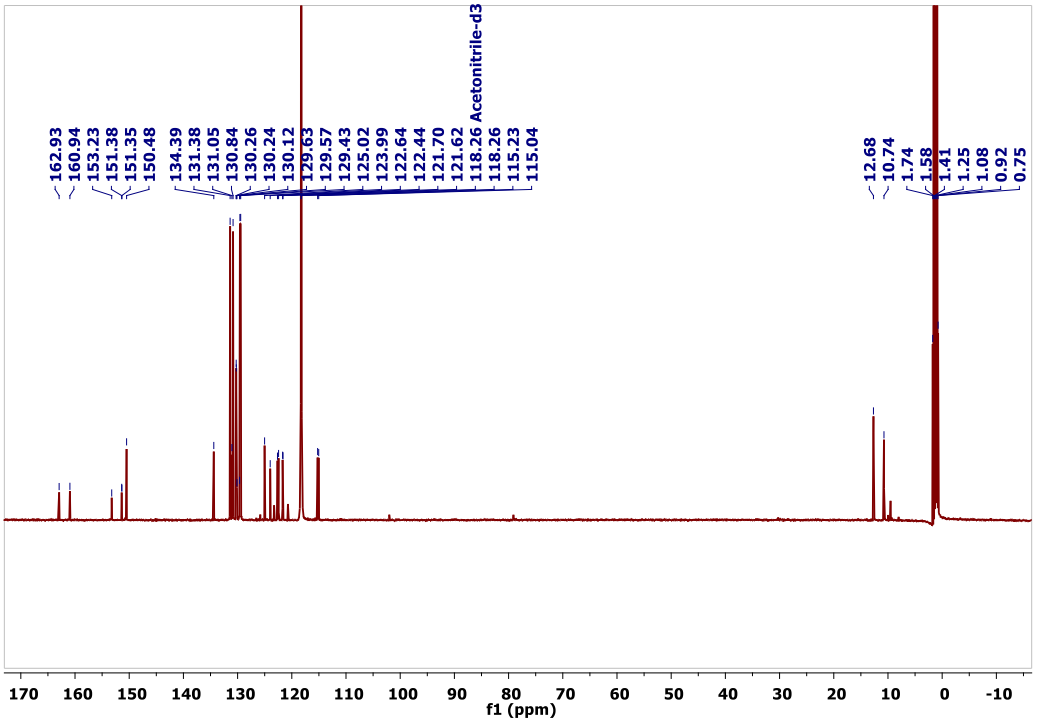

^{13}C{^{1}H} NMR spectrum of **3j** (126 MHz, CD_3CN)

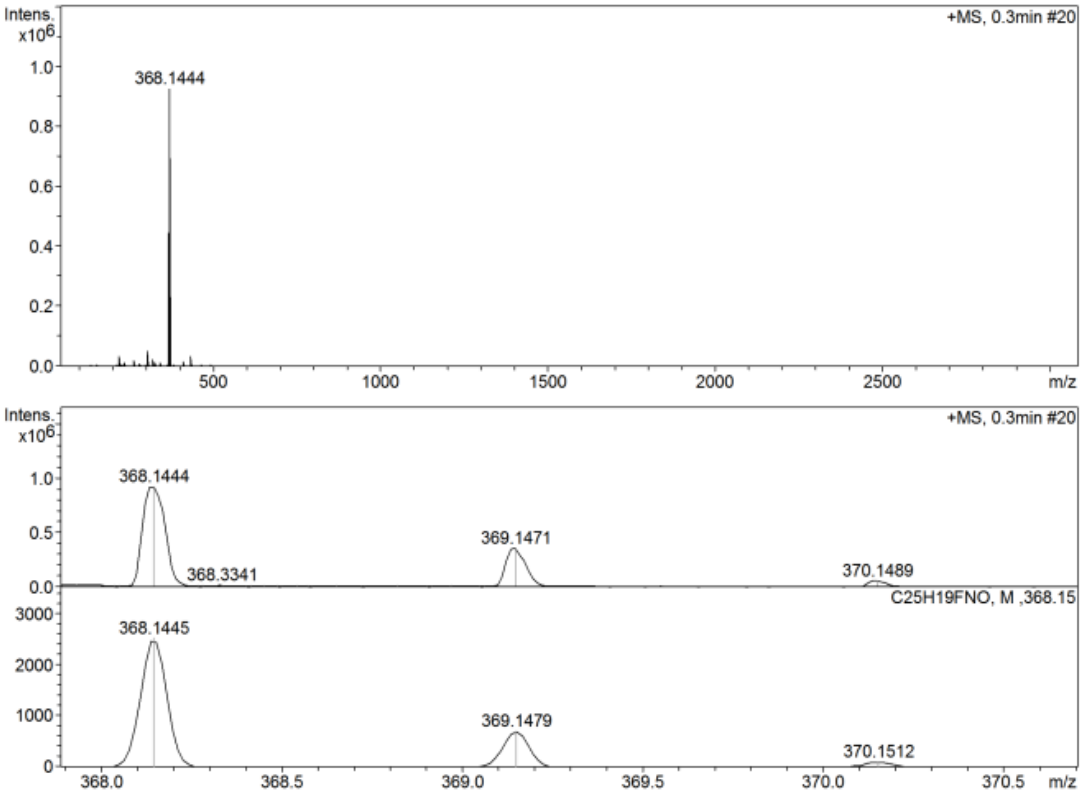

ESI-HRMS (positive ion mode) spectrum of **3j**

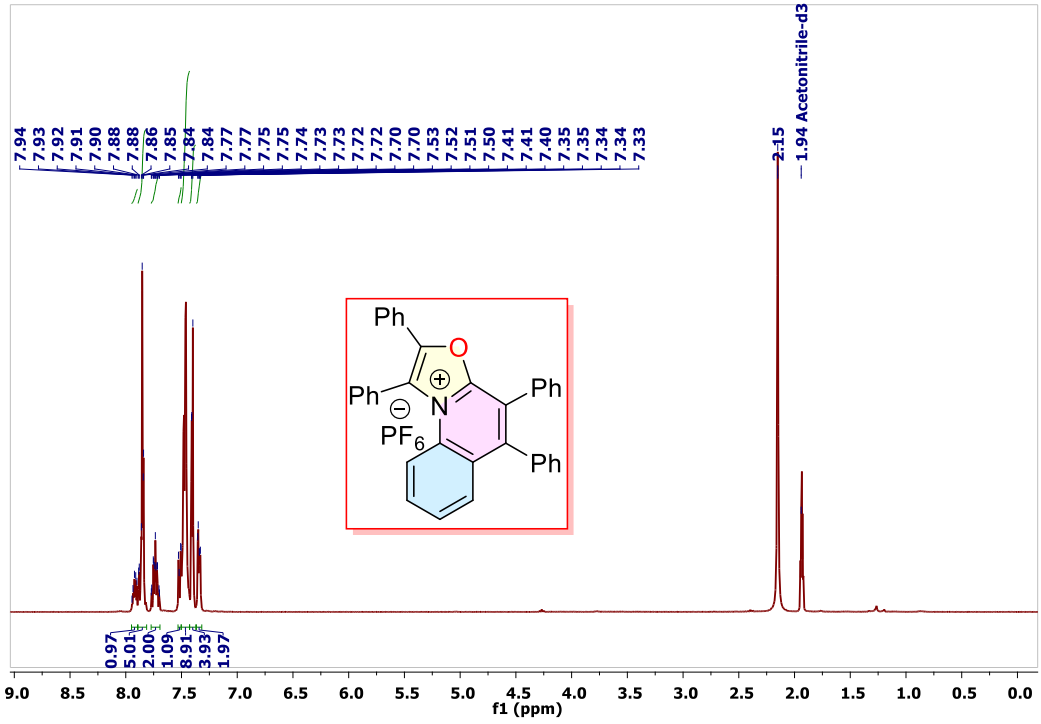

^{1}H NMR spectrum of **3k** (400 MHz, CD_3CN)

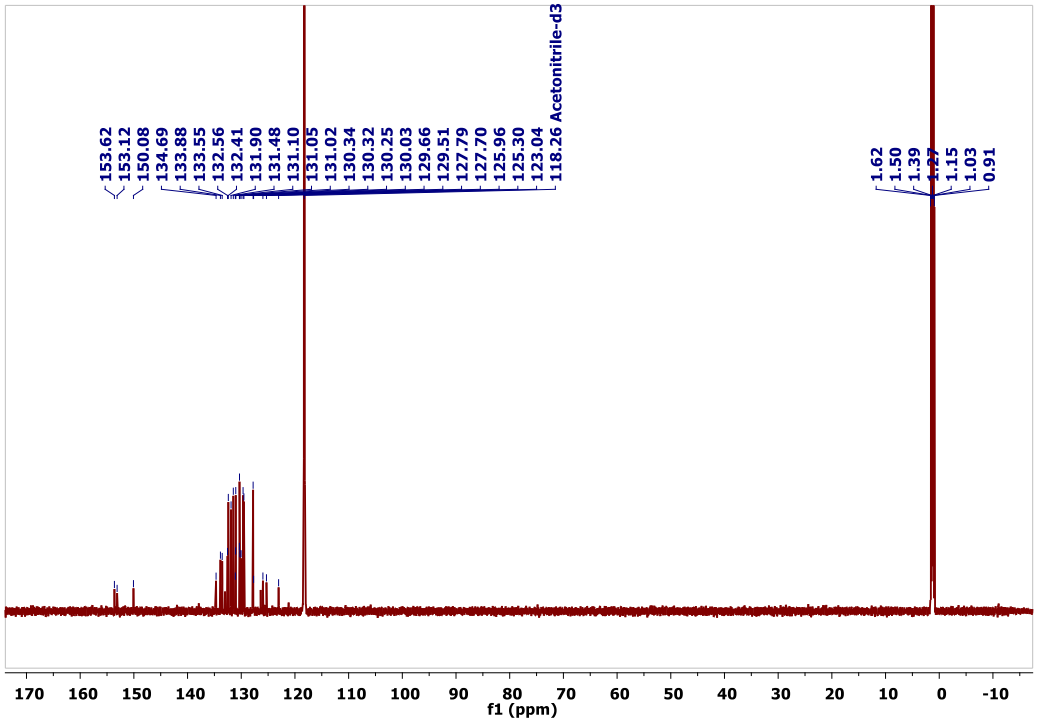

$^{13}C\{^{1}H\}$ NMR spectrum of **3k** (176 MHz, CD_3CN)

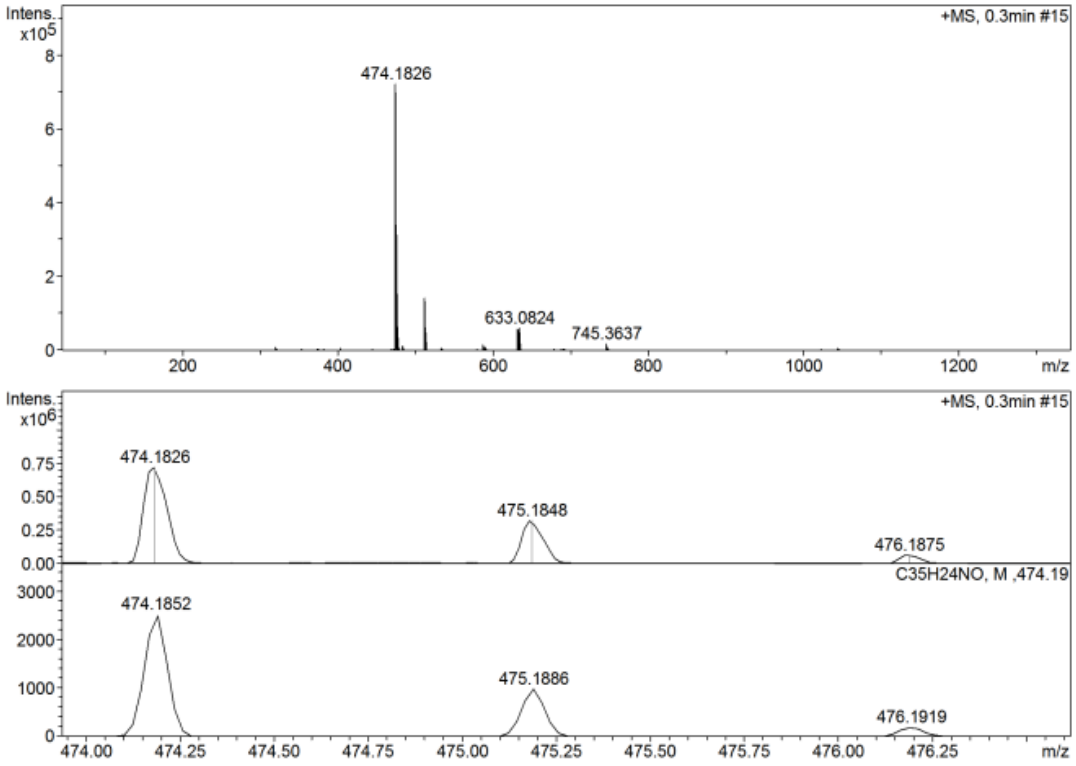

ESI-HRMS (positive ion mode) spectrum of **3k**

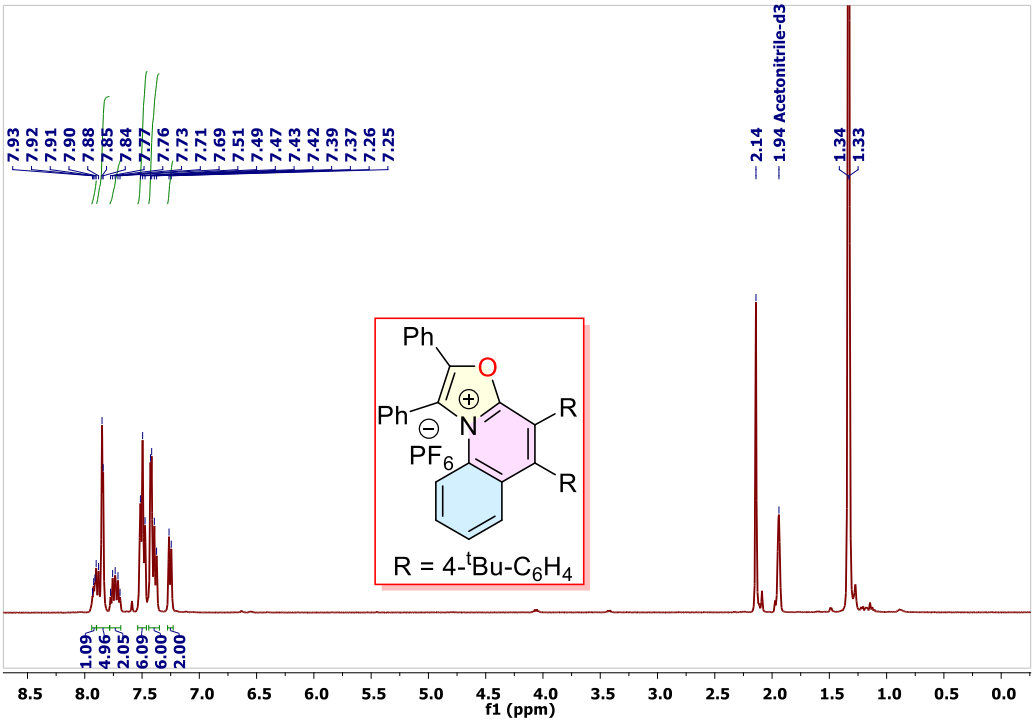

^{1}H NMR spectrum of **3l** (400 MHz, CD_3CN)

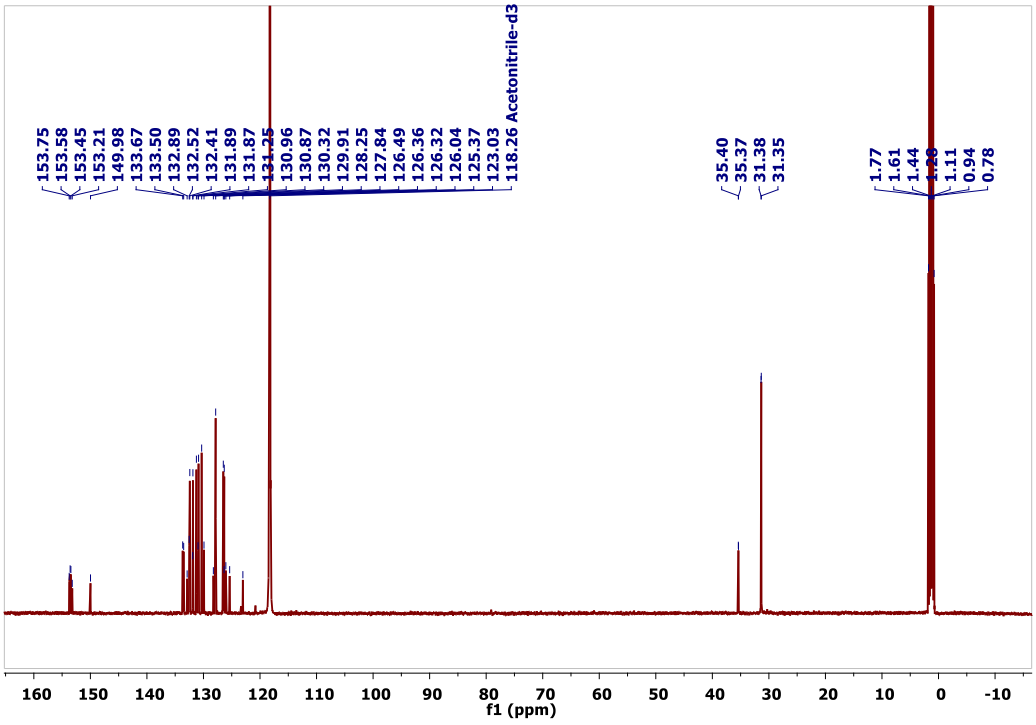

^{13}C{^{1}H} NMR spectrum of **3l** (126 MHz, CD_3CN)

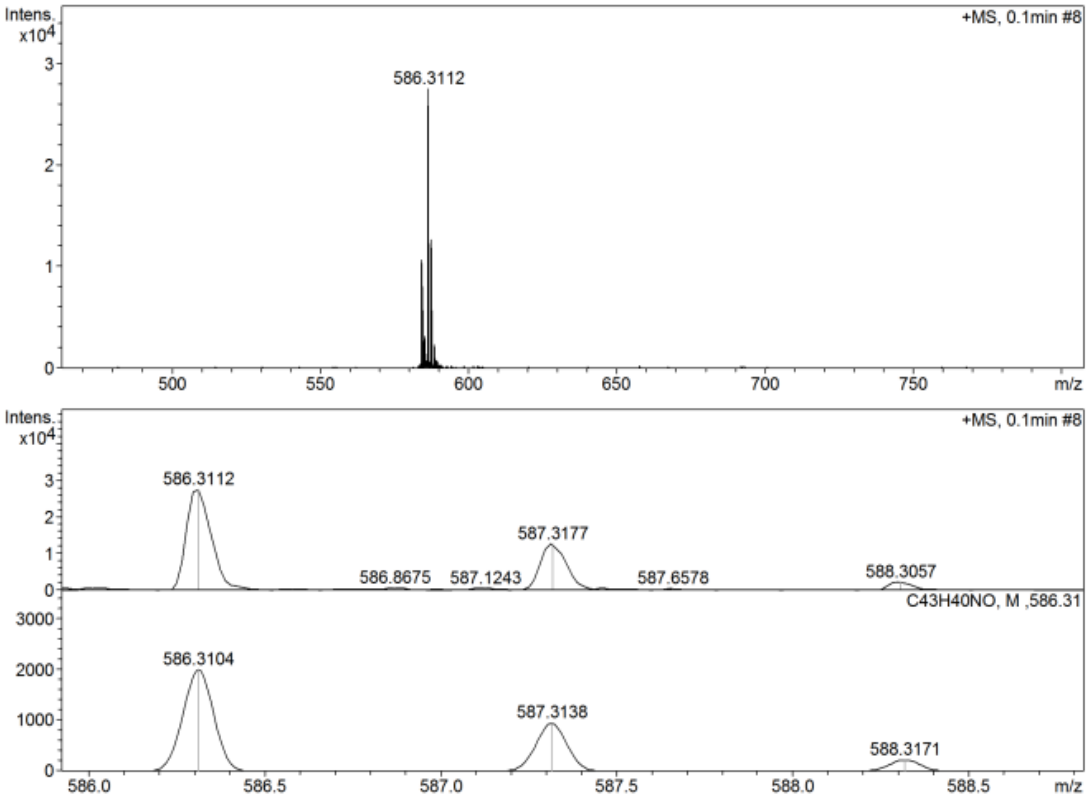

ESI-HRMS (positive ion mode) spectrum of **3l**

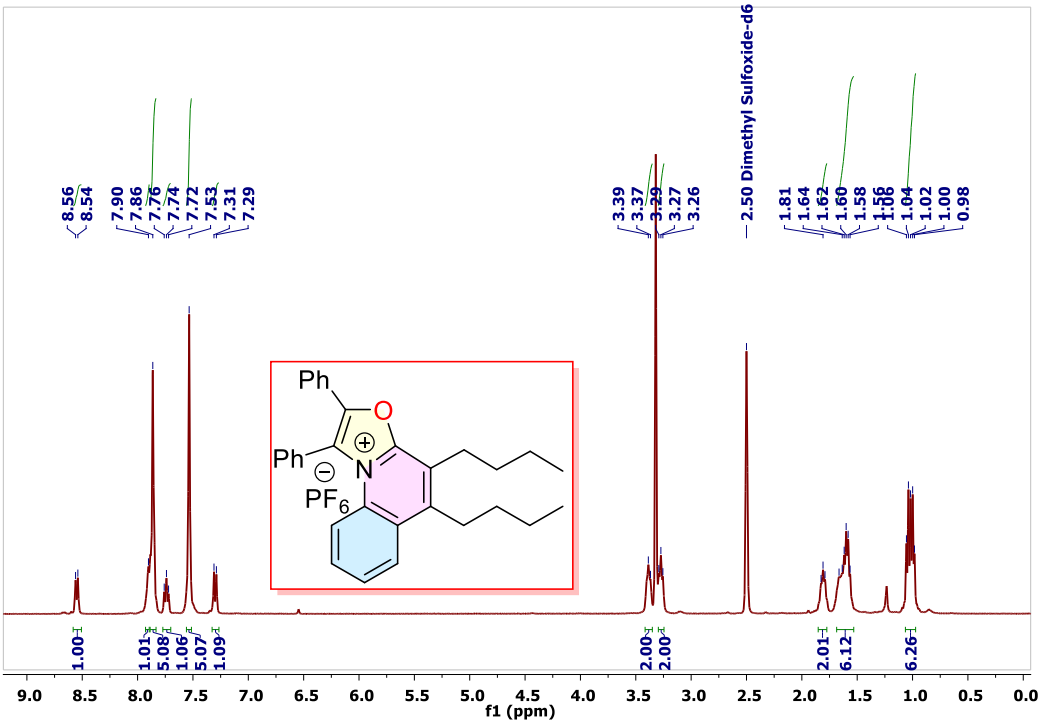

^{1}H NMR spectrum of **3m** (400 MHz, DMSO-d_6)

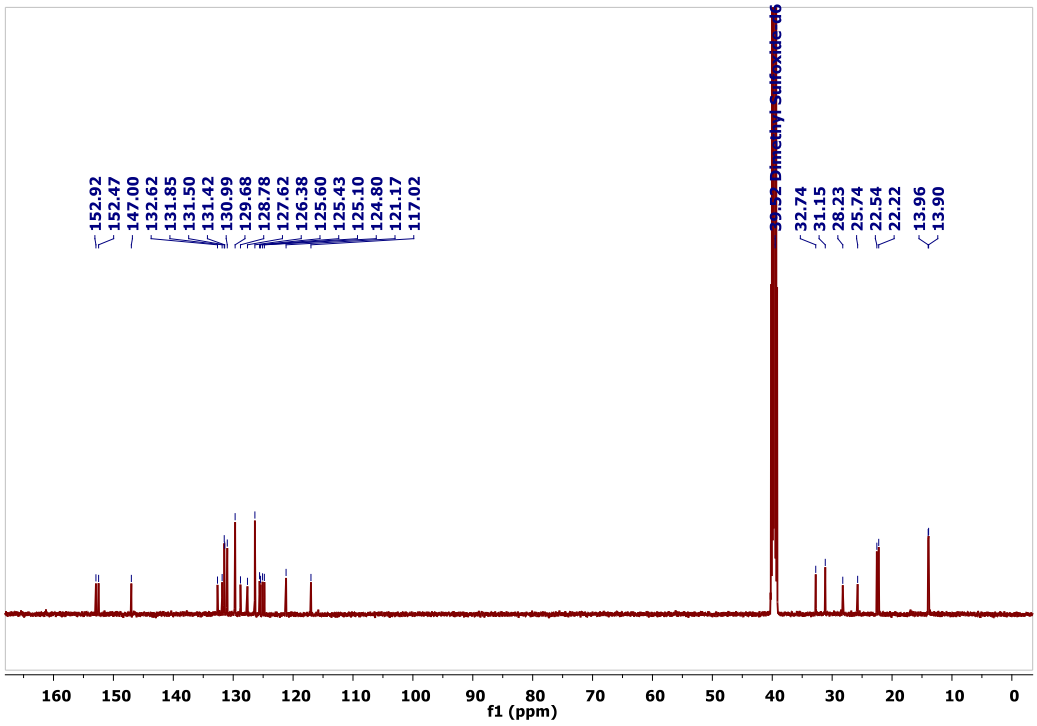

$^{13}C\{^{1}H\}$ NMR spectrum of **3m** (126 MHz, DMSO-d_6)

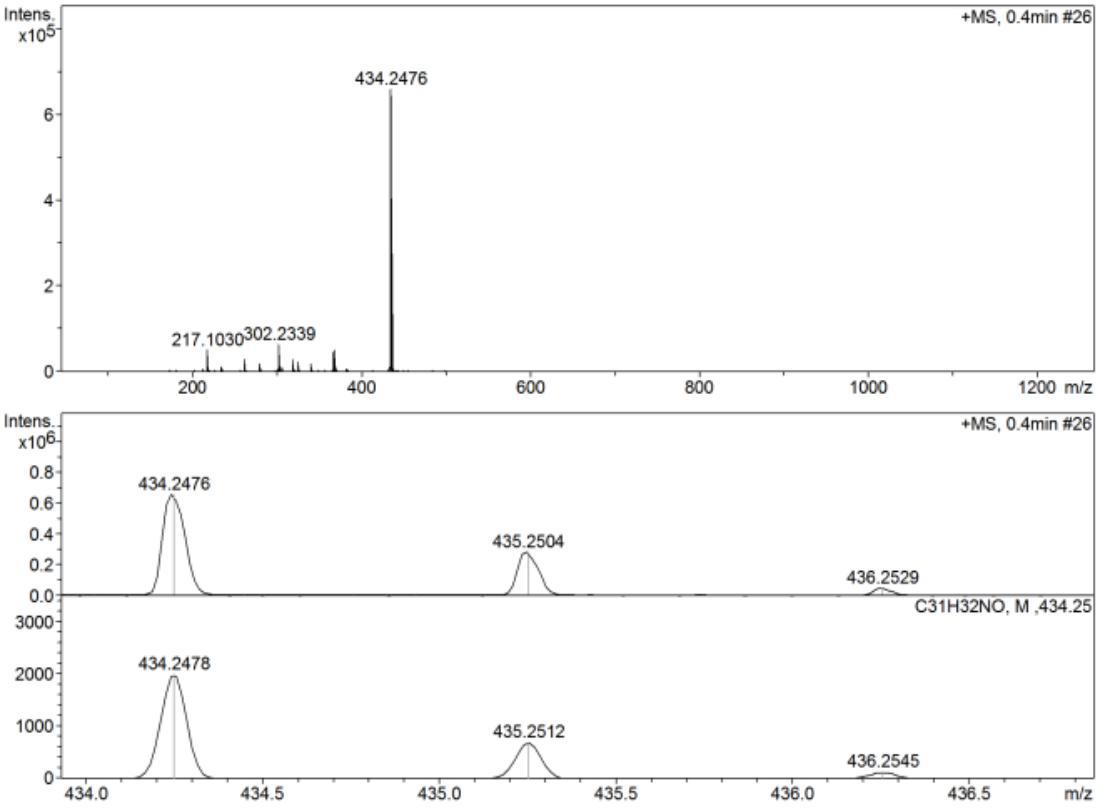

ESI-HRMS (positive ion mode) spectrum of **3m**

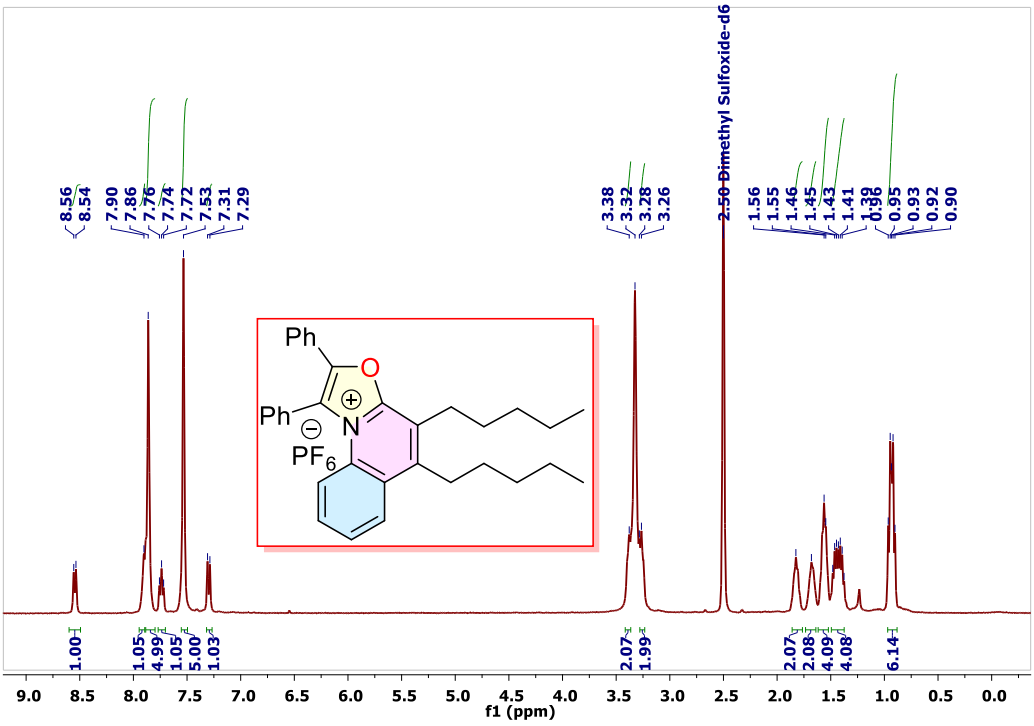

^{1}H NMR spectrum of **3n** (400 MHz, DMSO-d_6)

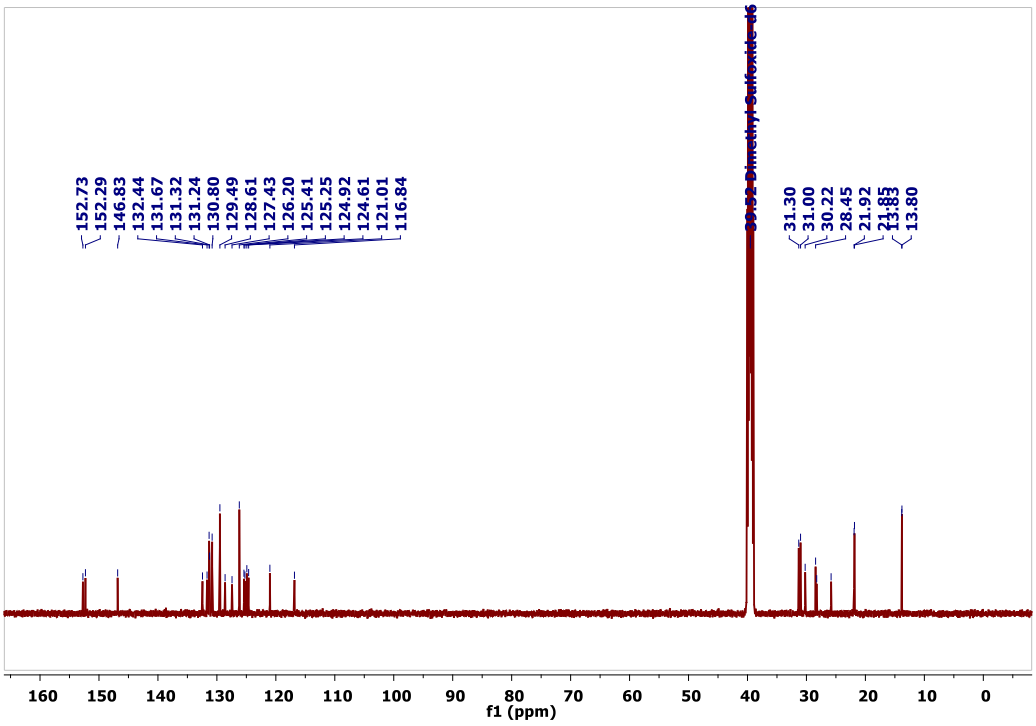

^{13}C{^{1}H} NMR spectrum of **3n** (126 MHz, DMSO-d_6)

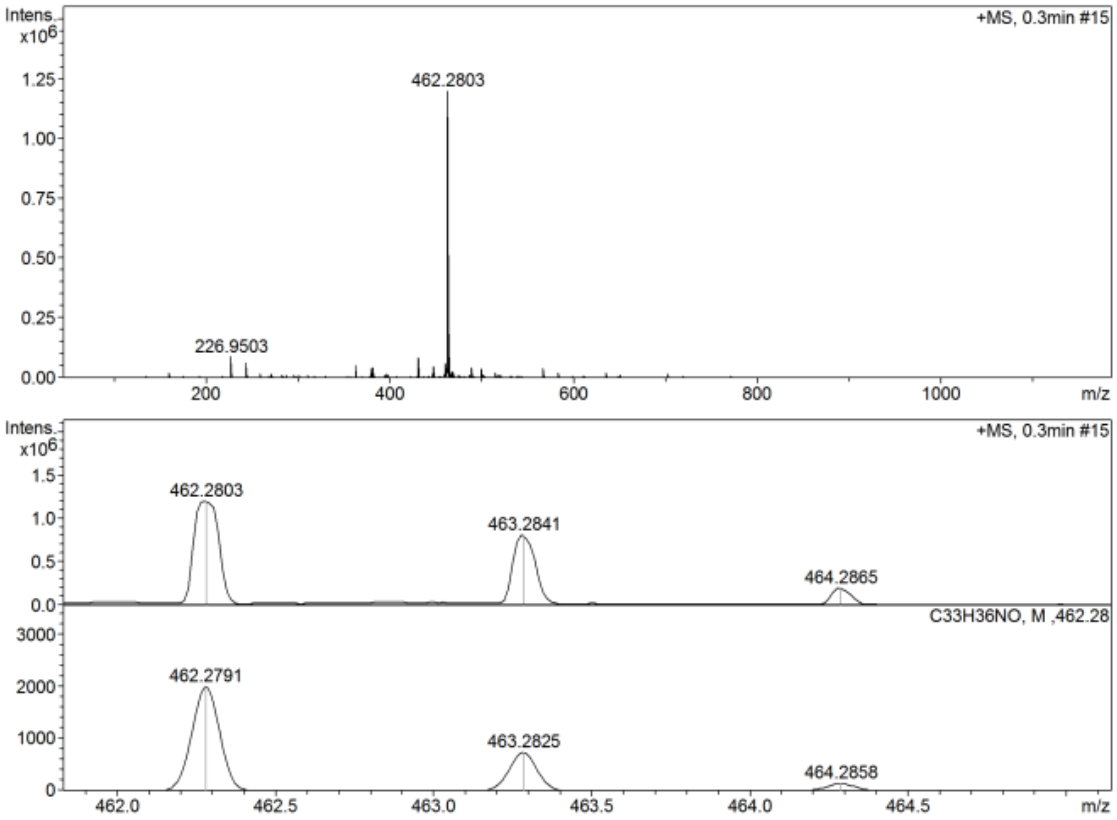

ESI-HRMS (positive ion mode) spectrum of **3n**

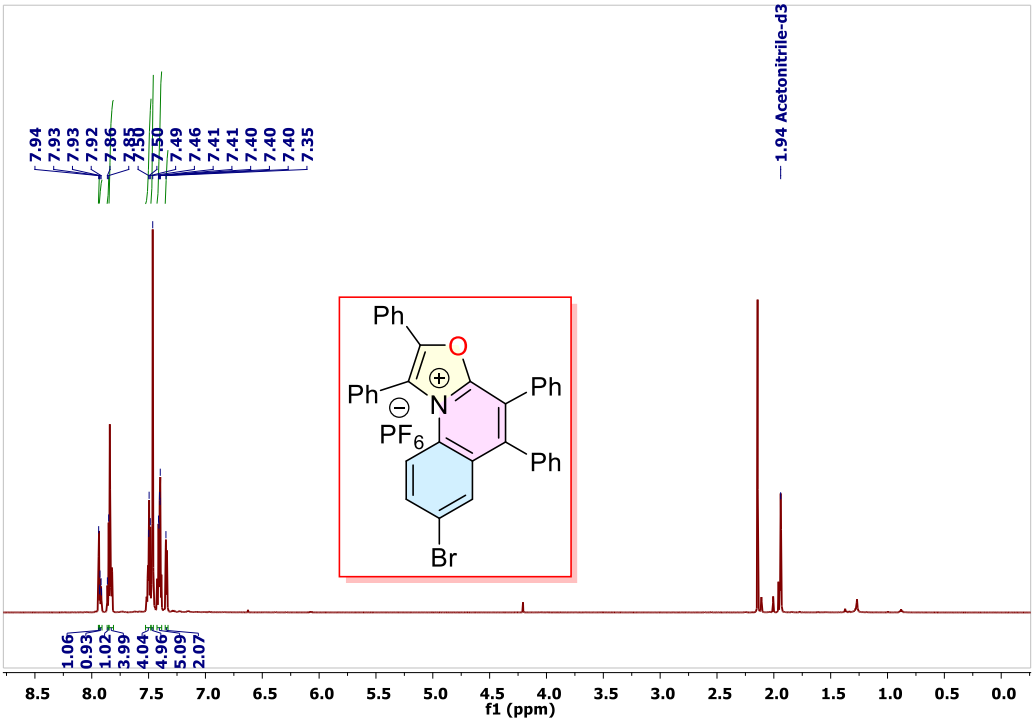

^{1}H NMR spectrum of **3o** (700 MHz, CD_3CN)

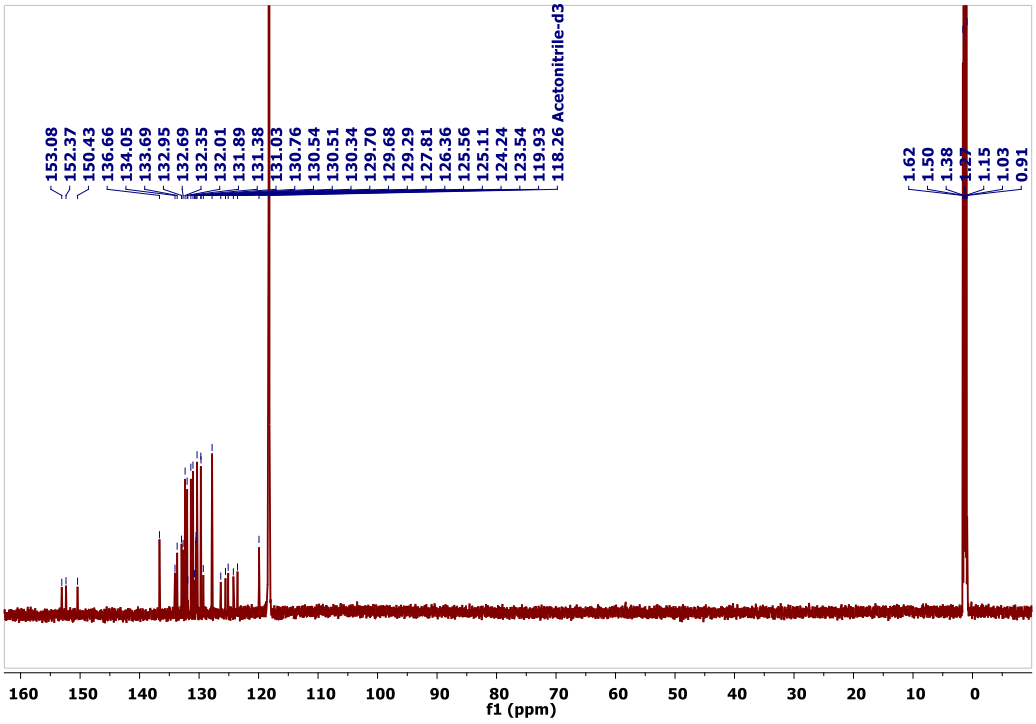

$^{13}C\{^{1}H\}$ NMR spectrum of **3o** (176 MHz, CD_3CN)

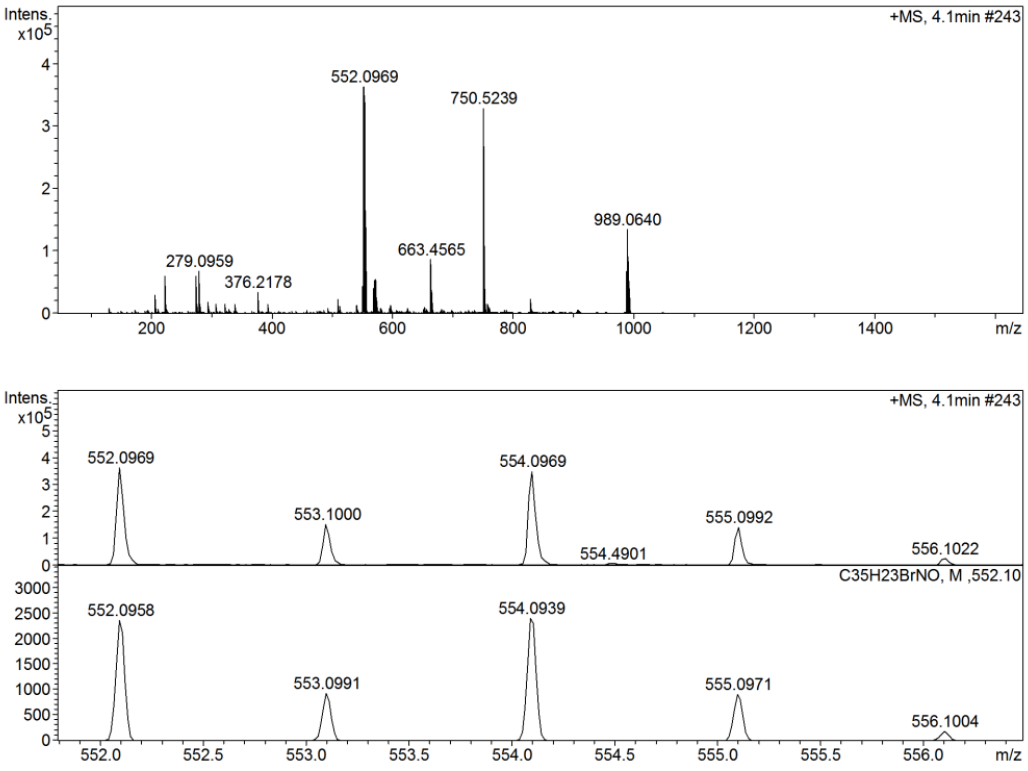

ESI-HRMS (positive ion mode) spectrum of **3o**

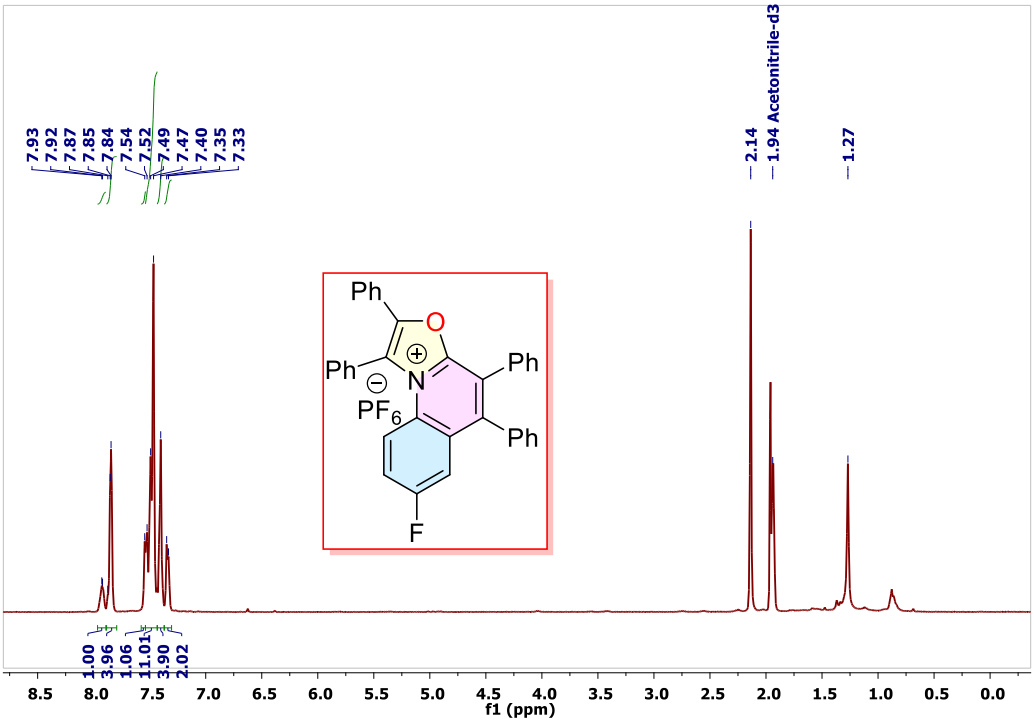

^{1}H NMR spectrum of **3p** (400 MHz, CD_3CN)

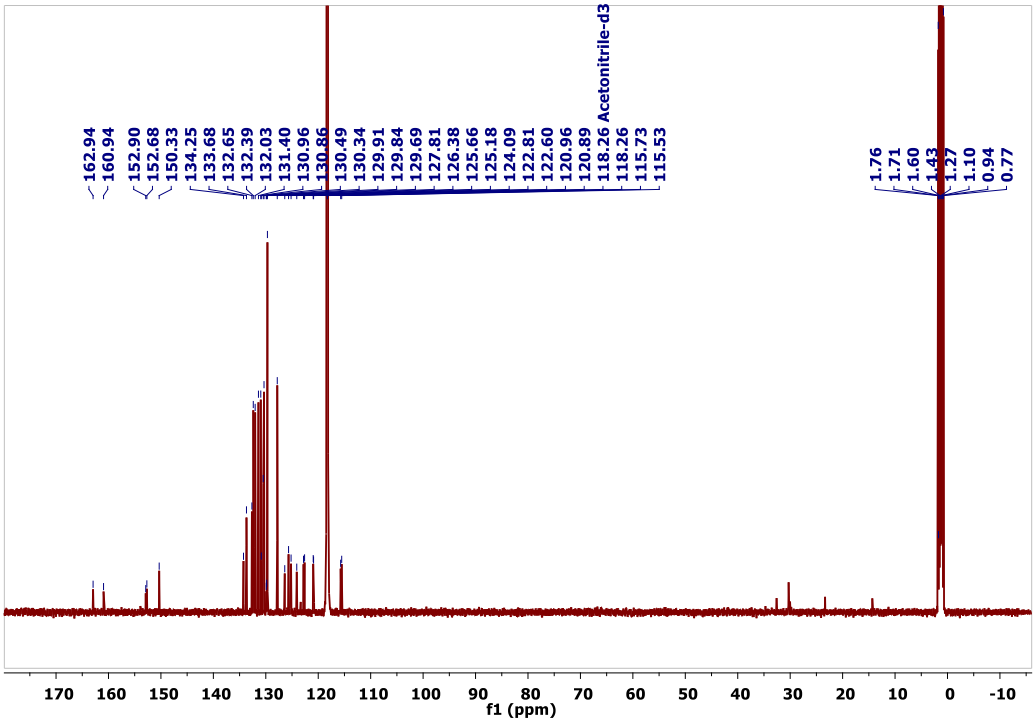

^{13}C{^{1}H} NMR spectrum of **3p** (126 MHz, CD_3CN)

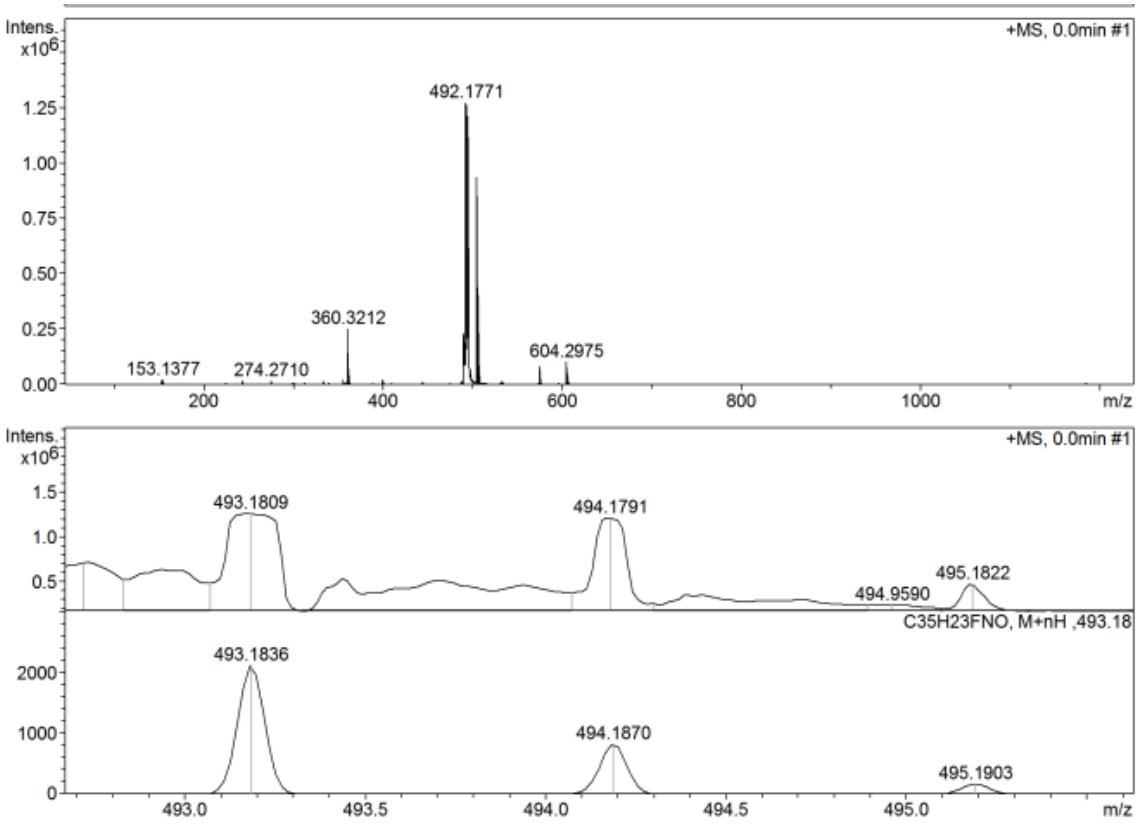

ESI-HRMS (positive ion mode) spectrum of **3p**

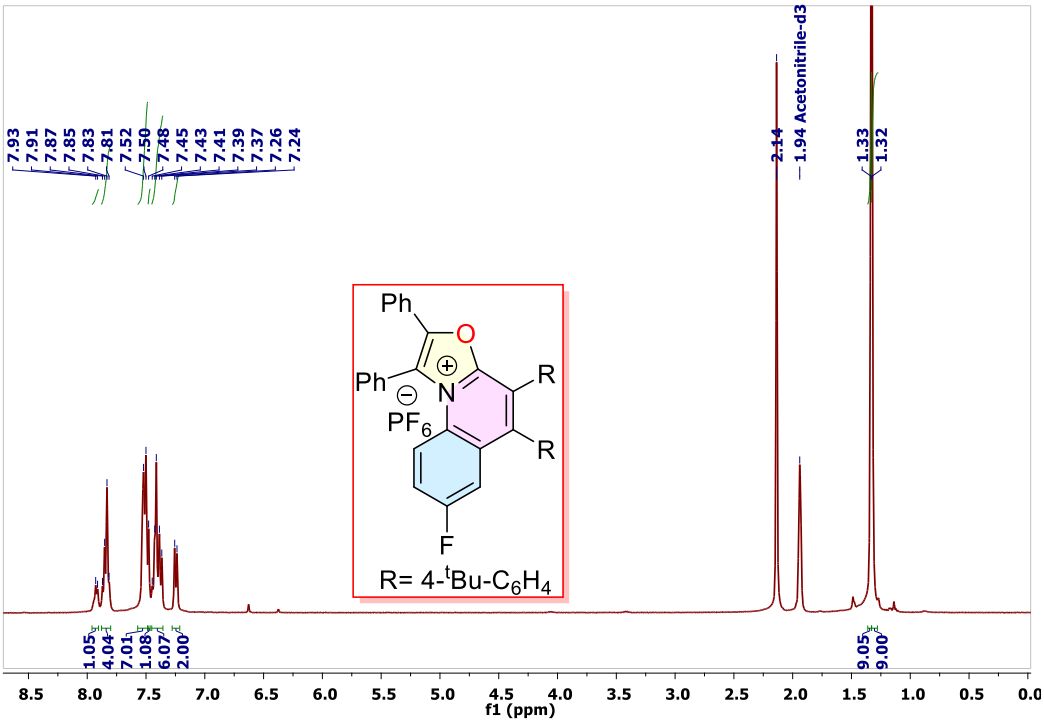

^{1}H NMR spectrum of **3q** (400 MHz, CD_3CN)

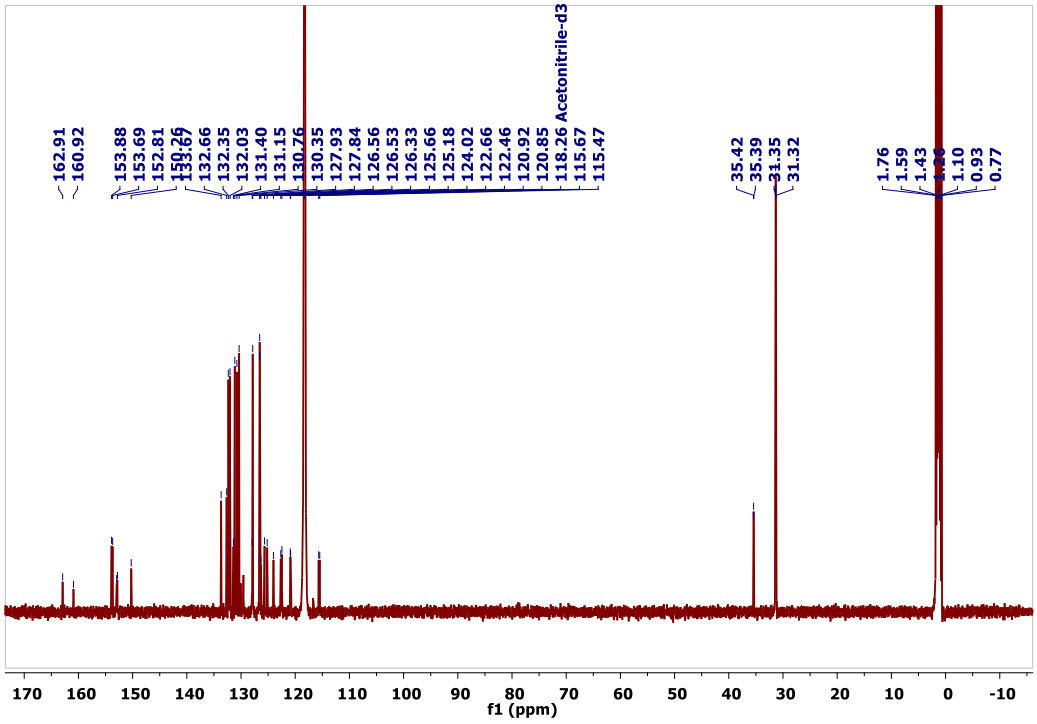

$^{13}C\{1H\}$ NMR spectrum of **3q** (126 MHz, CD_3CN)

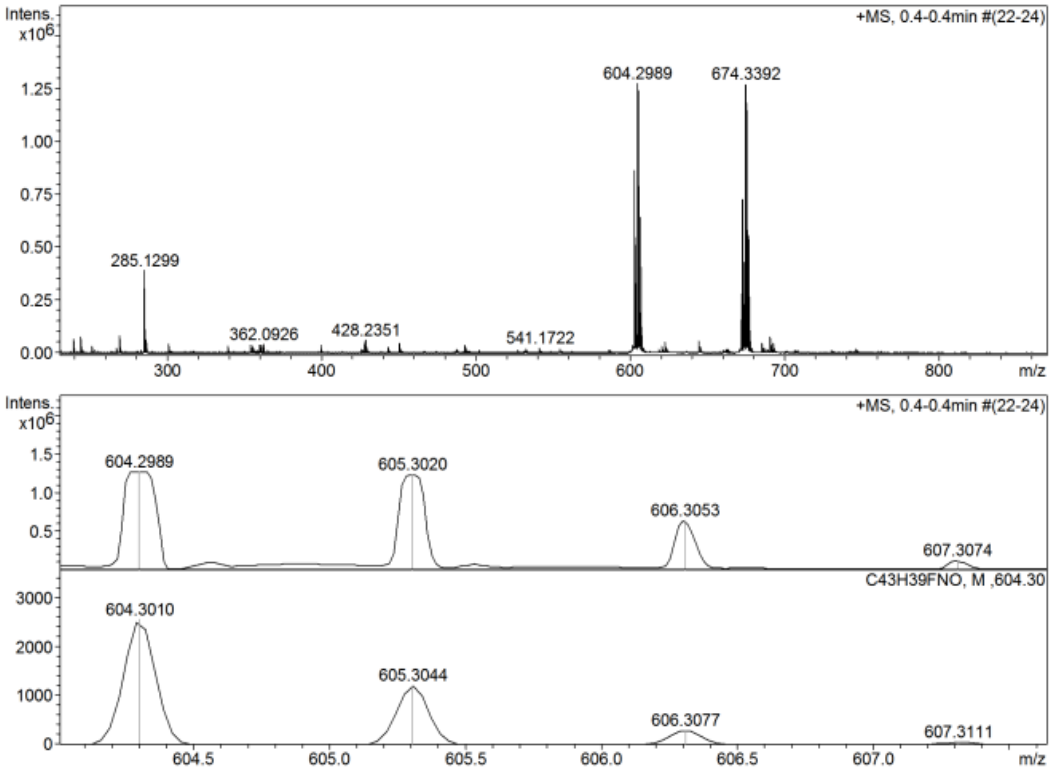

ESI-HRMS (positive ion mode) spectrum of **3q**

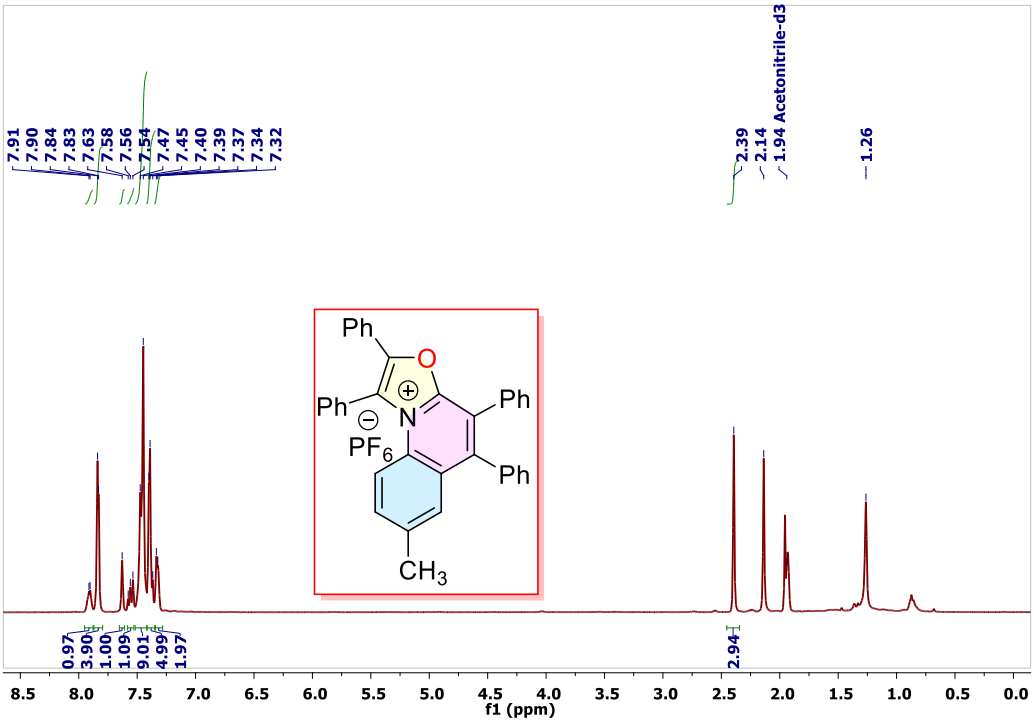

^{1}H NMR spectrum of **3r** (400 MHz, CD_3CN)

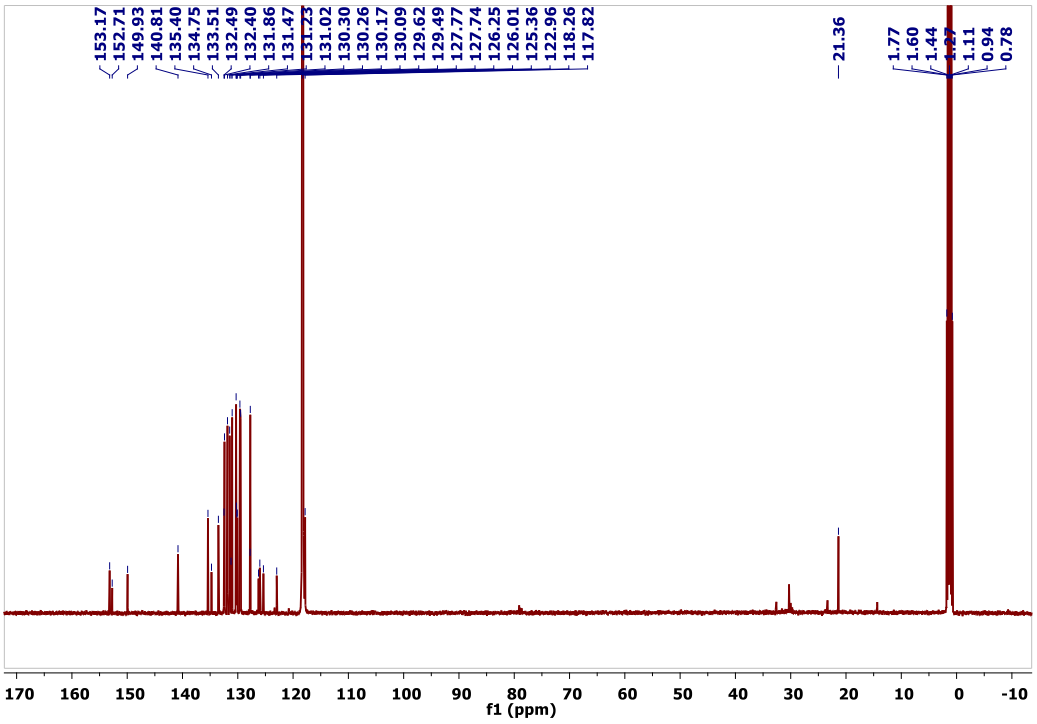

^{13}C{1H} NMR spectrum of **3r** (126 MHz, CD_3CN)

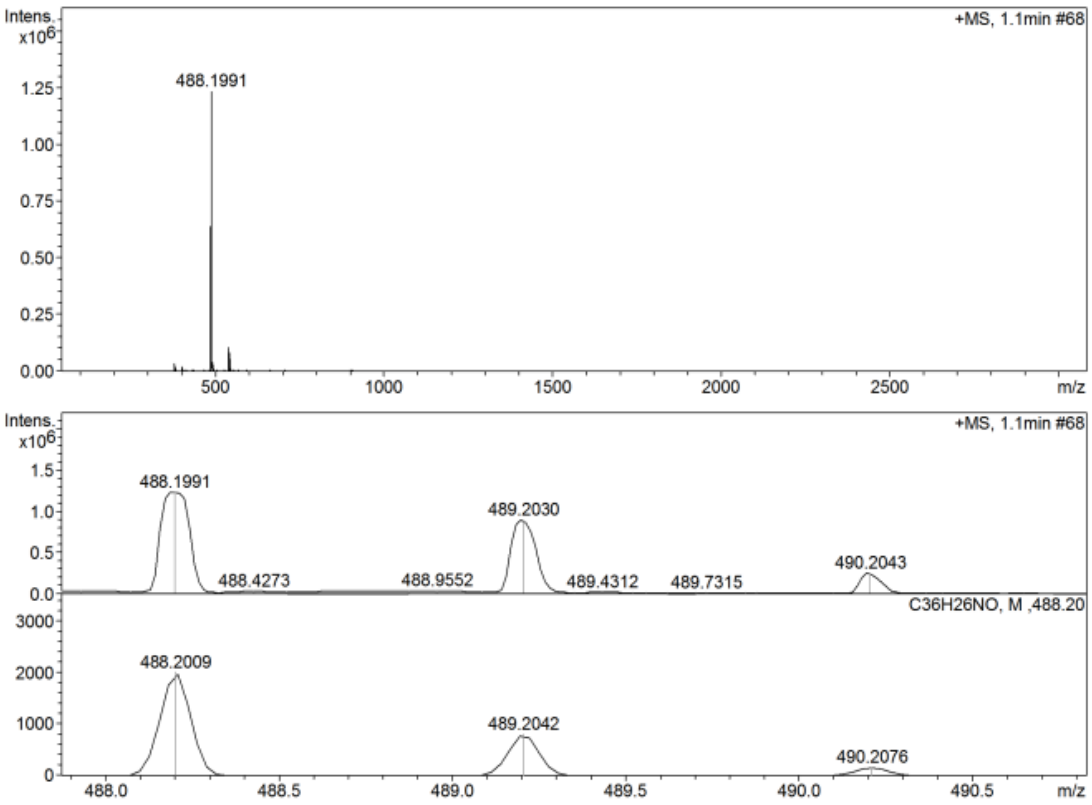

ESI-HRMS (positive ion mode) spectrum of **3r**

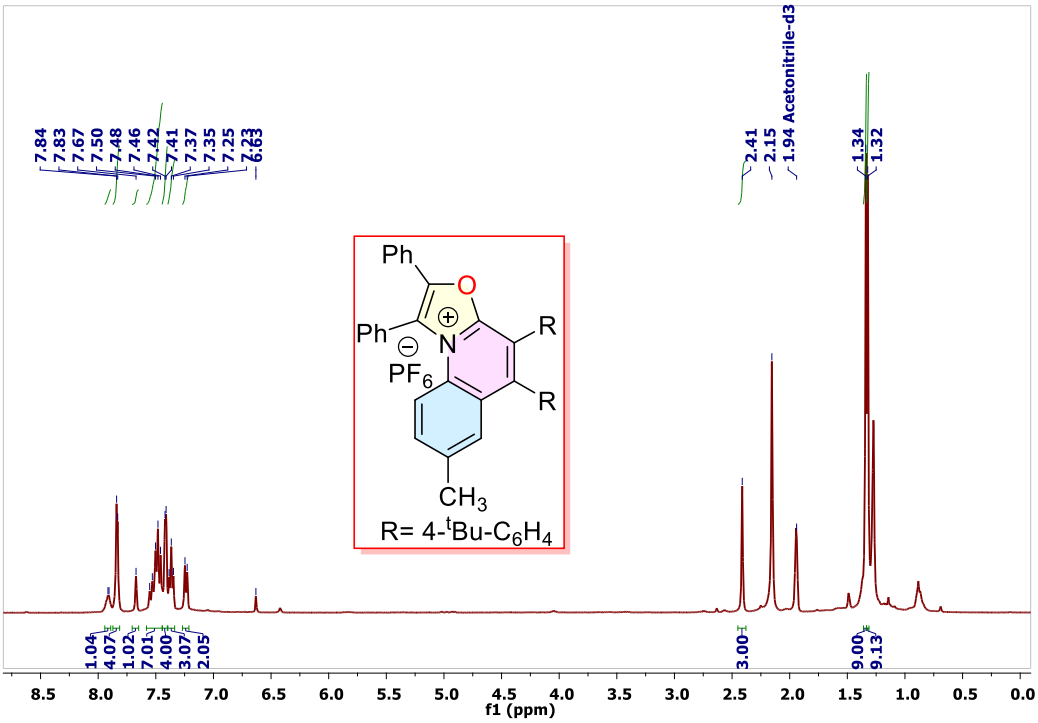

^{1}H NMR spectrum of **3s** (400 MHz, CD_3CN)

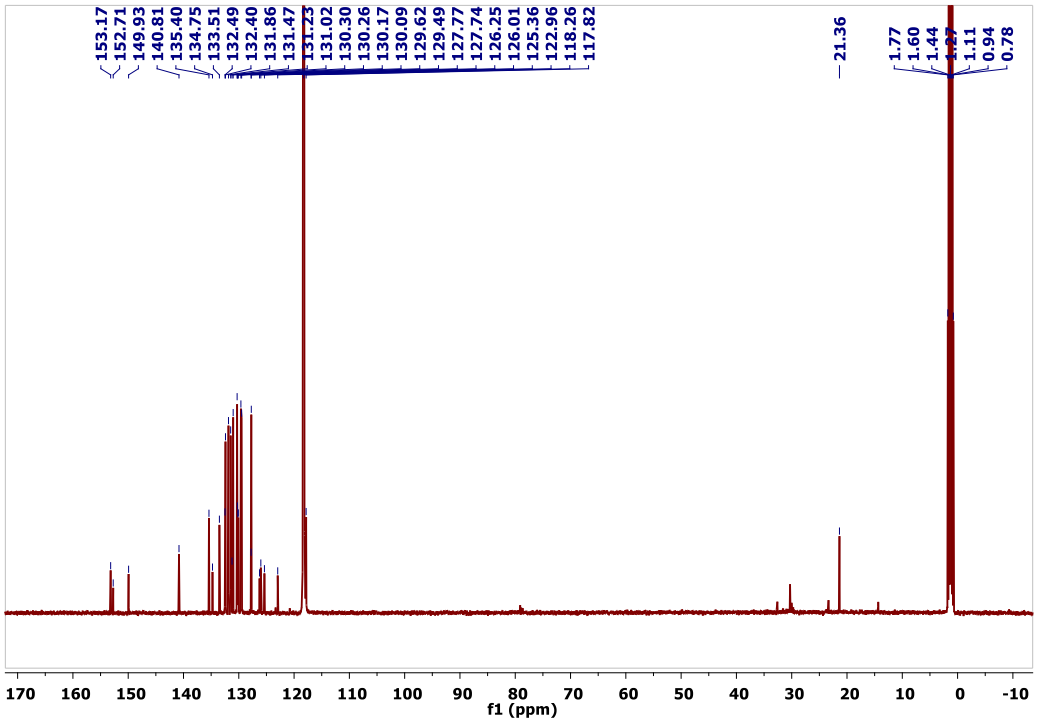

$^{13}C\{1H\}$ NMR spectrum of **3s** (126 MHz, CD_3CN)

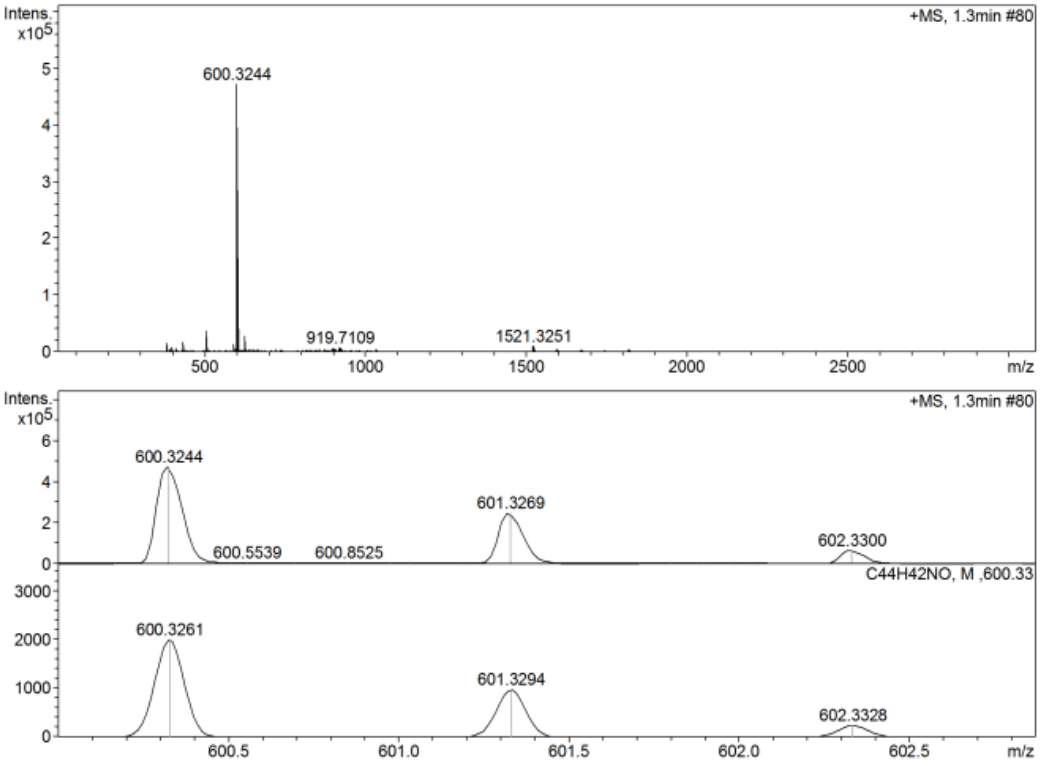

ESI-HRMS (positive ion mode) spectrum of **3s**

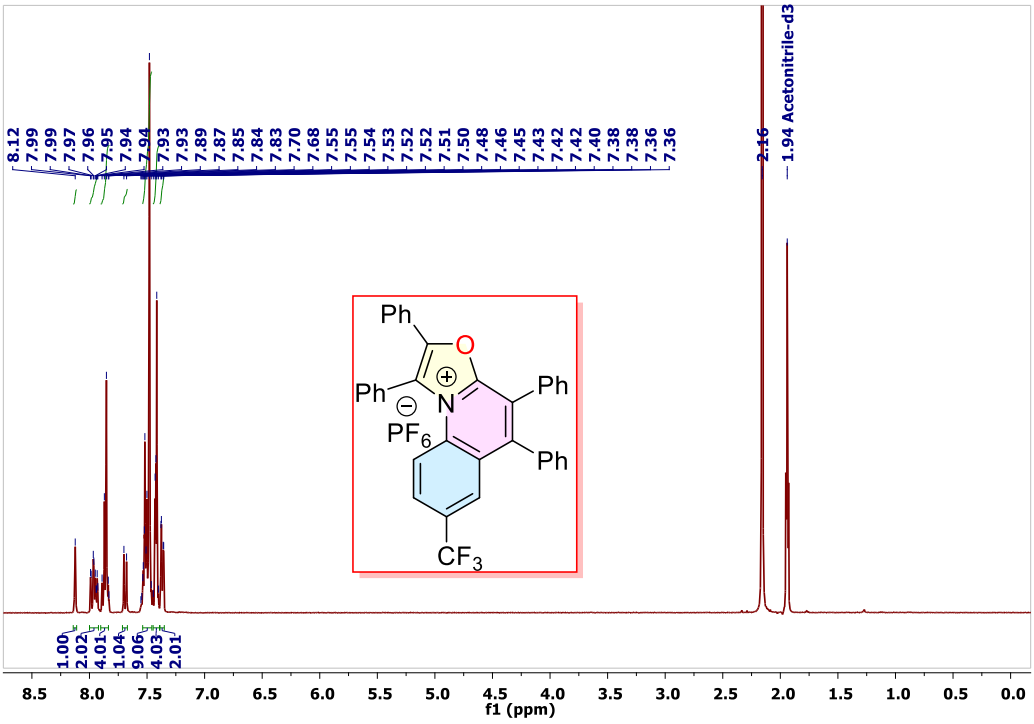

^{1}H NMR spectrum of **3t** (400 MHz, CD_3CN)

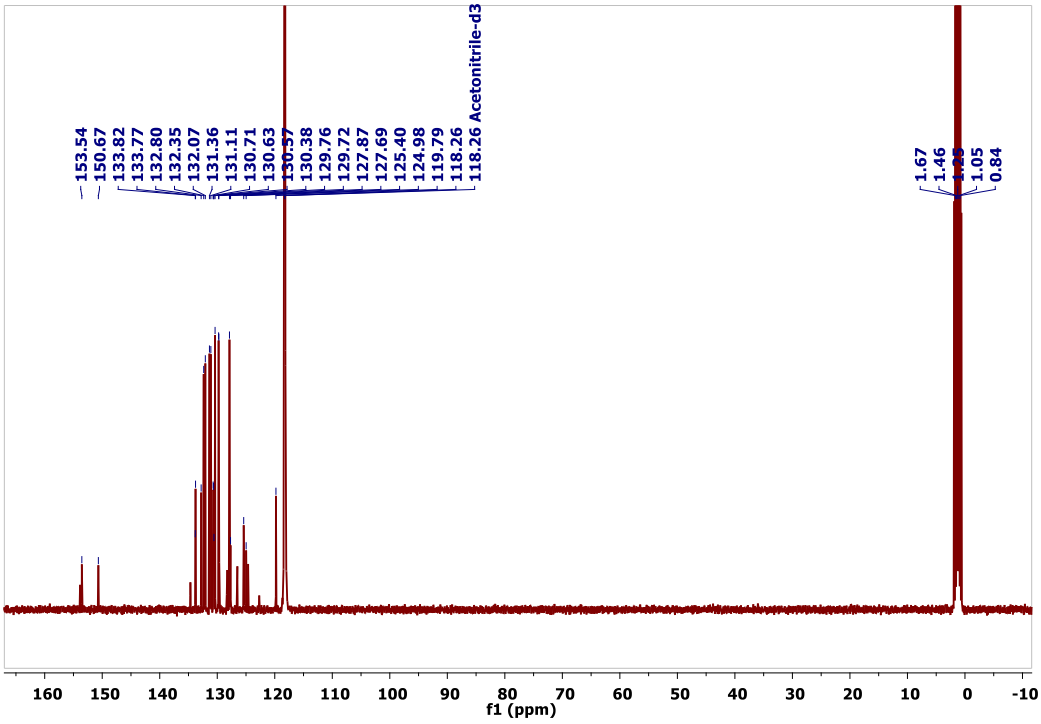

^{13}C{^{1}H} NMR spectrum of **3t** (101 MHz, CD_3CN)

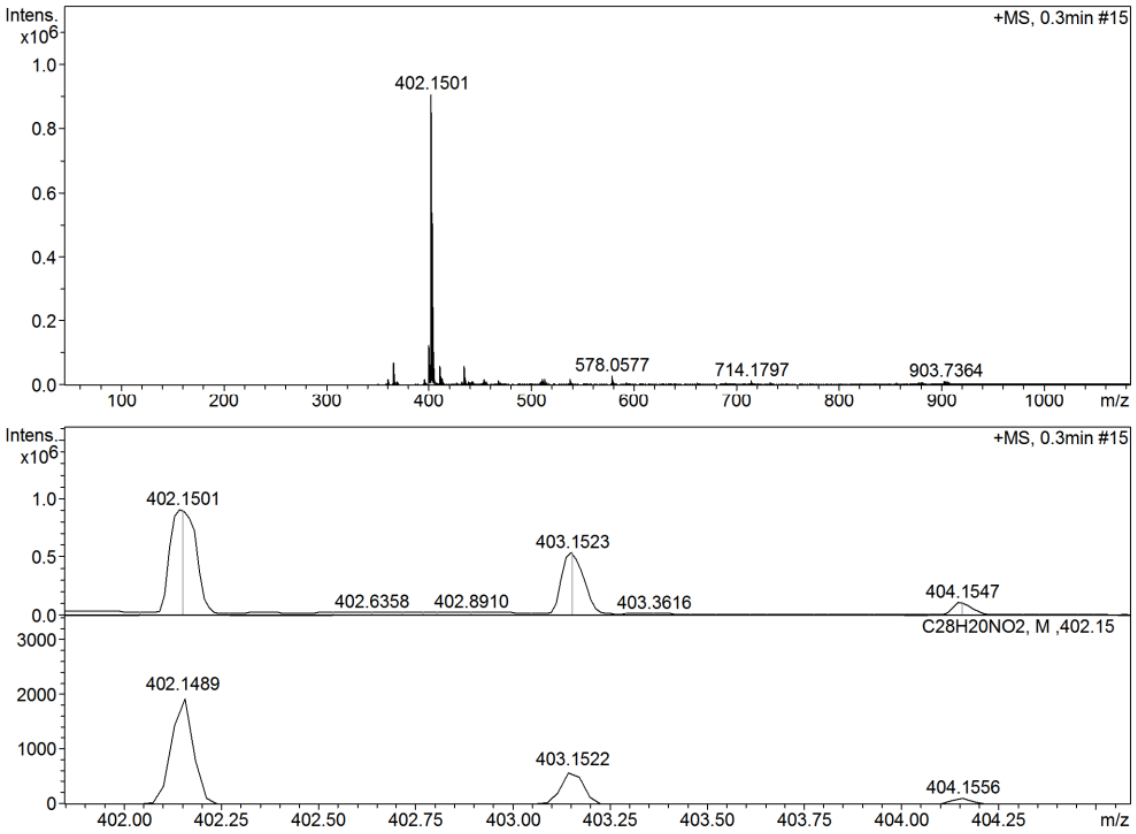

ESI-HRMS (positive ion mode) spectrum of **3t**

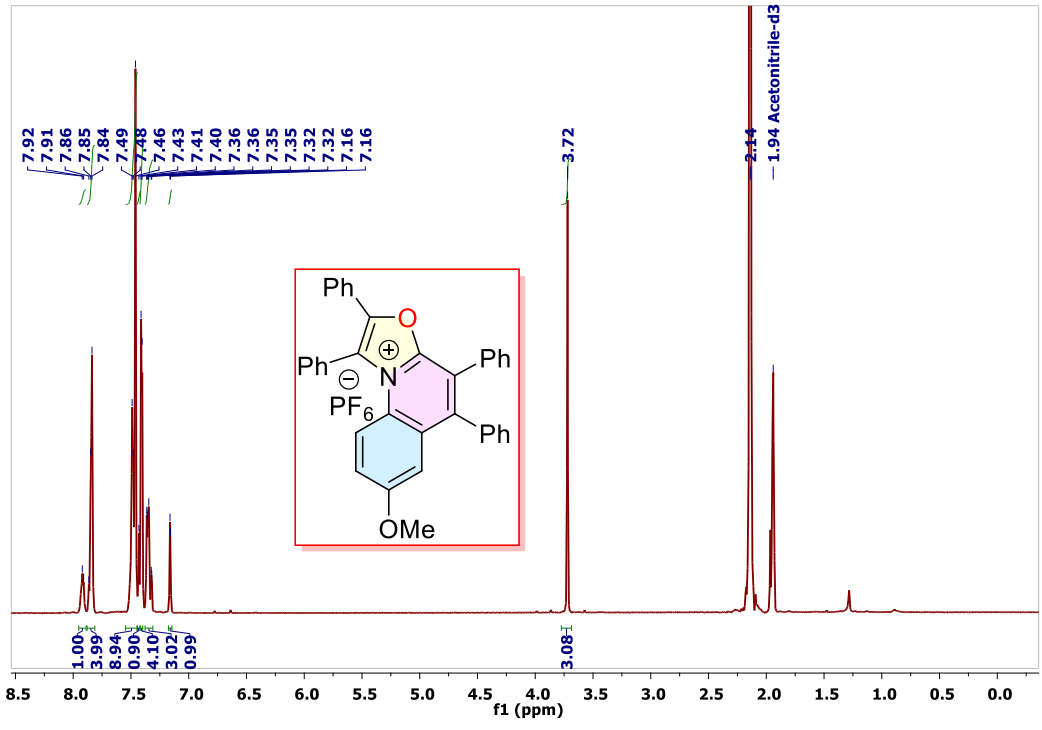

^{1}H NMR spectrum of **3u** (400 MHz, CD_3CN)

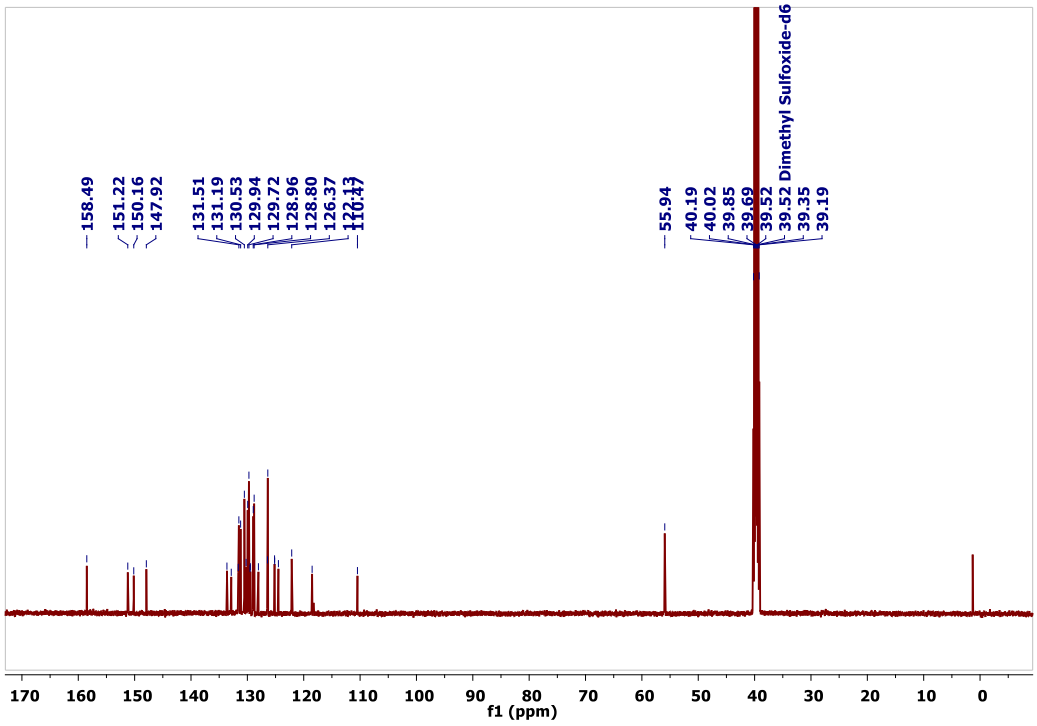

$^{13}C\{^{1}H\}$ NMR spectrum of **3u** (126 MHz, CD_3CN)

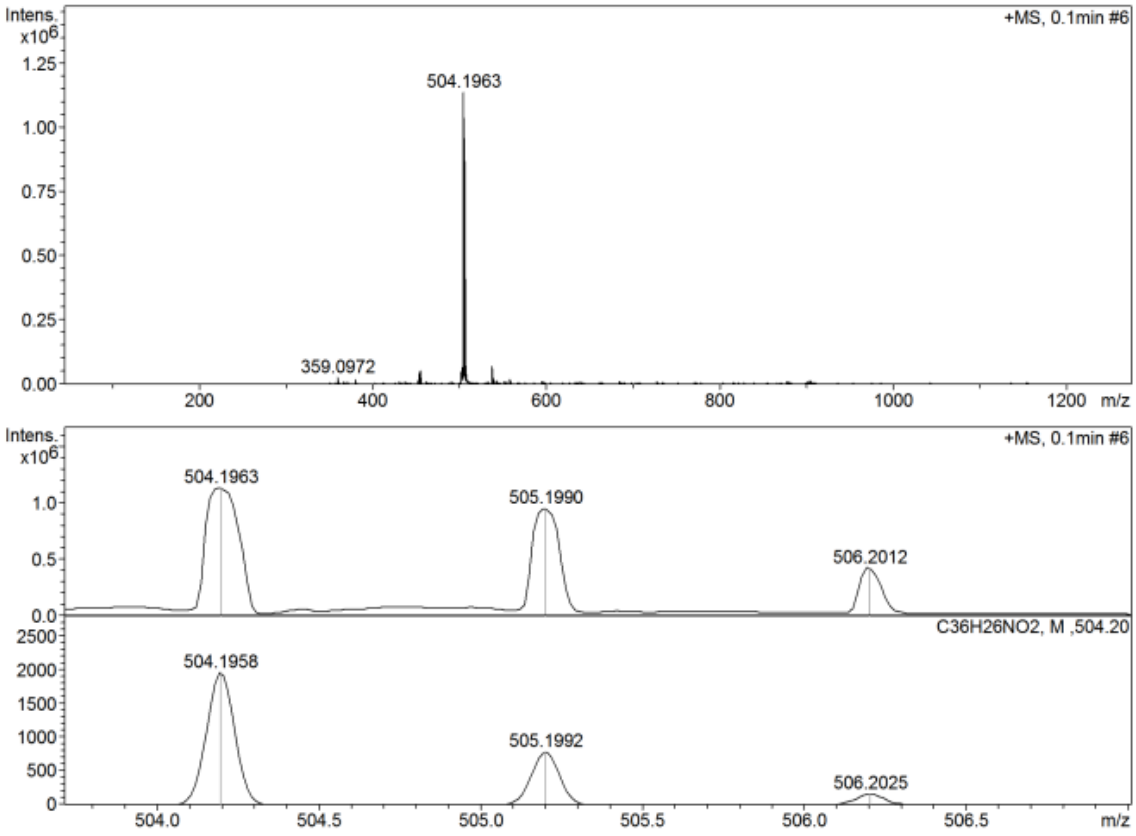

ESI-HRMS (positive ion mode) spectrum of **3u**

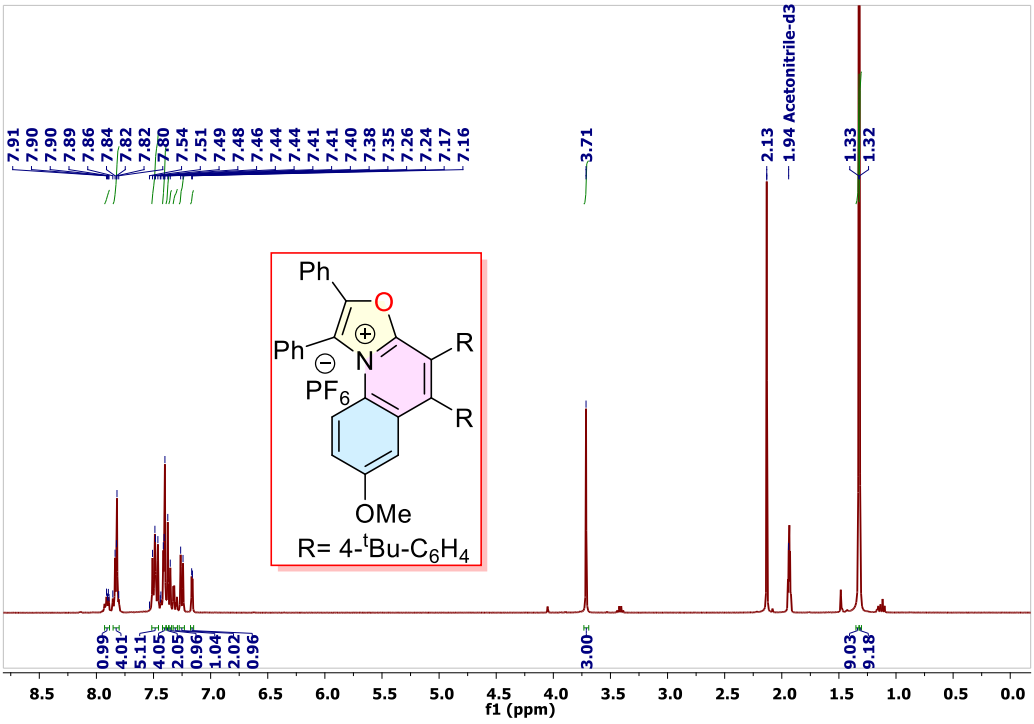

^{1}H NMR spectrum of **3v** (400 MHz, CD_3CN)

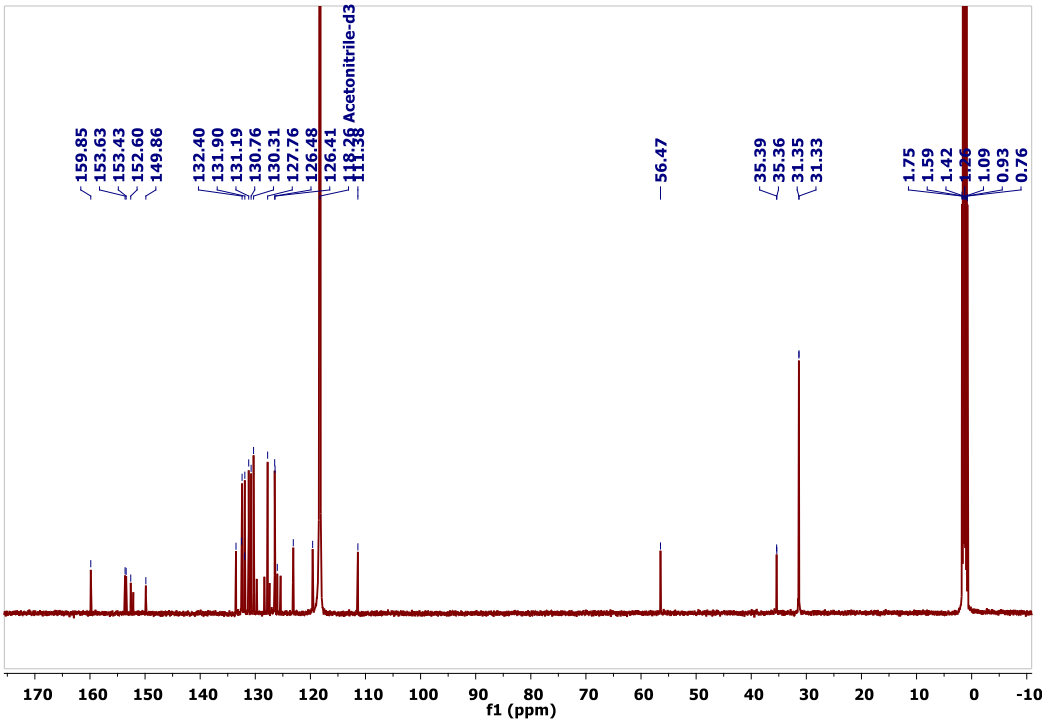

^{13}C{^{1}H} NMR spectrum of **3v** (126 MHz, CD_3CN)

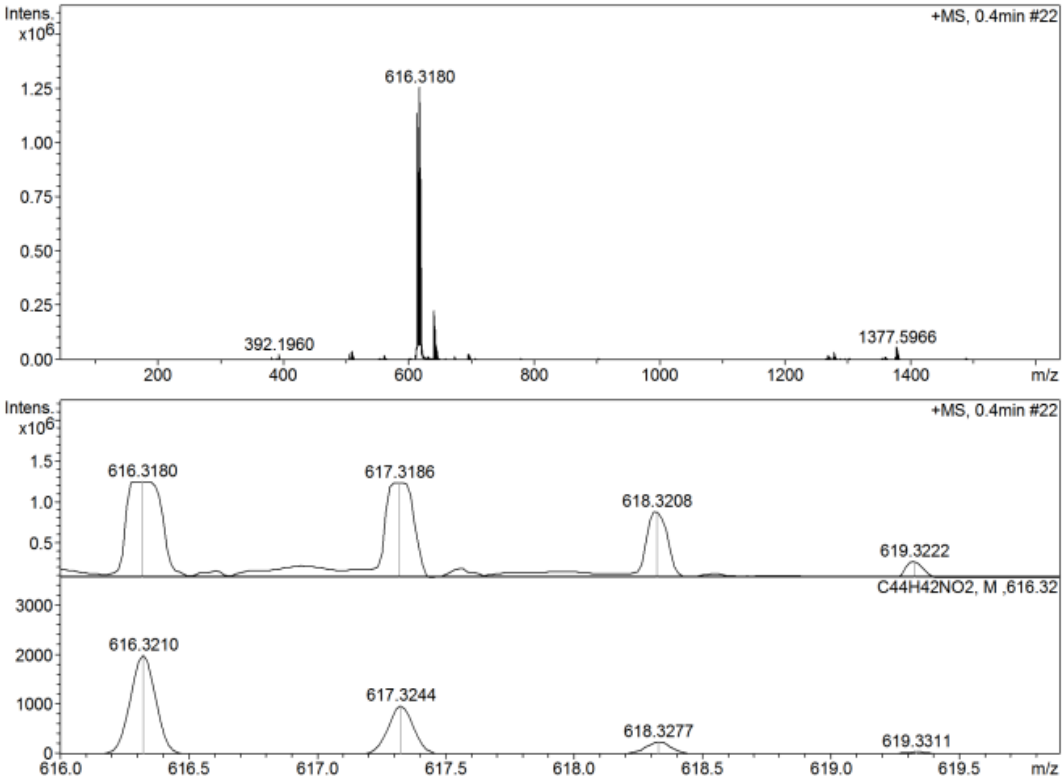

ESI-HRMS (positive ion mode) spectrum of **3v**

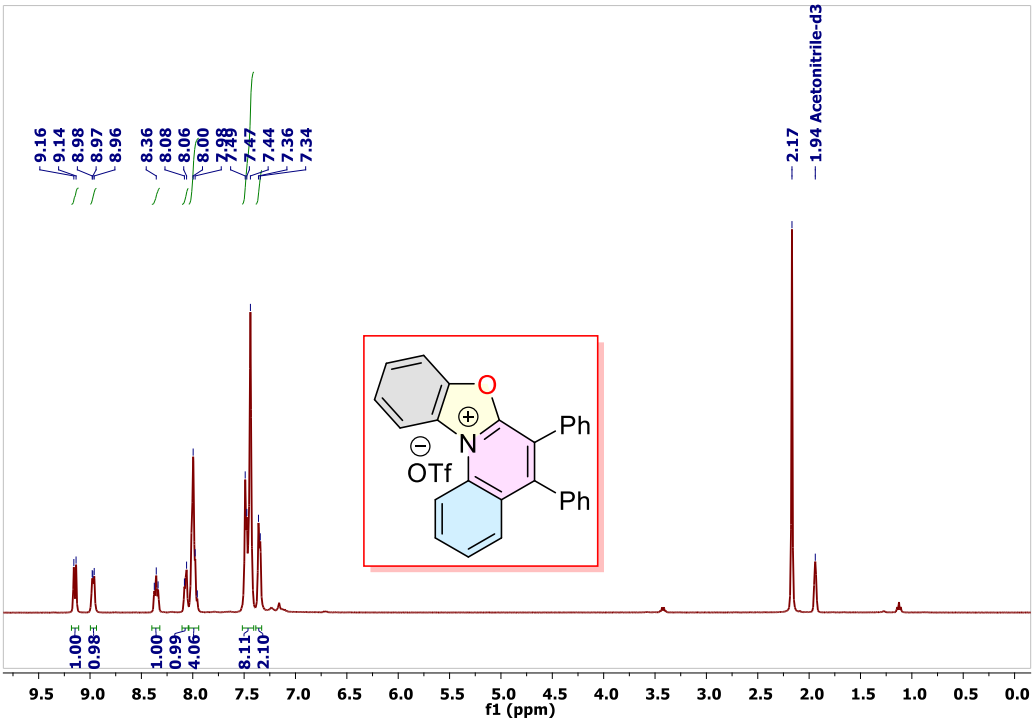

^{1}H NMR spectrum of **3w** (400 MHz, CD_3CN)

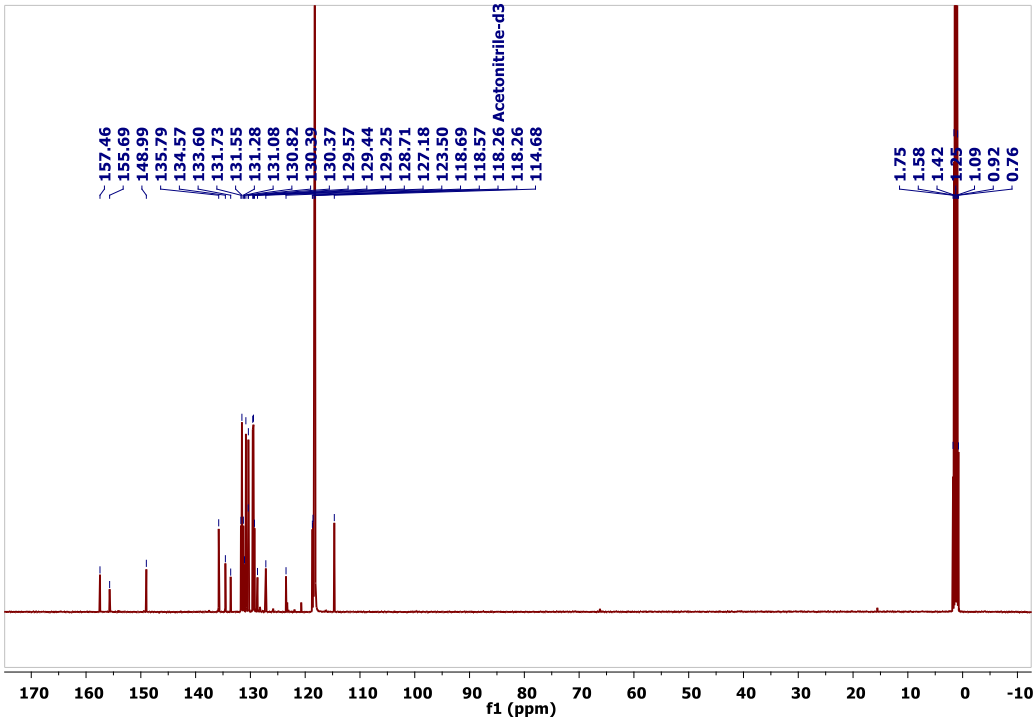

$^{13}C\{^{1}H\}$ NMR spectrum of **3w** (126 MHz, CD_3CN)

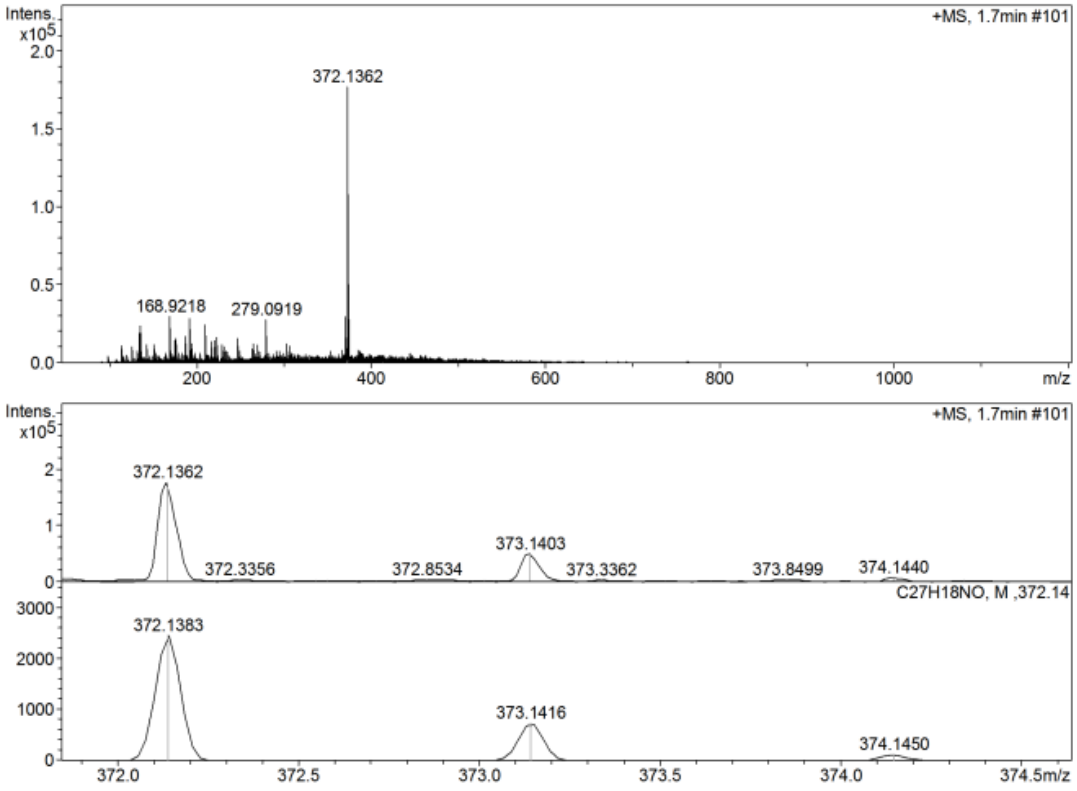

ESI-HRMS (positive ion mode) spectrum of **3w**

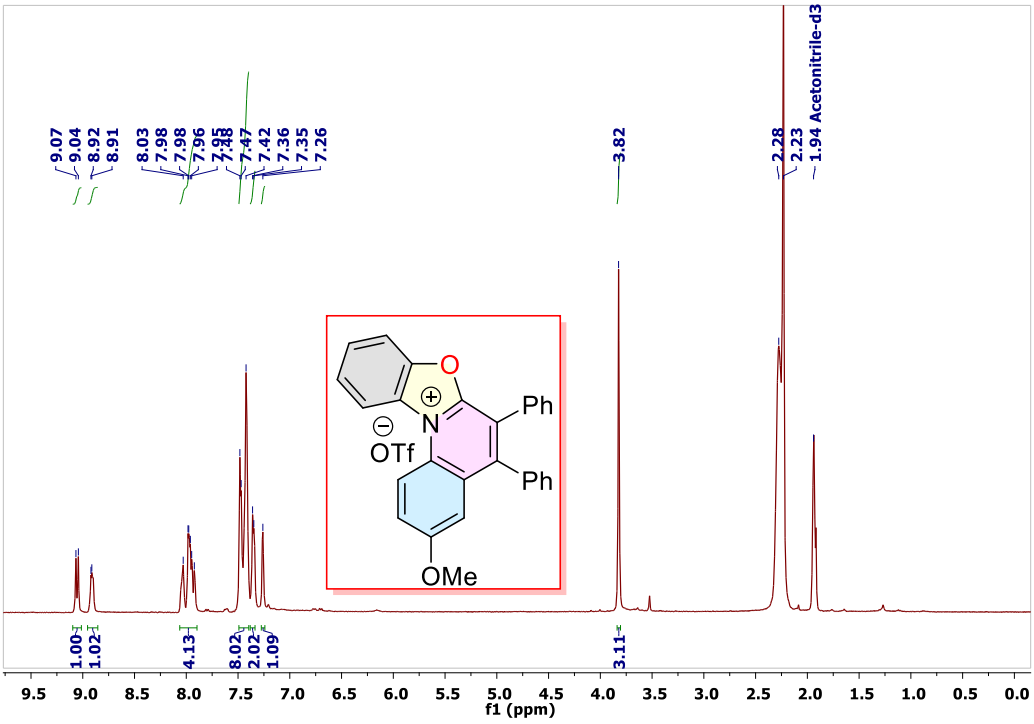

^{1}H NMR spectrum of **3x** (400 MHz, CD_3CN)

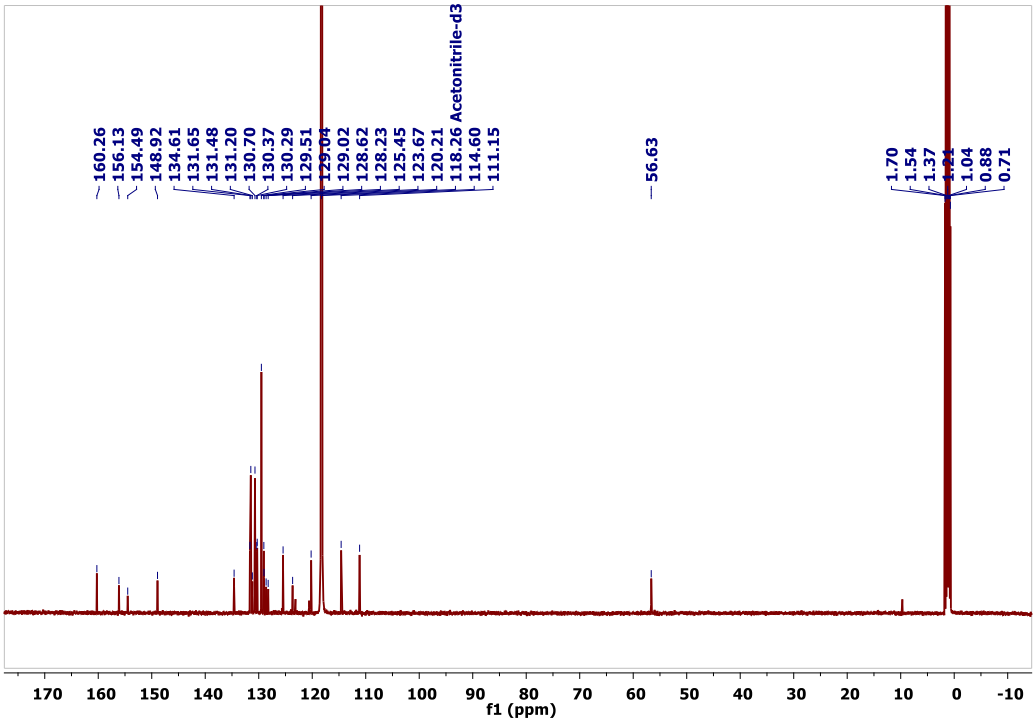

^{13}C{^{1}H} NMR spectrum of **3x** (126 MHz, CD_3CN)

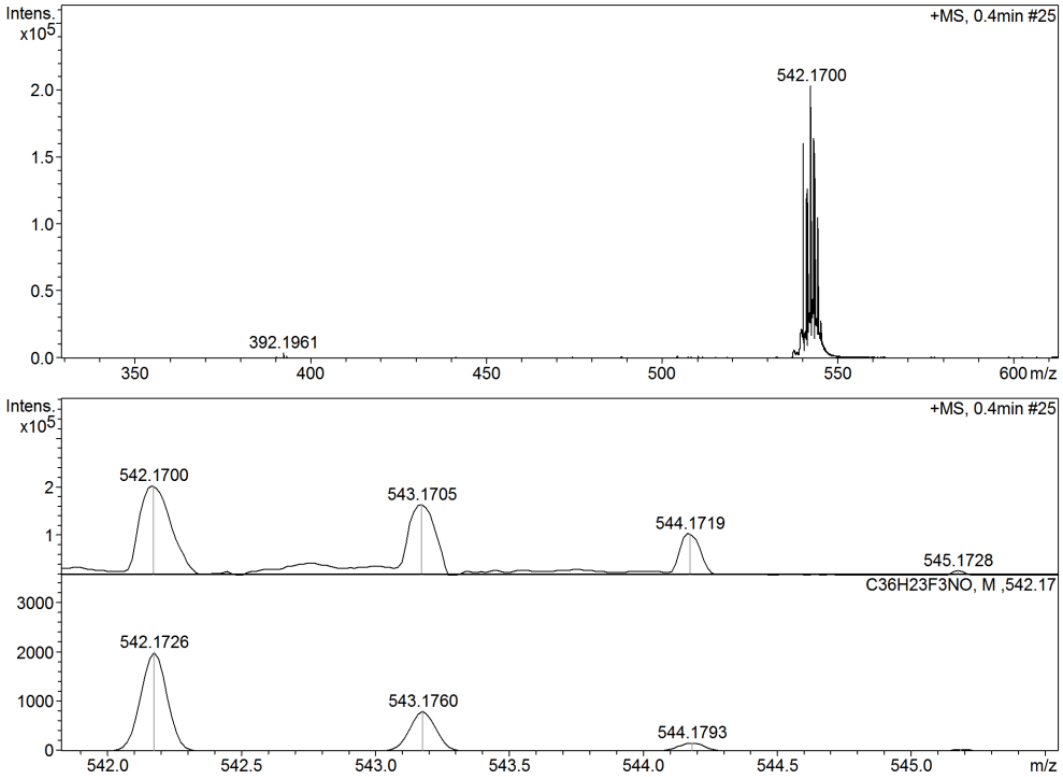

ESI-HRMS (positive ion mode) spectrum of **3x**

18. References

S1 Y. Du, T. K. Hyster, and T. Rovi, *Chem. Commun.*, 2011, **47**, 12074-12076.

S2. V. K. R. Garapati, and M. Gravel, *Org. Lett.* 2018, **20**, 6372−6375.

S3. N. Sanosa, D. Ambrosi, P. R. Campos, D. Sampedro and I.F. Ardoiz, *Chem. Eur. J.* 2023, **29**, e202301406.

S4. J. Wang, X. Gu, P. Zhang, X. Huang, X. Zheng, M. Chen, H. Feng, R. T. K. Kwok, J. W. Y. Lam and B. Z. Tang, *J. Am. Chem. Soc.*, 2017, **139**, 16974–16979.

S5. G. Jiang, R. Hu, C. Li, J. Gong, J. Wang, J. W. Y. Lam, A. Qin and B. Z. Tang, *Chem. Eur. J.*, 2022, **28**, e202202388.

S6. Voskuhl, J.; Giese, M.; *Aggregate*, **2022**, *3*, e124.